

Theory and Phenomenology of an Exceptional Supersymmetric Standard Model

S. F. King¹, S. Moretti², R. Nevzorov^{3 4}

*School of Physics and Astronomy, University of Southampton,
Highfield, Southampton, SO17 1BJ, U.K.*

Abstract

We make a comprehensive study of the theory and phenomenology of a low energy supersymmetric standard model originating from a string-inspired E_6 grand unified gauge group. The Exceptional Supersymmetric Standard Model (ESSM) considered here is based on the low energy SM gauge group together with an extra Z' corresponding to an extra $U(1)_N$ gauge symmetry under which right-handed neutrinos have zero charge. The low energy matter content of the ESSM corresponds to three 27 representations of the E_6 symmetry group, to ensure anomaly cancellation, plus an additional pair of Higgs-like doublets as required for high energy gauge coupling unification. The ESSM is therefore a low energy alternative to the MSSM or NMSSM. The ESSM involves extra matter beyond the MSSM contained in three $5 + 5^*$ representations of $SU(5)$, plus three $SU(5)$ singlets which carry $U(1)_N$ charges, one of which develops a VEV, providing the effective μ term for the Higgs doublets, as well as the necessary exotic fermion masses. We explore the RG flow of the ESSM and examine theoretical restrictions on the values of new Yukawa couplings caused by the validity of perturbation theory up to the Grand Unification scale. We then discuss electroweak symmetry breaking and Higgs phenomenology, and establish an upper limit on the mass of the lightest Higgs particle which can be significantly heavier than in the MSSM and NMSSM, in leading two-loop approximation. We also discuss the phenomenology of the Z' and the extra matter, whose discovery will provide a smoking gun signal of the model.

¹E-mail: sfk@hep.phys.soton.ac.uk

²E-mail: stefano@hep.phys.soton.ac.uk

³E-mail: nevzorov@phys.soton.ac.uk

⁴On leave of absence from the Theory Department, ITEP, Moscow, Russia.

1. Introduction

Despite the absence of any evidence for new particles beyond those contained in the Standard Model (SM), the cancellation of quadratic divergences [1] remains a compelling theoretical argument in favour of softly broken supersymmetry (SUSY) which stabilises the Electro-Weak (EW) scale and solves the hierarchy problem [2] (for a recent review see [3]). SUSY also facilitates the high energy convergence of the SM gauge couplings [4] which allows the SM gauge group to be embedded into Grand Unified Theories (GUTs) [5] based on simple gauge groups such as $SU(5)$, $SO(10)$ or E_6 . The rational $U(1)_Y$ charges, which are postulated “ad hoc” in the case of the SM, then appear in a natural way in the context of SUSY GUT models after the breakdown of the extended symmetry at some high energy scale M_X , providing a simple explanation of electric charge quantisation.

An additional motivation to consider models with softly broken SUSY is associated with the possible incorporation of the gravitational interactions. The local version of SUSY (supergravity) leads to a partial unification of the SM gauge interactions with gravity. However SuperGRAvity (SUGRA) itself is a non-renormalisable theory and has to be considered as an effective low energy limit of some renormalisable or even finite theory. Currently, the best candidate for such an underlying theory is ten-dimensional heterotic superstring theory based on $E_8 \times E'_8$ [6]. In the strong coupling regime of an $E_8 \times E'_8$ heterotic string theory described by eleven dimensional SUGRA (M-theory) [7], the string scale can be compatible with the unification scale M_X [8]. Compactification of the extra dimensions results in the breakdown of E_8 down to E_6 or one of its subgroups in the observable sector [9]. The remaining E'_8 plays the role of a hidden sector that gives rise to spontaneous breakdown of SUGRA, which results in a set of soft SUSY breaking terms [10] characterised by the gravitino mass ($m_{3/2}$) of order the EW scale¹.

Although the theoretical argument for low energy SUSY is quite compelling, it is worth emphasising that the choice of low energy effective theory at the TeV scale consistent with high energy conventional (or string) unification is not uniquely specified. Although the Minimal Supersymmetric Standard Model (MSSM) is the best studied and simplest candidate for such a low energy effective theory, the MSSM suffers from the μ problem: the superpotential of the MSSM contains one bilinear term $\mu \hat{H}_d \hat{H}_u$ which can be present before SUSY is broken. As a result one would naturally expect it to be of the order of the Planck scale M_{Pl} . If $\mu \simeq M_{\text{Pl}}$ then the Higgs scalars get a huge positive contribution $\sim \mu^2$ to their squared masses and EW Symmetry Breaking (EWSB) does not occur. On the other hand the parameter μ cannot be simply omitted. If $\mu = 0$ at some scale Q the

¹A large mass hierarchy between $m_{3/2}$ and Planck scale can appear because of non-perturbative sources of SUSY breaking in the hidden sector gauge group (for a review see [11]).

mixing between Higgs doublets is not generated at any scale below Q due to the non-renormalisation theorems [12]. In this case the minimum of the Higgs boson potential is attained for $\langle H_d \rangle = 0$. Because of this down-type quarks and charged leptons remain massless. In order to get the correct pattern of EWSB, μ is required to be of the order of the SUSY breaking (or EW) scale.

The Next-to-Minimal Supersymmetric Standard Model (NMSSM) is an attempt to solve the μ problem of the MSSM in the most direct way possible, by generating μ dynamically as the low energy Vacuum Expectation Value (VEV) of a singlet field. The superpotential of the NMSSM is given by [13]–[14]

$$W_{NMSSM} = \lambda \hat{S}(\hat{H}_d \hat{H}_u) + \frac{1}{3} \kappa \hat{S}^3 + W_{MSSM}(\mu = 0). \quad (1)$$

The cubic term of the new singlet superfield \hat{S} in the superpotential breaks an additional $U(1)$ global symmetry that would appear and is a common way to avoid the axion that would result. However the NMSSM itself is not without problems. The NMSSM superpotential is still invariant under the transformations of a discrete Z_3 symmetry. This Z_3 symmetry should lead to the formation of domain walls in the early universe between regions which were causally disconnected during the period of EWSB [15]. Such domain structure of vacuum create unacceptably large anisotropies in the cosmic microwave background radiation [16]. In an attempt to break the Z_3 symmetry operators suppressed by powers of the Planck scale could be introduced. But it has been shown that these operators give rise to quadratically divergent tadpole contributions, which destabilise the mass hierarchy once again [17].

One solution to these difficulties is to consider the simplest gauge extensions of the SM gauge group that involve an additional non-anomalous $U(1)'$ gauge symmetry. Models with an additional $U(1)'$ factor can arise naturally out of string-inspired constructions [18, 19]. In particular one or two extra $U(1)'$ factors may emerge in the breaking of a string-inspired E_6 gauge group and the phenomenology of such models has been extensively studied in the literature [18]. Such theories may lead to a $U(1)'$ extension of the NMSSM in which a SM singlet field S couples to the Higgs doublets and yields an effective μ parameter $\sim \lambda \langle S \rangle$, while the \hat{S}^3 term is forbidden by the $U(1)'$ gauge symmetry. In such models the Peccei–Quinn (PQ) symmetry becomes embedded in the new $U(1)'$ gauge symmetry. Clearly there are no domain wall problems in such a model since there is no discrete Z_3 symmetry. The field S is charged under the $U(1)'$ so that its expectation value also gives mass to the new Z' gauge boson breaking the $U(1)'$, in other words the would-be PQ axion is eaten by the Z' . The extended gauge symmetry forbids an elementary μ term as well as terms like \hat{S}^n in the superpotential. The role of the S^3 term in generating quartic terms in the scalar potential, which stabilise the physical vacuum, is played by

D -terms.

In this paper we explore a specific E_6 inspired supersymmetric realisation of the above $U(1)'$ type model which is capable of resolving the μ problem as in the NMSSM, but without facing any of its drawbacks. The total matter content of our model corresponds to three families of 27_i representations, plus two Higgs-like doublets, consistent with SUSY unification. A particular feature of our model is that we assume that the E_6 gauge group is broken at high energies down to the SM gauge group plus a particular extra $U(1)_N$ gauge symmetry in which right-handed neutrinos have zero charge and so are singlets and do not participate in the gauge interactions. Since right-handed neutrinos have zero charges they can acquire very heavy Majorana masses and are thus suitable to take part in the standard seesaw mechanism which yields small neutrino masses. Having heavy right-handed neutrinos also avoids any stringent constraints on the mass of the Z' boson coming from the nucleosynthesis and astrophysical data which would be present if the right-handed neutrinos were light.

The above superstring inspired E_6 SUSY model, henceforth referred to as the Exceptional Supersymmetric Standard Model (ESSM), provides a theoretically attractive solution to the μ problem of the MSSM since the bilinear Higgs μ terms are forbidden by the $U(1)_N$ gauge symmetry. This model contains three pairs of candidate Higgs doublets H_{1i}, H_{2i} , plus three singlets S_i , which carry $U(1)_N$ charge. These states all originate from three 27_i representations and couple together according to a $27_i 27_j 27_k$ coupling resulting in NMSSM type superpotential couplings of the form:

$$W_H = \sum_{ijk} \lambda_{ijk} \hat{S}_i \hat{H}_{1j} \hat{H}_{2k}. \quad (2)$$

The breaking of the EW and $U(1)_N$ gauge symmetry down to $U(1)_{em}$ takes place when some of these Higgs fields acquire VEVs. It is possible to work in a basis where only one family of Higgs fields and singlets acquire non-zero VEVs, which we can define to be the third family, and we can then define $S \equiv S_3$, $H_d \equiv H_{1,3}$, $H_u \equiv H_{2,3}$. We shall then refer to the remaining first two families $S_i, H_{1,i}, H_{2,i}$, with $i = 1, 2$ as non-Higgs doublets and singlets. The relation of the third family Higgs so defined to the third family quarks and leptons is more model dependent, but in the context of Radiative EWSB (REWSB) it is natural to associate the third family Higgs to the third family quarks and leptons, since it is the large Yukawa coupling of the third family which drives the Higgs VEVs. This also avoids the appearance of Flavour Changing Neutral Currents (FCNCs). Then, restricting ourselves to Higgs fields which develop VEVs, the superpotential (2) reduces to

$$W_H \rightarrow \lambda \hat{S}(\hat{H}_d \hat{H}_u) \quad (3)$$

which is just the NMSSM coupling in Eq. (1). After the spontaneous symmetry breakdown at the EW scale the scalar component of the superfield \hat{S} acquires non-zero VEV

($\langle S \rangle = s/\sqrt{2}$) and an effective μ -term ($\mu = \lambda s/\sqrt{2}$) of the required size is automatically generated. The Higgs sector of the considered model contains only one additional singlet field and one extra parameter compared to the MSSM. Therefore it can be regarded as the simplest extension of the Higgs sector of the MSSM.

It is interesting to compare the ESSM to other related models with an extra $U(1)'$. In general anomaly cancellation requires either the presence of exotic chiral supermultiplets [20]–[21] or family–non–universal $U(1)'$ couplings [22]. Any family dependence of the $U(1)'$ charges would result in FCNCs mediated by the Z' which can be suppressed for the first two generation and manifest themselves in rare B decays and $B - \bar{B}$ mixing [23]. In the ESSM, because the $U(1)_N$ charge assignment is flavour–independent, the considered model does not suffer from the FCNC problem. In the ESSM anomalies are cancelled in a flavour–independent way since the model contains an extra $U(1)_N$ arising from E_6 together with the matter content of (three) complete 27 representations of E_6 down to the TeV scale, apart from the three right–handed neutrinos which are singlets under the low energy gauge group. The existence of exotic supermultiplets in the ESSM is consistent with gauge coupling unification since the extra matter is in complete 27 representations. However exotic quarks and non–Higgses naturally appear in the E_6 inspired model, with the quantum numbers of three families of $5+5^*$ $SU(5)$ representations, which phenomenologically correspond to three families of extra down–type quark singlets and three families of matter with the quantum numbers of Higgs doublets, where each multiplet is accompanied by its conjugate representation. The large third family coupling of the extra coloured chiral superfields (D, \bar{D}) to the singlet S of the form $\kappa S(D\bar{D})$ may help to induce radiative breakdown of the $SU(2) \times U(1)_Y \times U(1)'$ symmetry [20], [24]–[27].

Before describing the phenomenological work performed in this paper it is worth briefly reviewing the phenomenological studies performed so far on related models in the literature. Recently the implications of SUSY models with an additional $U(1)'$ gauge symmetry have been studied for CP–violation [28], neutrino physics [29]–[30], dark matter [31], leptogenesis [32], EW baryogenesis [33]–[34], muon anomalous magnetic moment [35], electric dipole moment of electron [36], lepton flavour violating processes like $\mu \rightarrow e\gamma$ [37] (forbidding R–parity violating terms [21], [38]). An important property of $U(1)'$ models is that the tree–level mass of the lightest Higgs particle can be larger than M_Z even for moderate values of $\tan\beta \simeq 1 - 2$ [27]–[28], [39], hence the existing LEP bounds can be satisfied with almost no need for large radiative corrections. Models with a $U(1)_N$ gauge symmetry in which right–handed neutrinos have zero charge have been studied in [30] in the context of non–standard neutrino models with extra singlets, in [40] from the point of view of $Z - Z'$ mixing and a discussion of the neutralino sector, in [25] where the RG was studied, in [27] where a one–loop Higgs mass upper bound was presented.

The phenomenological analysis presented here goes well beyond what has appeared so far in the literature. Our analysis begins with a detailed RG analysis of the dimensionless couplings in the ESSM, and an examination of the fixed points of the model. This analysis is completely new as it has not appeared before. We later use the results of this analysis in determining an upper bound on the lightest CP-even (or scalar) Higgs boson mass, using the effective potential and including two-loop corrections, which had also not been considered previously, and we make a detailed comparison with similar bounds obtained in the MSSM and NMSSM. We then make a comprehensive phenomenological study of the full Higgs spectrum and couplings, which includes the low energy allowed regions in which EWSB is successful, and comment on the crucial phenomenological aspects of the Higgs sector of the ESSM. The chargino and neutralino spectrum expected in the ESSM is also studied in some depth. We then discuss the phenomenology of the extra particles predicted by the ESSM, including the Z' and some exotic fermions, and provide a numerical estimate and a full discussion of their production cross sections and signatures at the upcoming CERN Large Hadron Collider (LHC) and a future International Linear Collider (ILC).

The paper is organised as follows. In section 2 we specify our model. In section 3 we examine the RG flow of gauge and Yukawa couplings assuming that gauge coupling unification takes place at high energies. The EWSB and Higgs phenomenology are studied in sections 4 and 5 respectively. In section 6 we consider the chargino and neutralino spectrum in the ESSM while in section 7 the potential discovery of a Z' boson and new exotic particles at future colliders are discussed. Our results are summarised in section 8.

2. The ESSM

2.1 Overview of the model

As it is clear from the discussion in the Introduction, the ESSM is a low energy alternative to the MSSM or NMSSM defined as follows. The ESSM originates from an E_6 GUT gauge group which is broken at the GUT scale to the SM gauge group together with an additional $U(1)_N$ gauge group which is not broken until a scale not very far above the EW scale, giving rise to an observable Z' gauge boson. The $U(1)_N$ gauge group is defined such that right-handed neutrinos N_i^c carry zero charges under it. The matter content below the GUT scale corresponds to three 27-plets of E_6 (labelled as 27_i) which contain the three ordinary families of quarks and leptons including right-handed neutrinos N_i^c , three families of candidate Higgs doublets H_{1i} , H_{2i} , three families of extra down-type quark singlets D_i, \bar{D}_i , and three families of extra singlets S_i . However only the third family

Higgs doublets H_u and H_d and singlet S develop VEVs. In addition, in order to achieve gauge coupling unification, there is a further pair of Higgs-like doublet supermultiplets H' and \bar{H}' which do not develop VEVs, arising from an incomplete $27' + \bar{27}'$ representation. All the extra matter described above is expected to have mass of order the TeV scale and may be observable at the LHC or at an ILC. The ESSM has the following desirable features:

- Anomalies are cancelled generation by generation within each complete 27_i representation.
- Gauge coupling unification is accomplished due to the complete 27_i representations together with the additional pair of Higgs-like doublets H' and \bar{H}' from the incomplete $27' + \bar{27}'$ representation.
- The seesaw mechanism is facilitated due to the right-handed neutrinos N_i^c arising from the 27_i representations having zero gauge charges.
- The μ -problem of the MSSM is solved since the μ -term is forbidden by the $U(1)_N$ gauge symmetry. It is replaced by a singlet coupling $\hat{S}(\hat{H}_d \hat{H}_u)$ as in the NMSSM, but without the \hat{S}^3 term of the NMSSM which resulted in domain wall problems. Besides, in the ESSM the would-be Goldstone boson is eaten by the Z' associated with the $U(1)_N$ gauge group.

The purpose of the remainder of this section is to develop the theoretical aspects of the ESSM defined above, and define the matter content, charges, couplings and symmetries of the ESSM more precisely.

2.2 The choice of the surviving $U(1)_N$ gauge group

Since all matter and Higgs superfields must originate from 27 and $\bar{27}$ -plets of E_6 , one cannot break E_6 in a conventional manner as the required Higgs fields are in larger representations than the 27. However, at the string scale, E_6 can be broken via the Hosotani mechanism [41]. Because the rank of the E_6 group is six the breakdown of the E_6 symmetry results in several models based on rank-5 or rank-6 gauge groups. As a consequence E_6 inspired SUSY models in general may lead to low-energy gauge groups with one or two additional $U(1)'$ factors in comparison to the SM. Indeed E_6 contains the maximal subgroup $SO(10) \times U(1)_\psi$ while $SO(10)$ can be decomposed in terms of the $SU(5) \times U(1)_\chi$ subgroup. By means of the Hosotani mechanism E_6 can be broken directly to $SU(3)_C \times SU(2)_W \times U(1)_Y \times U(1)_\psi \times U(1)_\chi$ which has rank 6. For suitable large VEVs of the symmetry breaking Higgs fields this rank-6 model can be reduced further to an

effective rank-5 model with only one extra gauge symmetry. Then an extra $U(1)'$ that appears at low energies is a linear combination of $U(1)_\chi$ and $U(1)_\psi$:

$$U(1)' = U(1)_\chi \cos \theta + U(1)_\psi \sin \theta. \quad (4)$$

In general the right-handed neutrinos will carry non-zero charges with respect to the extra gauge interaction $U(1)'$. It means that their mass terms are forbidden by the gauge symmetry. The right-handed neutrinos can gain masses only after the breakdown of the $SU(2)_W \times U(1)_Y \times U(1)'$ symmetry. But even in this case one can expect that the corresponding mass terms should be suppressed due to the invariance of the low-energy effective Lagrangian under the $U(1)_L$ symmetry associated with lepton number conservation². If the right-handed neutrinos were lighter than a few MeV they would be produced prior to big bang nucleosynthesis by the Z' interactions leading to a faster expansion rate of the Universe and to a higher ${}^4\text{He}$ relic abundance [42]. The current cosmological observations of cosmic microwave background radiation and nuclear abundances restrict the total effective number of extra neutrino species ΔN_ν to 0.3 [43]. The strength of the interactions of right-handed neutrinos with other particles and the equivalent number of additional neutrinos rises with a decreasing Z' boson mass. Thus cosmological and astrophysical observations set a stringent limit on the Z' mass which has to be larger than 4.3 TeV [42].

The situation changes dramatically if the right-handed neutrinos remain sterile after the breakdown of the E_6 symmetry, i.e. have zero charges under the surviving gauge group. The extra $U(1)'$ factor for which right-handed neutrinos transform trivially is called $U(1)_N$. It corresponds to the angle $\theta = \arctan \sqrt{15}$ in Eq. (4). In this case, considered here, the right-handed neutrinos may be superheavy. Then the three known doublet neutrinos ν_e , ν_μ and ν_τ acquire small Majorana masses via the seesaw mechanism. This allows for a comprehensive understanding of the mass hierarchy in the lepton sector and neutrino oscillations data. The successful leptogenesis in the early epoch of the Universe is the distinctive feature of the ESSM with an extra $U(1)_N$ factor [32]. Because right-handed neutrinos are allowed to have large masses, they may decay into final states with lepton number $L = \pm 1$, thereby creating a lepton asymmetry in the early Universe [44]. Since sphalerons violate $B + L$ but conserve $B - L$, this lepton asymmetry subsequently gets converted into the present observed baryon asymmetry of the Universe through the EW phase transition [45]. Any other E_6 inspired supersymmetric extension with the extra $U(1)$ factor would result in $B - L$ violating interactions at $O(1)$ TeV as it is broken down to the SM. This $B - L$ violating interactions together with $B + L$ violating sphalerons

²In many supersymmetric models the invariance under the lepton and baryon $U(1)$ symmetries are caused by R-parity conservation which is normally imposed to prevent rapid proton decay.

would erase any lepton or baryon asymmetry that may have been created during the earlier epoch of the Universe. Different phenomenological aspects of supersymmetric models with an extra $U(1)_N$ gauge symmetry were studied in [25], [27], [30], [32], [34], [40].

One of the most important issues in $U(1)'$ models is the cancellation of the gauge and gravitational anomalies. In E_6 theories the anomalies are cancelled automatically. Therefore all models that are based on the E_6 subgroups and contain complete representations should be anomaly-free. As a result in order to make the chosen supersymmetric model with the extra $U(1)_N$ factor anomaly-free one is forced to augment the minimal spectrum by a number of exotics which, together with ordinary quarks and leptons, form complete fundamental 27 representations of E_6 . These decompose under the surviving low energy gauge group as discussed in the next subsection.

2.3 The low energy matter content of the ESSM

The three families of fundamental 27_i representations decompose under the $SU(5) \times U(1)_N$ subgroup of E_6 [25] as follows:

$$27_i \rightarrow (10, 1)_i + (5^*, 2)_i + (5^*, -3)_i + (5, -2)_i + (1, 5)_i + (1, 0)_i . \quad (5)$$

The first and second quantities in the brackets are the $SU(5)$ representation and extra $U(1)_N$ charge while i is a family index that runs from 1 to 3. An ordinary SM family which contains the doublets of left-handed quarks Q_i and leptons L_i , right-handed up- and down-type quarks (u_i^c and d_i^c) as well as right-handed charged leptons, is assigned to the $(10, 1)_i + (5^*, 2)_i$. These representations decompose under

$$SU(5) \times U(1)_N \rightarrow SU(3)_C \times SU(2)_W \times U(1)_Y \times U(1)_N \quad (6)$$

to give ordinary quarks and leptons:

$$\begin{aligned} (10, 1)_i &\rightarrow Q_i = (u_i, d_i) \sim \left(3, 2, \frac{1}{6}, 1\right), \\ &u_i^c \sim \left(3^*, 1, -\frac{2}{3}, 1\right), \\ &e_i^c \sim (1, 1, 1, 1); \\ (5^*, 2)_i &\rightarrow d_i^c \sim \left(3^*, 1, \frac{1}{3}, 2\right), \\ &L_i = (\nu_i, e_i) \sim \left(1, 2, -\frac{1}{2}, 2\right), \end{aligned} \quad (7)$$

where the third quantity in the brackets is the $U(1)_Y$ hypercharge. (In Eq. (7) and further we omit all isospin and colour indexes related to $SU(2)$ and $SU(3)$ gauge interactions.)

The right-handed neutrinos N_i^c transform trivially under $SU(5) \times U(1)_N$ by definition. Therefore N_i^c should be associated with the last term in Eq. (5) $(1, 0)_i$. The next-to-last

term in Eq. (5), $(1, 5)_i$, represents SM singlet fields S_i which carry non-zero $U(1)_N$ charges and therefore survive down to the EW scale.

The remaining representations in Eq. (5) decompose as follows:

$$\begin{aligned}
(5^*, -3)_i &\rightarrow H_{1i} = (H_{1i}^0, H_{1i}^-) \sim \left(1, 2, -\frac{1}{2}, -3\right), \\
&\quad \bar{D}_i \sim \left(3^*, 1, \frac{1}{3}, -3\right), \\
(5, -2)_i &\rightarrow H_{2i} = (H_{2i}^+, H_{2i}^0) \sim \left(1, 2, \frac{1}{2}, -2\right), \\
&\quad D_i \sim \left(3, 1, -\frac{1}{3}, -2\right).
\end{aligned} \tag{8}$$

The pair of $SU(2)$ -doublets (H_{1i} and H_{2i}) that are contained in $(5^*, -3)_i$ and $(5, -2)_i$ have the quantum numbers of Higgs doublets. Other components of these exotic $SU(5)$ multiplets form extra colour triplet but EW singlet quarks D_i and anti-quarks \bar{D}_i with electric charges $-1/3$ and $+1/3$ respectively. The exotic multiplets in Eq. (8) form vector pairs under the SM gauge group.

In addition to the three complete 27_i representations just discussed, some components of additional $27'$ and $\bar{27}'$ representations can and must survive to low energies, in order to preserve gauge coupling unification. We assume that an additional $SU(2)$ doublet and anti-doublet H' and \bar{H}' originate as incomplete multiplets of an additional $27'$ and $\bar{27}'$. Specifically we assume that they originate from the $SU(2)$ doublet components of a $(5^*, 2)$ from a $27'$, and the corresponding anti-doublet from a $\bar{27}'$.

The low energy matter content of the ESSM may then be summarised as:

$$3[(Q_i, u_i^c, d_i^c, L_i, e_i^c, N_i^c)] + 3(S_i) + 3(H_{2i}) + 3(H_{1i}) + 3(D_i, \bar{D}_i) + H' + \bar{H}', \tag{9}$$

where the right-handed neutrinos N_i^c are expected to gain masses at some intermediate scale, while the remaining matter survives down to the EW scale near which the gauge group $U(1)_N$ is broken.

2.4 The low energy symmetries and couplings of the ESSM

In E_6 models the renormalisable part of the superpotential comes from the $27 \times 27 \times 27$ decomposition of the E_6 fundamental representation. The most general renormalisable superpotential which is allowed by the $SU(3) \times SU(2) \times U(1)_Y \times U(1)_N$ gauge symmetry can be written in the following form:

$$W_{\text{total}} = W_0 + W_1 + W_2 + W_{\cancel{6}}. \tag{10}$$

The first, second and third terms in Eq. (10) represent the most general form of the superpotential allowed by the E_6 symmetry. W_0 , W_1 and W_2 are given by

$$\begin{aligned}
W_0 &= \lambda_{ijk} S_i(H_{1j} H_{2k}) + \kappa_{ijk} S_i(D_j \overline{D}_k) + h_{ijk}^N N_i^c(H_{2j} L_k) + h_{ijk}^U u_i^c(H_{2j} Q_k) + \\
&\quad + h_{ijk}^D d_i^c(H_{1j} Q_k) + h_{ijk}^E e_i^c(H_{1j} L_k), \\
W_1 &= g_{ijk}^Q D_i(Q_j Q_k) + g_{ijk}^q \overline{D}_i d_j^c u_k^c, \\
W_2 &= g_{ijk}^N N_i^c D_j d_k^c + g_{ijk}^E e_i^c D_j u_k^c + g_{ijk}^D (Q_i L_j) \overline{D}_k.
\end{aligned} \tag{11}$$

The part of the superpotential (10) coming from the $27 \times 27 \times 27$ decomposition of the E_6 fundamental representation (i.e. $W_0 + W_1 + W_2$) possesses a global $U(1)$ symmetry that can be associated with $B - L$ number conservation. This enlarged global symmetry is broken explicitly by most of the terms in $W_{\cancel{E}_6}$.

The last part of the superpotential (10) includes the E_6 violating set of terms:

$$W_{\cancel{E}_6} = \frac{1}{2} M_{ij} N_i^c N_j^c + W'_0 + W'_1 + W'_2, \tag{12}$$

where

$$\begin{aligned}
W'_0 &= \mu'(H' \overline{H}') + \mu'_i(\overline{H}' L_i) + h_{ij} N_i^c(H_{2j} H') + h_{ij}^{H'} e_i^c(H_{1j} H'), \\
W'_1 &= \frac{\sigma_{ijk}}{3} N_i^c N_j^c N_k^c + \Lambda_k N_k^c + \lambda_{ij} S_i(H_{1j} \overline{H}') + g_{ij}^N N_i^c(\overline{H}' L_j) \\
&\quad + g_i^N N_i^c(\overline{H}' H') + g_{ij}^U u_i^c(\overline{H}' Q_j) + \mu_{ij}(H_{2i} L_j) + \mu_i(H_{2i} H') + \mu'_{ij} D_i d_j^c, \\
W'_2 &= g_{ij}^{H'} (Q_i H') \overline{D}_j, \quad i, j, k = 1, 2, 3.
\end{aligned} \tag{13}$$

The terms in Eq. (12) are invariant with respect to the SM gauge group and extra $U(1)_N$ transformations but are either forbidden by the E_6 symmetry itself or by the splitting of complete 27 and $\overline{27}$ representations that also breaks E_6 . Some of the interactions listed in Eq. (12) can play a crucial role in low-energy phenomenology. For example, Majorana mass terms of the right-handed neutrinos at some intermediate scales provide small Majorana masses for the three species of left-handed neutrinos via the seesaw mechanism. Some other terms in Eqs. (12)–(13) (like $\mu_{ij} H_{2i} L_j$) may be potentially dangerous from the phenomenological point of view.

Although the $B - L$ number is conserved automatically in E_6 inspired SUSY models, some Yukawa interactions in Eq. (11) violate baryon number resulting in rapid proton decay. The baryon and lepton number violating operators can be suppressed by postulating the invariance of the Lagrangian under R-parity transformations. In the MSSM the R-parity quantum numbers are

$$R = (-1)^{3(B-L)+2S}. \tag{14}$$

The straightforward generalisation of the definition of R-parity to E_6 inspired supersymmetric models, assuming $B_D = 1/3$ and $B_{\overline{D}} = -1/3$, implies that W_1 and W_2 are forbidden by the discrete symmetry (14). In this case the rest of the Lagrangian of the considered model, which is allowed by the E_6 symmetry, is invariant not only with respect to $U(1)_L$ and $U(1)_B$ but also under $U(1)_D$ symmetry transformations³

$$D \rightarrow e^{i\alpha} D, \quad \overline{D} \rightarrow e^{-i\alpha} \overline{D}. \quad (15)$$

The $U(1)_D$ invariance ensures that the lightest exotic quark is stable. Any heavy stable particle would have been copiously produced during the very early epochs of the Big Bang. Those strong or electromagnetically interacting fermions and bosons which survive annihilation would subsequently have been confined in heavy hadrons which would annihilate further. The remaining heavy hadrons originating from the Big Bang should be present in terrestrial matter. There are very strong upper limits on the abundances of nuclear isotopes which contain such stable relics in the mass range from 1 GeV to 10 TeV. Different experiments set limits on their relative concentrations from 10^{-15} to 10^{-30} per nucleon [46]. At the same time various theoretical estimations [47] show that if remnant particles would exist in nature today their concentration is expected to be at the level of 10^{-10} per nucleon. Therefore E_6 inspired models with stable exotic quarks or non-Higgsinos are ruled out.

To prevent rapid proton decay in E_6 supersymmetric models the definition of R-parity should be modified. There are 8 different ways to impose an appropriate Z_2 symmetry resulting in baryon and lepton number conservation [48]. The requirements of successful leptogenesis and non-zero neutrino masses single out only two ways to do that. If H_{1i} , H_{2i} , S_i , D_i , \overline{D}_i and quark superfields (Q_i, u_i^c, d_i^c) are even under Z_2 while lepton superfields (L_i, e_i^c, N_i^c) and survival components of 27 and $\overline{27}$ (H' and \overline{H}') are odd, all terms in W_2 are forbidden. Then the part of the superpotential allowed by the E_6 symmetry is invariant with respect to $U(1)_B$ and $U(1)_L$ global symmetries if the exotic quarks D_i and \overline{D}_i carry twice larger baryon number than the ordinary quark fields d_i^c and Q_i respectively. It implies that \overline{D}_i and D_i are diquark and anti-diquark, i.e. $B_D = -2/3$ and $B_{\overline{D}} = 2/3$. This way of suppressing baryon and lepton number violating operators will be called further Model I. An alternative possibility is to assume that the exotic quarks D_i and \overline{D}_i as well as ordinary lepton superfields and survivors are all odd under Z_2 whereas the others remain even. Then we get Model II in which all Yukawa interactions in W_1 are ruled out by the discrete Z_2 symmetry. Model II possesses two extra $U(1)$ global symmetries. They can be associated with $U(1)_L$ and $U(1)_B$ if the exotic quarks carry baryon ($B_D = 1/3$ and

³The term $\mu'_{ij} D_i d_j^c$ in $W_{\cancel{E_6}}$ spoils the invariance under $U(1)_D$ symmetry but the mechanism of its generation remains unclear.

$B_{\overline{D}} = -1/3$) and lepton ($L_D = 1$ and $L_{\overline{D}} = -1$) numbers simultaneously. It means that D_i and \overline{D}_i are leptoquarks in Model II.

In Model II the imposed Z_2 symmetry forbids all the terms in the W'_1 part of $W_{\cancel{E}_6}$, leaving only the mass terms for the right-handed neutrinos, W'_0 and W'_2 . The discrete symmetry postulated in the Model I also rules out W'_2 but permits $\mu'_{ij} D_i d_j^c$ which violate baryon number making possible the transition $p \rightarrow \pi^+ \chi^0$, where χ^0 is a neutralino. In order to suppress dangerous operators one can impose another Z_2 symmetry that changes the sign of the ordinary quark superfields Q_i , u_i^c , d_i^c leaving all others unchanged. Finally for the superpotentials of Model I and II we get

$$\begin{aligned} I) \quad W_{\text{ESSMI}} &= W_0 + W_1 + \frac{1}{2} M_{ij} N_i^c N_j^c + W'_0, \\ II) \quad W_{\text{ESSMII}} &= W_0 + W_2 + \frac{1}{2} M_{ij} N_i^c N_j^c + W'_0 + W'_2. \end{aligned} \tag{16}$$

2.5 Origin of bilinear mass terms in the ESSM

In the superpotentials (16) the non-Higgs doublets and the survival components from the $27'$ can be redefined in such a way that only one $SU(2)$ doublet H' interacts with the \overline{H}' from the $\overline{27}'$. As a result without loss of generality μ'_i in W'_0 may be set to zero. Then the superpotentials of the considered supersymmetric models include two types of bilinear terms only. One of them, $\frac{1}{2} M_{ij} N_i^c N_j^c$, determines the spectrum of the right-handed neutrinos which are expected to be heavy so that the corresponding mass parameters M_{ij} are at intermediate mass scales. Another one, $\mu' H' \overline{H}'$, is characterised by the mass parameter μ' which should not be too large otherwise it spoils gauge coupling unification in the ESSM. On the other hand, the parameter μ cannot be too small since $\mu' H' \overline{H}'$ is solely responsible for the mass of the charged and neutral components of \overline{H}' . Therefore we typically require $\mu' \sim O(1 \text{ TeV})$ as in the MSSM, potentially giving rise to the μ problem once again.

Within SUGRA models the appropriate term $\mu' H' \overline{H}'$ in the superpotentials (16) can be induced just after the breakdown of local SUSY if the Kähler potential contains an extra term $(Z(H' \overline{H}') + h.c)$ [49]. This mechanism is of course just the same one used in the MSSM to solve the μ problem. But in superstring inspired models the bilinear terms involving H_d and H_u are forbidden by the E_6 symmetry both in the Kähler potential and superpotential. As a result the mechanism mentioned above cannot be applied for the generation of $\mu H_d H_u$ in the ESSM superpotential. However this mechanism may be used to give mass to the non-Higgs doublets H' and \overline{H}' from additional $27'$ and $\overline{27}'$ since the corresponding bilinear terms are allowed by the E_6 symmetry both in the Kähler potential and superpotential.

The other bilinear terms in the superpotential of the E_6 inspired SUSY models responsible for right-handed neutrino masses can be induced through the non-renormalisable interactions of 27 and $\overline{27}$ of the form $\frac{\kappa_{\alpha\beta}}{M_{Pl}}(27_\alpha \overline{27}_\beta)^2$. If the N_H^c and \overline{N}_H^c components of some extra 27_H and $\overline{27}_H$ representations develop VEVs along the D -flat direction $\langle N_H^c \rangle = \langle \overline{N}_H^c \rangle$ the original gauge symmetry of the rank-6 superstring inspired model with extra $U(1)_\psi$ and $U(1)_\chi$ reduces to $SU(3)_C \times SU(2)_W \times U(1)_Y \times U(1)_N$. In this case the effective mass terms for the right-handed neutrinos are generated automatically if the extra $\overline{27}_H$ -plet couples to the ordinary matter representations

$$\delta W = \frac{\kappa_{ij}}{M_{Pl}}(\overline{27}_H 27_i)(\overline{27}_H 27_j) \quad \implies \quad M_{ij} = \frac{2\kappa_{ij}}{M_{Pl}} \langle \overline{N}_H^c \rangle^2. \quad (17)$$

To get a reasonable pattern for the left-handed neutrino masses and mixing the $U(1)_\psi$ and $U(1)_\chi$ gauge symmetries should be broken down to the $U(1)_N$ one around the Grand Unification or Planck scale. A similar mechanism could be applied for the generation of the μ term discussed earlier. However it is rather difficult to use the same fields N_H^c and \overline{N}_H^c in both cases because the values of the corresponding mass parameters are too different. In order to obtain μ in the TeV range one should assume the existence of additional pair of $N_H^{c'}$ and $\overline{N}_H^{c'}$ which acquire VEVs of order 10^{11} GeV.

2.6 Yukawa couplings in the ESSM

The superpotential (16) of the ESSM involves a lot of new Yukawa couplings in comparison to the SM. But only large Yukawa couplings are significant for the study of the renormalisation group flow and spectrum of new particles which will be analysed in the subsequent sections. The observed mass hierarchy of quarks and charged leptons implies that most of the Yukawa couplings in the SM and MSSM are small. Therefore it is natural to assume some hierarchical structure of the Yukawa interactions of new exotic particles with ordinary quarks and leptons as well. As discussed earlier, without loss of generality we can assume that only the third family Higgs doublets and singlets $S \equiv S_3$, $H_d \equiv H_{13}$, $H_u \equiv H_{23}$ gain VEVs, and furthermore the third family Higgs sector couples most strongly with the third family quarks and leptons. The third family SM singlet field S will also couple to the exotic quarks D_i and \overline{D}_i and $SU(2)$ non-Higgs doublets $H_{1\alpha}$ and $H_{2\alpha}$ ($\alpha = 1, 2$).

Discrete and extended gauge symmetries, which were specified before, do not guarantee the absence of FCNCs in the ESSM. Indeed the considered model contains many $SU(2)$ doublets and exotic quarks which interact with ordinary quarks and charged leptons of different generations. Therefore one may expect that even in the basis of their mass eigenstates the non-diagonal flavour transitions are not forbidden. For example, non-diagonal flavour interactions contribute to the amplitude of $K^0 - \overline{K}^0$ oscillations and

give rise to new channels of muon decay like $\mu \rightarrow e^- e^+ e^-$. To suppress flavour changing processes one can postulate Z_2^H symmetry. If all superfields except H_u , H_d and S are odd under Z_2^H symmetry transformations then only one Higgs doublet H_d interacts with the down-type quarks and charged leptons and only one Higgs doublet H_u couples to up-type quarks while the couplings of all other exotic particles to the ordinary quarks and leptons are forbidden. This eliminates any problems related with the non-diagonal flavour transitions in the considered model.

The most general Z_2^H and gauge invariant part of the ESSM superpotential that describes the interactions of the SM singlet fields S_i with exotic quarks, $SU(2)$ Higgs and non-Higgs doublets can be written as

$$\begin{aligned} \lambda_{ijk} S_i (H_{1j} H_{2k}) + \kappa_{ijk} S_i (D_j \overline{D}_k) \longrightarrow \lambda_i S (H_{1i} H_{2i}) + \kappa_i S (D_i \overline{D}_i) + \\ + f_{\alpha\beta} S_\alpha (H_d H_{2\beta}) + \tilde{f}_{\alpha\beta} S_\alpha (H_{1\beta} H_u), \end{aligned} \quad (18)$$

where $\alpha, \beta = 1, 2$ and $i = 1, 2, 3$. In Eq. (18) we choose the basis of non-Higgs and exotic quark superfields so that the Yukawa couplings of the singlet field S have flavour diagonal structure. Here we define $\lambda \equiv \lambda_3$ and $\kappa \equiv \kappa_3$ ⁴. If λ or κ are large at the Grand Unification scale they affect the evolution of the soft scalar mass m_S^2 of the singlet field S rather strongly resulting in negative values of m_S^2 at low energies that triggers the breakdown of $U(1)_N$ symmetry. The singlet VEV must be large enough to generate sufficiently large masses for the exotic particles to avoid conflict with direct particle searches at present and former accelerators. This also implies that the Yukawa couplings λ_i and κ_i ($i \neq 3$) involving the new exotic particles although small must be large enough. The Yukawa couplings of other SM singlets $f_{\alpha\beta}$ and $\tilde{f}_{\alpha\beta}$ are expected to be considerably less than λ_i and κ_i to ensure that only one singlet field S gains a VEV. At the same time $f_{\alpha\beta}$ and $\tilde{f}_{\alpha\beta}$ cannot be negligibly small because in this case the fermion components of superfields S_1 and S_2 becomes extremely light⁵. The induced masses of singlinos \tilde{S}_1 and \tilde{S}_2 should be larger a few MeV otherwise the extra states could contribute to the expansion rate prior to nucleosynthesis changing nuclear abundances.

The Z_2^H symmetry discussed above forbids all terms in W_1 and W_2 that would allow the exotic quarks to decay. Therefore discrete Z_2^H symmetry can only be approximate. In our model we allow only the third family $SU(2)$ doublets H_d and H_u to have Yukawa couplings to the ordinary quarks and leptons of the order unity. As discussed, this is a self-consistent assumption since the large Yukawa couplings of the third generation (in

⁴Note that κ as defined here in the ESSM refers to the coupling of the singlet S to the third family exotic quarks $D\overline{D}$, and is not related to the κ of the NMSSM which refers to the cubic singlet coupling S^3 which is absent in the ESSM.

⁵When $f_{\alpha\beta}$ and $\tilde{f}_{\alpha\beta}$ vanish singlinos \tilde{S}_1 and \tilde{S}_2 remain massless.

particular, the top–quark Yukawa coupling) provides a radiative mechanism for generating the Higgs VEVs [50] which defines the third family direction. As a consequence the neutral components of H_u and H_d acquire non–zero VEVs inducing the masses of ordinary quarks and leptons. The Yukawa couplings of two other pairs of $SU(2)$ doublets H_{1i} and H_{2i} as well as H' and exotic quarks to the quarks and leptons of the third generation are supposed to be significantly smaller ($\lesssim 0.1$) so that none of the other exotic bosons gain a VEV. These couplings break Z_2^H symmetry explicitly resulting in flavour changing neutral currents. In order to suppress the contribution of new particles and interactions to the $K^0 - \bar{K}^0$ oscillations and to the muon decay channel $\mu \rightarrow e^- e^+ e^-$ in accordance with experimental limits, it is necessary to assume that the Yukawa couplings of exotic particles to the quarks of the first and second generations are less than 10^{-4} and their couplings to the leptons of the first two generations are smaller than 10^{-3} .

3. Renormalisation group analysis

3.1 The approximate superpotential to be studied

Following the discussion about the natural choice of the parameters in our model given at the end of section 2, we can now specify the superpotential couplings whose RG flow will be analysed in this section. In our RG analysis we shall retain only Yukawa couplings which appear on the right–hand side of Eq. (18), together with the $O(1)$ Yukawa couplings to the quarks and leptons. We shall neglect the neutrino Yukawa couplings as well as the small couplings involving the first and second family singlets in our analysis. Then the approximate superpotential studied is given by:

$$W_0 \approx \lambda S(H_d H_u) + \lambda_1 S(H_{1,1} H_{2,1}) + \lambda_2 S(H_{1,2} H_{2,2}) + \kappa S(D_3 \bar{D}_3) + \kappa_1 S(D_1 \bar{D}_1) + \kappa_2 S(D_2 \bar{D}_2) + h_t(H_u Q)t^c + h_b(H_d Q)b^c + h_\tau(H_d L)\tau^c, \quad (19)$$

where all ordinary quark and lepton superfields appeared in Eq. (19) belong to the third generation, i.e. $L = L_3$, $Q = Q_3$, $t^c = u_3^c$, $b^c = d_3^c$ and $\tau^c = e_3^c$. Here we adopt the notation $\lambda = \lambda_3$ and $\kappa = \kappa_3$. The obtained superpotential possesses the approximate Z_2^H symmetry specified in the previous section which ensures the natural suppression of FCNCs. To guarantee that only one pair of $SU(2)$ doublets H_u and H_d acquires a VEV we impose a certain hierarchy between the couplings of H_{1i} and H_{2i} to the SM singlet superfield S : $\lambda \gtrsim \lambda_{1,2}$. We assume further that the superpotential (19) is formed near the Grand Unification or Planck scale. But in order to compute the masses and couplings at the EW scale one has to determine the values of gauge and Yukawa couplings at the EW scale. The evolution of all masses and couplings from M_X to M_Z is described by a

system of RG equations. In this section we study the behaviour of the solutions to such equations describing the gauge and Yukawa couplings in the framework of the ESSM.

3.2 The mixing of $U(1)_Y$ and $U(1)_N$

In this subsection we address a mixing phenomenon related with the gauge sector of models containing two $U(1)$ gauge factors. In the Lagrangian of any gauge extension of the SM containing an additional $U(1)'$ gauge group there can appear a kinetic term consistent with all symmetries which mixes the gauge fields of the $U(1)'$ and $U(1)_Y$ [51]. Our model is not an exception in this respect. In the basis in which the interactions between gauge and matter fields have the canonical form, i.e. for instance a covariant derivative D_μ which acts on the scalar and fermion components of the left-handed quark superfield given by

$$D_\mu = \partial_\mu - ig_3 A_\mu^a T^a - ig_2 W_\mu^b \tau^b - ig_Y Q_i^Y B_\mu^Y - ig_N Q_i^N B_\mu^N, \quad (20)$$

the pure gauge kinetic part of the Lagrangian can be written as

$$\mathcal{L}_{kin} = -\frac{1}{4} (F_{\mu\nu}^Y)^2 - \frac{1}{4} (F_{\mu\nu}^N)^2 - \frac{\sin \chi}{2} F_{\mu\nu}^Y F_{\mu\nu}^N - \frac{1}{4} (G_{\mu\nu})^2 - \frac{1}{4} (W_{\mu\nu})^2. \quad (21)$$

In Eqs. (20)–(21) A_μ^a , W_μ^b , B_μ^Y and B_μ^N represent $SU(3)$, $SU(2)$, $U(1)_Y$ and $U(1)_N$ gauge fields, $G_{\mu\nu}^a$, $W_{\mu\nu}^b$, $F_{\mu\nu}^Y$ and $F_{\mu\nu}^N$ are field strengths for the corresponding gauge interactions, while g_3 , g_2 , g_Y and g_N are $SU(3)$, $SU(2)$, $U(1)_Y$ and $U(1)_N$ gauge couplings respectively.

Because $U(1)_Y$ and $U(1)_N$ arise from the breaking of the simple gauge group E_6 the parameter $\sin \chi$ that parametrises the gauge kinetic term mixing is equal to zero at tree-level. However it arises from loop effects since

$$Tr(Q^Y Q^N) = \sum_{i=\text{chiral fields}} (Q_i^Y Q_i^N) \neq 0. \quad (22)$$

Here the trace is restricted to the states lighter than the energy scale being considered. The complete E_6 multiplets do not contribute to this trace. Its non-zero value is due to the incomplete $27' + \overline{27}'$ multiplets of the original E_6 symmetry from which only H' and \overline{H}' survive to low energy in order to ensure gauge coupling unification.

The mixing in the gauge kinetic part of the Lagrangian (21) can be easily eliminated by means of a non-unitary transformation of the two $U(1)$ gauge fields [26], [52]–[53]:

$$B_\mu^Y = B_{1\mu} - B_{2\mu} \tan \chi, \quad B_\mu^N = B_{2\mu} / \cos \chi. \quad (23)$$

In terms of the new gauge variables $B_{1\mu}$ and $B_{2\mu}$ the gauge kinetic part of the Lagrangian (21) is now diagonal and the covariant derivative (20) becomes [51]

$$D_\mu = \partial_\mu - ig_3 A_\mu^a T^a - ig_2 W_\mu^b \tau^b - ig_1 Q_i^Y B_{1\mu} - i(g_1' Q_i^N + g_{11} Q_i^Y) B_{2\mu}, \quad (24)$$

where the redefined gauge coupling constants, written in terms of the original ones, are

$$g_1 = g_Y, \quad g'_1 = g_N / \cos \chi, \quad g_{11} = -g_Y \tan \chi. \quad (25)$$

In the new Lagrangian written in terms of the new gauge variables $B_{1\mu}$ and $B_{2\mu}$ (defined in Eq. (23)) the mixing effect is concealed in the interaction between the $U(1)_N$ gauge field and matter fields. The gauge coupling constant g'_1 is varied from the original one and also a new off-diagonal gauge coupling g_{11} appears. The covariant derivative (24) can be rewritten in a more compact form

$$D_\mu = \partial_\mu - ig_3 A_\mu^a T^a - ig_2 W_\mu^b \tau^b - iQ^T G B_\mu, \quad (26)$$

where $Q^T = (Q_i^Y, Q_i^N)$, $B_\mu^T = (B_{1\mu}, B_{2\mu})$ and G is a 2×2 matrix of new gauge couplings (25)

$$G = \begin{pmatrix} g_1 & g_{11} \\ 0 & g'_1 \end{pmatrix}. \quad (27)$$

Now all physical phenomena can be considered by using this new Lagrangian with the modified structure of the extra $U(1)_N$ interaction (24)–(26). In the considered approximation the gauge kinetic mixing changes effectively the $U(1)_N$ charges of the fields to

$$\tilde{Q}_i \equiv Q_i^N + Q_i^Y \delta, \quad (28)$$

where $\delta = g_{11}/g'_1$ while the $U(1)_Y$ charges remain the same. As the gauge coupling constants are scale dependent, the effective $U(1)_N$ charges defined here as \tilde{Q}_i are scale dependent as well. The particle spectrum now depends on the effective $U(1)_N$ charges \tilde{Q}_i .

In Eq. (28) the correct E_6 normalisation of the charges should be used, and thus the $U(1)_Y$ hypercharges in Eqs. (7)–(8) should be multiplied by a factor $\sqrt{\frac{3}{5}}$, and the Q^N charges in Eqs. (7)–(8) should be multiplied by $1/\sqrt{40}$. The correctly normalised charges of all the matter fields in the ESSM are summarised in Table 1. The charges are family independent, and the index i here refers to the different multiplets as well as the different families.

3.3 The running of the gauge couplings

At the one-loop level the full set of RG equations describing the running of gauge and Yukawa couplings splits into two parts. One of them includes RG equations for the gauge couplings. In the one-loop approximation β functions of the gauge couplings do not

	Q	u^c	d^c	L	e^c	N^c	S	H_2	H_1	D	\overline{D}	H'	$\overline{H'}$
$\sqrt{\frac{5}{3}}Q_i^Y$	$\frac{1}{6}$	$-\frac{2}{3}$	$\frac{1}{3}$	$-\frac{1}{2}$	1	0	0	$\frac{1}{2}$	$-\frac{1}{2}$	$-\frac{1}{3}$	$\frac{1}{3}$	$-\frac{1}{2}$	$\frac{1}{2}$
$\sqrt{40}Q_i^N$	1	1	2	2	1	0	5	-2	-3	-2	-3	2	-2

Table 1: The $U(1)_Y$ and $U(1)_N$ charges of matter fields in the ESSM, where Q_i^N and Q_i^Y are here defined with the correct E_6 normalisation factor required for the RG analysis.

depend on the Yukawa ones. Therefore this part of the system of RG equations can be analysed separately, and is discussed in this subsection.

The RG flow of the Abelian gauge couplings is affected by the kinetic term mixing as discussed in the previous subsection. Using the matrix notation for the structure of $U(1)$ interactions with G defined in Eq. (27) one can write down the RG equations for the Abelian couplings in a compact form [26], [52]–[53]

$$\frac{dG}{dt} = G \times B, \quad (29)$$

where B is a 2×2 matrix of β functions given by

$$B = \begin{pmatrix} B_1 & B_{11} \\ 0 & B'_1 \end{pmatrix} = \frac{1}{(4\pi)^2} \begin{pmatrix} \beta_1 g_1^2 & 2g_1 g'_1 \beta_{11} + 2g_1 g_{11} \beta_1 \\ 0 & g_1'^2 \beta'_1 + 2g'_1 g_{11} \beta_{11} + g_{11}^2 \beta_1 \end{pmatrix}. \quad (30)$$

In the ESSM with $N_g = 3$ the one-loop β functions β_1 , β'_1 and β_{11} are

$$\beta_1 = \sum_i (Q_i^Y)^2 = \frac{48}{5}, \quad \beta'_1 = \sum_i (Q_i^N)^2 = \frac{47}{5}, \quad \beta_{11} = \sum_i Q_i^Y Q_i^N = \mp \frac{\sqrt{6}}{5}. \quad (31)$$

The index i is summed over all possible chiral superfields and all families. Note that $\beta_1 \approx \beta'_1 \gg \beta_{11}$. This implies that the effect of $U(1)$ gauge mixing is ultimately rather small, and furthermore that, if the (properly normalised) g_Y and g_N start out equal at the GUT scale, then they will remain approximately equal at low energies.

The running of $SU(2)$ and $SU(3)$ couplings obey the RG equations of the standard form:

$$\frac{dg_2}{dt} = \frac{\beta_2 g_2^3}{(4\pi)^2}, \quad \frac{dg_3}{dt} = \frac{\beta_3 g_3^3}{(4\pi)^2}, \quad (32)$$

with β functions

$$\beta_2 = -5 + 3N_g, \quad \beta_3 = -9 + 3N_g, \quad (33)$$

where $t = \ln(\mu/M_X)$ and μ is the RG scale. The parameter N_g appeared in the expressions for β_2 and β_3 is the number of generations forming E_6 fundamental representations which the considered SUSY model involves at low energies. As one can easily see from Eq. (33) $N_g = 3$ is the critical value for the one-loop β function of strong interactions. Since by

construction three complete 27-plets survive to low energies in the ESSM β_3 is equal to zero in our case and $SU(3)$ gauge coupling remains constant everywhere from M_Z to M_X . Because complete 27-plets do not violate E_6 symmetry each generation should give the same contribution to all β functions. It takes place automatically in the case of $SU(2)$ and $SU(3)$ β functions and allows to obtain a correct normalisation for the charges of two $U(1)$'s.

The RG equations for the gauge couplings in Eqs. (29) and (32) should be supplemented by the boundary conditions. Since we deal with an E_6 inspired model it seems to be natural to assume that at high energies E_6 symmetry is restored and all gauge interactions are characterised by a unique E_6 gauge coupling g_0 which is defined as

$$g_3(M_X) = g_2(M_X) = g_1(M_X) = g'_1(M_X) = g_0. \quad (34)$$

Also we expect that there is no mixing in the gauge kinetic part of the Lagrangian just after the breakdown of the E_6 symmetry, i.e.

$$g_{11}(M_X) = 0. \quad (35)$$

The hypothesis of gauge coupling unification (34) permits to evaluate the overall gauge coupling g_0 and the Grand Unification scale M_X using the values of $g_1(M_Z)$, $g_2(M_Z)$ and $g_3(M_Z)$ which are fixed by LEP measurements and other experimental data [54]. The high energy scale where the unification of the gauge couplings takes place is almost insensitive to the matter content of the supersymmetric model. Indeed, in the one-loop approximation we have

$$\frac{1}{(4\pi)^2} \ln \frac{M_X^2}{M_Z^2} = \frac{1}{\beta_1 - \beta_2} \left[\frac{1}{g_1^2(M_Z^2)} - \frac{1}{g_2^2(M_Z^2)} \right]. \quad (36)$$

Because the dependence of the scale M_X , where $U(1)_Y$ and $SU(2)$ gauge couplings meet, on the particle content of any model comes from the difference of the corresponding β functions, in which the contribution of any complete $SU(5)$ multiplets is cancelled, the Grand Unification scale in the ESSM remains the same as in the MSSM, i.e in the one-loop approximation $M_X \simeq 2 \cdot 10^{16}$ GeV. At the same time the value of the overall gauge coupling is rather sensitive to the matter content of SUSY models. In the ESSM the appropriate values of the $SU(2)$, $SU(3)$ and $U(1)_Y$ gauge couplings at the EW scale can be reproduced for $g_0 \simeq 1.21$ which differs from the value of $g_0 \simeq 0.72$ found in the minimal SUSY model. The growth of g_0 in our model is caused by the extra exotic supermultiplets of matter.

The interesting point concerning the matter content in our model is that β_1 , β'_1 , β_2 and β_3 are quite close to their saturation limits when the gauge couplings blow up at the Grand Unification scale. The ESSM allows to accommodate only one additional pair of

$5 + \bar{5}$ representations of the usual $SU(5)$ which form extra exotic quark and non-Higgs multiplets. Further enlargement of the particle content leads to the appearance of the Landau pole during the evolution of the gauge couplings from M_Z to M_X .

Using the boundary conditions (34) and (35) as well as the obtained values of g_0 and M_X it is possible to solve the RG equations for g'_1 and g_{11} . It turns out that $g'_1(Q)$ is very close to $g_1(Q)$ for any value of renormalisation scale Q from M_X to M_Z while $g_{11}(Q)$ is negligibly small compared to all other gauge couplings. At the EW scale we get

$$\frac{g_1(M_Z)}{g'_1(M_Z)} \simeq 0.99, \quad g_{11}(M_Z) \simeq 0.020, \quad g_1(M_Z) \simeq 0.46. \quad (37)$$

Eq. (37) tells us that if the (properly normalised) g_Y and g_N couplings start out equal at the GUT scale, then they will remain approximately equal at low energies to within an accuracy of two per cent at the one-loop level. As previously noted, this results from $\beta_1 \approx \beta'_1 \gg \beta_{11}$ which implies that the effect of $U(1)$ gauge mixing is small. In the following analysis we shall continue to include the effects of $U(1)$ gauge mixing in the correct way. However, it should be noted that to excellent approximation we could take $g_1 = g'_1 = g_Y = g_N$ and $\tilde{Q}_i = Q_i^N$, which is within the accuracy of the one-loop result.

3.4 The running of the Yukawa couplings

The running of the Yukawa couplings appearing in the superpotential in Eq. (19) obey the following system of differential equations⁶:

$$\begin{aligned} \frac{dh_t}{dt} &= \frac{h_t}{(4\pi)^2} \left[\lambda^2 + 6h_t^2 + h_b^2 - \frac{16}{3}g_3^2 - 3g_2^2 - \frac{13}{15}g_1^2 - 2 \left(\tilde{Q}_2^2 + \tilde{Q}_Q^2 + \tilde{Q}_u^2 \right) g_1'^2 \right], \\ \frac{dh_b}{dt} &= \frac{h_b}{(4\pi)^2} \left[\lambda^2 + h_t^2 + 6h_b^2 + h_\tau^2 - \frac{16}{3}g_3^2 - 3g_2^2 - \frac{7}{15}g_1^2 - 2 \left(\tilde{Q}_1^2 + \tilde{Q}_Q^2 + \tilde{Q}_d^2 \right) g_1'^2 \right], \\ \frac{dh_\tau}{dt} &= \frac{h_\tau}{(4\pi)^2} \left[\lambda^2 + 3h_b^2 + 4h_\tau^2 - 3g_2^2 - \frac{9}{5}g_1^2 - 2 \left(\tilde{Q}_1^2 + \tilde{Q}_L^2 + \tilde{Q}_e^2 \right) g_1'^2 \right], \\ \frac{d\lambda_i}{dt} &= \frac{\lambda_i}{(4\pi)^2} \left[2\lambda_i^2 + 2\Sigma_\lambda + 3\Sigma_\kappa + (3h_t^2 + 3h_b^2 + h_\tau^2)\delta_{i3} - \right. \\ &\quad \left. - 3g_2^2 - \frac{3}{5}g_1^2 - 2 \left(\tilde{Q}_S^2 + \tilde{Q}_2^2 + \tilde{Q}_1^2 \right) g_1'^2 \right], \\ \frac{d\kappa_i}{dt} &= \frac{\kappa_i}{(4\pi)^2} \left[2\kappa_i^2 + 2\Sigma_\lambda + 3\Sigma_\kappa - \frac{16}{3}g_3^2 - \frac{4}{15}g_1^2 - 2 \left(\tilde{Q}_S^2 + \tilde{Q}_D^2 + \tilde{Q}_\bar{D}^2 \right) g_1'^2 \right], \end{aligned} \quad (38)$$

where $\Sigma_\lambda = \lambda_1^2 + \lambda_2^2 + \lambda_3^2$ and $\Sigma_\kappa = \kappa_1^2 + \kappa_2^2 + \kappa_3^2$ and where the index $i = 1, 2, 3$.

The couplings h_t , h_b and h_τ in Eq. (38) determine the running masses of the fermions of the third generation at the EW scale

$$m_t(M_t) = \frac{h_t(M_t)v}{\sqrt{2}} \sin \beta, \quad m_b(M_t) = \frac{h_b(M_t)v}{\sqrt{2}} \cos \beta, \quad m_\tau(M_t) = \frac{h_\tau(M_t)v}{\sqrt{2}} \cos \beta, \quad (39)$$

⁶See also [25]–[26].

which are generated after EWSB. In Eq. (39) m_τ , m_t and m_b are the running masses of the τ -lepton, top- and bottom-quark respectively, M_t is a top quark pole mass, $v = \sqrt{v_1^2 + v_2^2} = 246 \text{ GeV}$, while $\tan \beta = v_2/v_1$, where v_2 and v_1 are the VEVs of the Higgs doublets H_u and H_d . Since the running masses of the fermions of the third generation are known, Eq. (39) can be used to derive the Yukawa couplings $h_\tau(M_t)$, $h_t(M_t)$ and $h_b(M_t)$ for each particular value of $\tan \beta$ establishing boundary conditions for the renormalisation group equations (38). In this paper we restrict our analysis to moderate values of $\tan \beta \ll m_t(M_t)/m_b(M_t)$ for which b -quark and τ -lepton Yukawa couplings are much smaller than h_t and thus can be safely neglected.

The boundary conditions for the Yukawa couplings of the SM singlet field S to the Higgs doublets and exotic particles are unknown. These couplings give rise to the masses of the exotic quarks and non-Higgsinos after the breakdown of gauge symmetry. Since none of the exotic particles or Higgs bosons have been found yet λ_i and κ_i should be considered as free parameters in our model. There are two different assumptions regarding these couplings that look rather natural and allow one to reduce the number of new parameters. One of them implies that the masses of the exotic particles mimic the hierarchy observed in the sector of ordinary quarks and charged leptons. Then non-observation of new exotic states may be related with the considerable hierarchy of VEVs of the singlet field S and Higgs doublets. In this case λ_1 , λ_2 , κ_1 and κ_2 are tiny and can be simply ignored.

Although the suggested pattern is quite simple and natural it does not permit to tell anything about the masses of the exotic particles of the first two generations because the corresponding Yukawa couplings are set to zero from the beginning. In the meantime one has to ensure that exotic fermions gain large enough masses to avoid any conflict with direct new particle searches at present and former colliders. Therefore it is worth to incorporate all Yukawa couplings of exotic particles to the SM singlet field S in our analysis of RG flow. Because the Yukawa interactions of extra coloured singlets D_i and \overline{D}_i in the superpotential (19) and as a consequence the corresponding RG equations are symmetric with respect to the generation index i exchange, i.e. $1 \leftrightarrow 2$, $2 \leftrightarrow 3$ and $3 \leftrightarrow 1$, there is a solution of the RG equations when all κ_i are equal to each other. Moreover the solutions for $\kappa_i(Q)$ tend to converge to each other during the evolution of these couplings from the Grand Unification to EW scale. Thus the choice $\kappa_1(M_t) = \kappa_2(M_t) = \kappa(M_t)$ is well motivated by the RG flow.

Similar results can be obtained for λ_1 and λ_2 . However the running of $\lambda_1(Q) = \lambda_2(Q)$ differs from the evolution of $\lambda(Q)$ because the top-quark and its superpartners give significant contributions to the renormalisation of $\lambda(Q)$. Nevertheless the difference between the RG flow of $\lambda_1(Q) = \lambda_2(Q)$ and $\lambda(Q)$ is not so appreciable in comparison with the running of $\kappa_i(Q)$ and $h_t(Q)$. The couplings of the Yukawa interactions involving quark

superfields renormalise by virtue of the strong interactions that push their values up considerably at low energies. Therefore it seems to be reasonable to ignore the difference between the evolution of $\lambda_i(Q)$ in first approximation and consider separately the limit in which $\lambda_1(M_t) = \lambda_2(M_t) = \lambda(M_t)$.

At first we consider the limit when the Yukawa couplings of the exotic quarks and non-Higgses of the first two generation are negligibly small. Then the system of the RG equations can be rewritten in the suggestive form

$$\begin{aligned} 8\pi^2 \frac{d}{dt} \left[\frac{\lambda^2}{h_t^2} \right] &= \left(3\lambda^2 + 3\kappa^2 - 3h_t^2 + \frac{16}{3}g_3^2 + \frac{4}{15}g_1^2 + \right. \\ &\quad \left. + 2(\tilde{Q}_Q^2 + \tilde{Q}_u^2 - \tilde{Q}_S^2 - \tilde{Q}_1^2) \right) \left[\frac{\lambda^2}{h_t^2} \right], \\ 8\pi^2 \frac{d}{dt} \left[\frac{\kappa^2}{h_t^2} \right] &= \left(5\kappa^2 + \lambda^2 - 6h_t^2 + 3g_2^2 + \frac{3}{5}g_1^2 + \right. \\ &\quad \left. + 2(\tilde{Q}_2^2 + \tilde{Q}_Q^2 + \tilde{Q}_u^2 - \tilde{Q}_S^2 - \tilde{Q}_D^2 - \tilde{Q}_{\bar{D}}^2) \right) \left[\frac{\kappa^2}{h_t^2} \right]. \end{aligned} \quad (40)$$

If we ignore gauge couplings the system of differential equations (40) has two fixed points

$$\begin{aligned} (I) \quad & \frac{\lambda^2}{h_t^2} = 1, \quad \frac{\kappa^2}{h_t^2} = 0; \\ (II) \quad & \frac{\lambda^2}{h_t^2} = 0, \quad \frac{\kappa^2}{h_t^2} = \frac{6}{5}. \end{aligned} \quad (41)$$

Of these fixed points only the last one is infrared stable. The presence of the infrared stable fixed point (II) means that if we start with random boundary conditions for the couplings λ , κ and h_t in the gaugeless ($g_0 = 0$) limit the solutions of the RG equations (40) tend to converge towards the values which respect the ratios (II). This is illustrated in Fig. 1a where the running λ/h_t versus κ/h_t for $h_t(M_X) = 10$, $g_0 = 0$ and regular distribution of boundary conditions for $\lambda(M_X)$ and $\kappa(M_X)$ at the Grand Unification scale is shown. A point in the plane $\lambda/h_t - \kappa/h_t$ will flow rapidly towards the valley, that corresponds to the invariant line which connects fixed points (I) and (II), and then more slowly along it to the stable fixed point (II). The properties of invariant lines and surfaces were reviewed in detail in [55].

So far we have neglected the effects of gauge couplings. However their role is quite important especially at low energies where the gauge coupling of the strong interactions is larger than the Yukawa ones. As one can see from Fig. 1b the inclusion of gauge couplings spoils the valley along which the solutions of RG equations flow to the fixed points (II). But the convergence of $h_t(Q)$, $\lambda(Q)$ and $\kappa(Q)$ to the quasi-fixed point, which becomes more close to unity, increases.

Similar analysis can be performed in the case when all Yukawa couplings of exotic particles have non-zero values. As before in the gaugeless limit there is only one stable fixed point of the RG equations (38) which corresponds to

$$\frac{\lambda^2}{h_t^2} = 0, \quad \frac{\kappa^2}{h_t^2} = \frac{\kappa_{1,2}^2}{h_t^2} = \frac{\lambda_{1,2}^2}{h_t^2} = \frac{2}{5}. \quad (42)$$

Turning the gauge couplings on induces a certain hierarchy between the Yukawa couplings of exotic quarks and non-Higgses. Due to the growth of the gauge coupling of strong interactions at low energies the Yukawa couplings of the top- and exotic quarks tend to dominate over λ_i . It shifts the position of the quasi-fixed point where the solutions of the RG equations are focused

$$\frac{\lambda^2}{h_t^2} \rightarrow 0, \quad \frac{\lambda_{1,2}^2}{h_t^2} \simeq 0.26, \quad \frac{\kappa^2}{h_t^2} = \frac{\kappa_{1,2}^2}{h_t^2} \simeq 0.66. \quad (43)$$

In spite of their attractiveness fixed points cannot provide a complete description of the RG flow of Yukawa couplings. Indeed, the strength of the attraction of the solutions to the RG equations (41) towards the invariant line and fixed point is governed by $h_t(M_X)$. The larger $h_t(M_X)$ the faster the stable fixed point is reached. However at small values of $h_t(M_X) = 0.2 - 0.4$ the convergence of $h_t(Q)$, $\lambda(Q)$ and $\kappa(Q)$ to the fixed points is extremely weak. Therefore even at moderate values of $\tan \beta = 1.5 - 3$ the values of the Yukawa couplings at the EW scale may be far away from the stable fixed point.

In this context it is worth to study the limits on the values of the Yukawa couplings imposed by the perturbative RG flow. The growth of Yukawa couplings at the EW scale entails the increase of their values at the Grand Unification scale resulting in the appearance of the Landau pole. Large values of the Yukawa couplings spoil the applicability of perturbation theory at high energies so that the one-loop RG equations cannot be used for an adequate description of the evolution of gauge and Yukawa couplings at high scales $Q \sim M_X$. The requirement of validity of perturbation theory up to the Grand Unification scale restricts the interval of variations of Yukawa couplings at the EW scale. In the simplest case when $\kappa_1 = \kappa_2 = \lambda_1 = \lambda_2 = 0$ the assumption that perturbative physics continues up to the scale M_X sets an upper limit on the low energy value of $\kappa(M_t)$, evaluated at the top mass M_t , for each fixed set of $\lambda(M_t)$ and $h_t(M_t)$ (or $\tan \beta$). With decreasing (increasing) $\lambda(M_t)$ the maximal possible value of $\kappa(M_t)$, which is consistent with perturbative gauge coupling unification, increases (decreases) forming a demarcating line that restricts the allowed range of the parameter space in the $\kappa/h_t - \lambda/h_t$ plane for each particular value of $\tan \beta$.

For $\tan \beta = 2$ the corresponding limits on the low energy Yukawa couplings evaluated at M_t are shown in Fig. 2a. Outside the permitted region the solutions of the RG equations blow up before the Grand Unification scale and perturbation theory is not valid at high

energies. The allowed range for the Yukawa couplings varies when $\tan\beta$ changes. When $\tan\beta$ tends to its lower bound caused by the applicability of perturbation theory, which is around unity in our model, the permitted part of the parameter space narrows in the direction of λ/h_t so that only a small interval of variations of λ/h_t is allowed. At large $\tan\beta$ the allowed range for the Yukawa couplings enlarges. The typical pattern of the RG flow of the ratios of Yukawa couplings from the permitted region of the parameter space is presented in Fig. 2b. It differs significantly from the analogous pattern obtained in the top-bottom approach (see Fig. 1) because the chosen value of top-quark Yukawa coupling, which corresponds to $\tan\beta = 2$, is quite far from the quasi-fixed point. The peculiar feature of both patterns is that the ratio of λ/h_t changes during the evolution more strongly than κ/h_t . Owing to this most trajectories in Fig. 2b are almost parallel to the axis λ/h_t .

A similar pattern for the RG flow can be found for most values of $\tan\beta$ and does not change much after the inclusion of the Yukawa couplings of exotic particles of the first two generations. But the introduction of κ_1 , κ_2 , λ_1 and λ_2 makes more rigorous the restrictions on the Yukawa couplings of the third generation. In Fig. 2c we plot the allowed range of the Yukawa couplings in the case when λ_1 and λ_2 are still negligibly small while $\kappa = \kappa_1 = \kappa_2$. It is easy to see that in this case the upper bounds on κ/h_t are more stringent than in Fig. 2a. Turning λ_1 and λ_2 on so that $\lambda(M_t) = \lambda_1(M_t) = \lambda_2(M_t)$ reduces the limit on λ/h_t (see Fig. 2d). The narrowing of the allowed range of the parameter space is not an unexpected effect. New Yukawa couplings appear in the right-hand side of the differential equations (38) with positive sign. As a consequence they increase the growth of the Yukawa couplings of the third generation and perturbation theory becomes inapplicable for lower values of $\lambda(M_t)$ and $\kappa(M_t)$.

Because the allowed range of the Yukawa couplings always shrinks when additional Yukawa couplings are introduced one can find an absolute upper limit on the value of $\lambda(M_t)$ as function of $h_t(M_t)$ or $\tan\beta$ by setting all other Yukawa couplings to zero. The dependence of this upper limit λ_{\max} on $\tan\beta$ is shown in Fig. 3. The upper bound on $\lambda(M_t)$ grows with increasing $\tan\beta$ because the top-quark Yukawa coupling decreases. The value of λ_{\max} vanishes at $\tan\beta \simeq 1$ when the top-quark Yukawa coupling attains a fixed point (see also Fig. 1b). At large $\tan\beta$ the upper bound on $\lambda(M_t)$ approaches the saturation limit where $\lambda_{\max} \simeq 0.84$. The restrictions on $\lambda(M_t)$ and other Yukawa couplings obtained in this section are extremely useful for the analysis of the Higgs particle spectrum which we are going to consider next.

4. Electroweak symmetry breaking and Higgs sector

4.1 The Higgs potential and its minimisation

The sector responsible for EWSB in the ESSM includes two Higgs doublets H_u and H_d as well as the SM singlet field S . The interactions between them are defined by the structure of the gauge interactions and by the superpotential in Eq. (19). Including soft SUSY breaking terms, and radiative corrections, the resulting Higgs effective potential is the sum of four pieces:

$$\begin{aligned}
V &= V_F + V_D + V_{soft} + \Delta V, \\
V_F &= \lambda^2 |S|^2 (|H_d|^2 + |H_u|^2) + \lambda^2 |(H_d H_u)|^2, \\
V_D &= \frac{g_2^2}{8} (H_d^\dagger \sigma_a H_d + H_u^\dagger \sigma_a H_u)^2 + \frac{g'^2}{8} (|H_d|^2 - |H_u|^2)^2 + \\
&\quad + \frac{g_1'^2}{2} (\tilde{Q}_1 |H_d|^2 + \tilde{Q}_2 |H_u|^2 + \tilde{Q}_S |S|^2)^2, \\
V_{soft} &= m_S^2 |S|^2 + m_1^2 |H_d|^2 + m_2^2 |H_u|^2 + \left[\lambda A_\lambda S (H_u H_d) + h.c. \right],
\end{aligned} \tag{44}$$

where $g' = \sqrt{3/5}g_1$ is the low energy (non-GUT normalised) gauge coupling and \tilde{Q}_1 , \tilde{Q}_2 and \tilde{Q}_S are effective $U(1)_N$ charges of H_d , H_u and S respectively. Here $H_d^T = (H_d^0, H_d^-)$, $H_u^T = (H_u^+, H_u^0)$ and $(H_d H_u) = H_u^+ H_d^- - H_u^0 H_d^0$. At tree-level the Higgs potential in Eq. (44) is described by the sum of the first three terms. The structure of the F -terms V_F is exactly the same as in the NMSSM without the self-interaction of the singlet superfield. However the D -terms in V_D contain a new ingredient: the terms in the expression for V_D proportional to $g_1'^2$ represent D -term contributions due to the extra $U(1)_N$ which are not present in the MSSM or NMSSM. The soft SUSY breaking terms are collected in V_{soft} .

The term ΔV represents the contribution of loop corrections to the Higgs effective potential. In the MSSM the dominant contribution to ΔV comes from the loops involving the top-quark and its superpartners because of their large Yukawa coupling. However the ESSM contains many new exotic supermultiplets and the RG analysis described in the previous section revealed that the Yukawa couplings of the exotic D -quarks to the SM singlet field S can be large at the EW scale. Therefore the contribution of D -quarks and their superpartners to ΔV can be enhanced as well. Keeping only leading one-loop corrections to the Higgs effective potential in Eq. (44) from the top- and exotic quarks and their superpartners we find

$$\Delta V = \frac{3}{32\pi^2} \left[m_{\tilde{t}_1}^4 \left(\ln \frac{m_{\tilde{t}_1}^2}{Q^2} - \frac{3}{2} \right) + m_{\tilde{t}_2}^4 \left(\ln \frac{m_{\tilde{t}_2}^2}{Q^2} - \frac{3}{2} \right) - 2m_t^4 \left(\ln \frac{m_t^2}{Q^2} - \frac{3}{2} \right) + \right. \tag{45}$$

$$+ \sum_{i=1,2,3} \left\{ m_{\tilde{D}_{1,i}}^4 \left(\ln \frac{m_{\tilde{D}_{1,i}}^2}{Q^2} - \frac{3}{2} \right) + m_{\tilde{D}_{2,i}}^4 \left(\ln \frac{m_{\tilde{D}_{2,i}}^2}{Q^2} - \frac{3}{2} \right) - 2\mu_{D_i}^4 \left(\ln \frac{\mu_{D_i}^2}{Q^2} - \frac{3}{2} \right) \right\},$$

where $\mu_{D_i} = \kappa_i < S > = \frac{\kappa_i S}{\sqrt{2}}$ are masses of exotic quarks, while $m_{\tilde{t}_1}$, $m_{\tilde{t}_2}$, $m_{\tilde{D}_{1,i}}$ and $m_{\tilde{D}_{2,i}}$ are the masses of the superpartners of the top and D -quarks which are given by

$$\begin{aligned} m_{\tilde{t}_1, \tilde{t}_2}^2 &= \frac{1}{2} \left[m_Q^2 + m_U^2 + 2 + 2m_t^2 \pm \sqrt{(m_Q^2 - m_U^2)^2 + 4m_t^2 \left(A_t - \frac{\lambda s}{\sqrt{2} \tan \beta} \right)^2} \right], \\ m_{\tilde{D}_{1,i}, \tilde{D}_{2,i}}^2 &= \frac{1}{2} \left[m_{D_i}^2 + m_{\tilde{D}_i}^2 + 2\mu_{D_i}^2 \pm \sqrt{(m_{D_i}^2 - m_{\tilde{D}_i}^2)^2 + 4 \left(A_{\kappa i} \mu_{D_i} - \frac{\kappa_i \lambda}{2} v_1 v_2 \right)^2} \right]. \end{aligned} \quad (46)$$

The couplings g_2 , g' , g'_1 and λ in the scalar potential (44) do not violate SUSY. Moreover the gauge couplings g_2 and g' are well known [54]. The value of the extra $U(1)_N$ coupling g'_1 and the effective $U(1)_N$ charges of H_d , H_u and S can be determined assuming gauge coupling unification (see Eq. (37)). The Yukawa coupling λ cannot be fixed as directly as the gauge couplings. But as we discussed in the previous section the requirement of validity of perturbation theory up to the GUT scale leads to an upper bound $\lambda \leq \lambda_{\max}$.

A set of soft SUSY breaking parameters in the tree-level Higgs boson potential includes the soft masses m_1^2 , m_2^2 , m_3^2 and the trilinear coupling A_λ . The part of the scalar potential (44) which contains soft SUSY breaking terms V_{soft} coincides with the corresponding one in the NMSSM when the NMSSM parameters κ and A_κ vanish. Since the only complex phase (of λA_λ) that appears in the tree-level scalar potential (44) can easily be absorbed by a suitable redefinition of the Higgs fields, CP-invariance is preserved in the Higgs sector of the considered model at tree-level. The inclusion of loop corrections draws into the analysis many other soft SUSY breaking parameters which define masses of different superparticles. Some of these parameters can be complex creating potential sources of CP-violation.

At the physical minimum of the scalar potential (44) the Higgs fields develop VEVs

$$< H_d > = \frac{1}{\sqrt{2}} \begin{pmatrix} v_1 \\ 0 \end{pmatrix}, \quad < H_u > = \frac{1}{\sqrt{2}} \begin{pmatrix} 0 \\ v_2 \end{pmatrix}, \quad < S > = \frac{s}{\sqrt{2}}. \quad (47)$$

The vacuum configuration (47) is not the most general one. Because of the $SU(2)$ invariance of the Higgs potential (44) one can always make $< H_u^+ > = 0$ by virtue of a suitable gauge rotation. Then the requirement $< H_d^- > = 0$, which is a necessary condition to preserve $U(1)_{em}$ associated with electromagnetism in the physical vacuum, is equivalent to requiring the squared mass of the physical charged scalar to be positive. It imposes additional constraints on the parameter space of the model.

The equations for the extrema of the Higgs boson potential in the directions (47) in field space read:

$$\begin{aligned}
\frac{\partial V}{\partial s} &= m_S^2 s - \frac{\lambda A_\lambda}{\sqrt{2}} v_1 v_2 + \frac{\lambda^2}{2} (v_1^2 + v_2^2) s + \\
&\quad + \frac{g_1'^2}{2} \left(\tilde{Q}_1 v_1^2 + \tilde{Q}_2 v_2^2 + \tilde{Q}_S s^2 \right) \tilde{Q}_S s + \frac{\partial \Delta V}{\partial s} = 0, \\
\frac{\partial V}{\partial v_1} &= m_1^2 v_1 - \frac{\lambda A_\lambda}{\sqrt{2}} s v_2 + \frac{\lambda^2}{2} (v_2^2 + s^2) v_1 + \frac{\bar{g}^2}{8} (v_1^2 - v_2^2) v_1 + \\
&\quad + \frac{g_1'^2}{2} \left(\tilde{Q}_1 v_1^2 + \tilde{Q}_2 v_2^2 + \tilde{Q}_S s^2 \right) \tilde{Q}_1 v_1 + \frac{\partial \Delta V}{\partial v_1} = 0, \\
\frac{\partial V}{\partial v_2} &= m_2^2 v_2 - \frac{\lambda A_\lambda}{\sqrt{2}} s v_1 + \frac{\lambda^2}{2} (v_1^2 + s^2) v_2 + \frac{\bar{g}^2}{8} (v_2^2 - v_1^2) v_2 + \\
&\quad + \frac{g_1'^2}{2} \left(\tilde{Q}_1 v_1^2 + \tilde{Q}_2 v_2^2 + \tilde{Q}_S s^2 \right) \tilde{Q}_2 v_2 + \frac{\partial \Delta V}{\partial v_2} = 0,
\end{aligned} \tag{48}$$

where $\bar{g} = \sqrt{g_2^2 + g'^2}$. Instead of v_1 and v_2 it is more convenient to use $\tan \beta$ and v defined above. To simplify the analysis of the Higgs spectrum it is worth to express the soft masses m_1^2 , m_2^2 , m_S^2 in terms of s , v , $\tan \beta$ and other parameters. Because from precision measurements we know that $v = 246 \text{ GeV}$ the tree-level Higgs masses and couplings depend on four variables only:

$$\lambda, \quad s, \quad \tan \beta, \quad A_\lambda. \tag{49}$$

4.2 Z - Z' mixing

Initially the sector of EWSB involves ten degrees of freedom. However four of them are massless Goldstone modes which are swallowed by the W^\pm , Z and Z' gauge bosons. The charged W^\pm bosons gain masses via the interaction with the neutral components of the Higgs doublets just in the same way as in the MSSM so that $M_W = \frac{g_2}{2} v$. Meanwhile the mechanism of the neutral gauge boson mass generation differs significantly. Letting Z' be the gauge boson associated with $U(1)_N$, i.e.

$$Z'_\mu = B_{2\mu}, \quad Z_\mu = W_\mu^3 \cos \theta_W - B_{1\mu} \sin \theta_W, \tag{50}$$

the $Z - Z'$ mass squared matrix is given by

$$M_{ZZ'}^2 = \begin{pmatrix} M_Z^2 & \Delta^2 \\ \Delta^2 & M_{Z'}^2 \end{pmatrix}, \tag{51}$$

where

$$\begin{aligned}
M_Z^2 &= \frac{\bar{g}^2}{4} v^2, & \Delta^2 &= \frac{\bar{g} g_1'}{2} v^2 \left(\tilde{Q}_1 \cos^2 \beta - \tilde{Q}_2 \sin^2 \beta \right), \\
M_{Z'}^2 &= g_1'^2 v^2 \left(\tilde{Q}_1^2 \cos^2 \beta + \tilde{Q}_2^2 \sin^2 \beta \right) + g_1'^2 \tilde{Q}_S^2 s^2.
\end{aligned} \tag{52}$$

The eigenvalues of this matrix are

$$M_{Z_1, Z_2}^2 = \frac{1}{2} \left[M_Z^2 + M_{Z'}^2 \mp \sqrt{(M_Z^2 - M_{Z'}^2)^2 + 4\Delta^4} \right]. \quad (53)$$

The eigenvalues $M_{Z_1}^2$ and $M_{Z_2}^2$ correspond to the mass eigenstates Z_1 and Z_2 which are linear superpositions of Z and Z'

$$\begin{aligned} Z_1 &= Z \cos \alpha_{ZZ'} + Z' \sin \alpha_{ZZ'}, & Z_2 &= -Z \sin \alpha_{ZZ'} + Z' \cos \alpha_{ZZ'}, \\ \alpha_{ZZ'} &= \frac{1}{2} \arctan \left(\frac{2\Delta^2}{M_{Z'}^2 - M_Z^2} \right). \end{aligned} \quad (54)$$

Phenomenological constraints typically require the mixing angle $\alpha_{ZZ'}$ to be less than $2 - 3 \times 10^{-3}$ [56] and the mass of the extra neutral gauge boson to be heavier than $500 - 600 \text{ GeV}$ [57]. A suitable mass hierarchy and mixing between Z and Z' are maintained if the field S acquires a large VEV $s \gtrsim 1.5 \text{ TeV}$. Then the mass of the lightest neutral gauge boson Z_1 is very close to M_Z whereas the mass of Z_2 is set by the VEV of the singlet field $M_{Z_2} \simeq M_{Z'} \approx g'_1 \tilde{Q}_S s$.

4.3 Charged Higgs

Due to electric-charge conservation the charged components of the Higgs doublets are not mixed with neutral Higgs fields. They form a separate sector whose spectrum is described by a 2×2 mass matrix. Its determinant has zero value leading to the appearance of two Goldstone states

$$G^- = H_d^- \cos \beta - H_u^{+*} \sin \beta, \quad (55)$$

which are absorbed into the longitudinal degrees of freedom of the W^\pm gauge boson. Their orthogonal linear combination

$$H^+ = H_d^{-*} \sin \beta + H_u^+ \cos \beta \quad (56)$$

gains mass

$$m_{H^\pm}^2 = \frac{\sqrt{2}\lambda A_\lambda}{\sin 2\beta} s - \frac{\lambda^2}{2} v^2 + \frac{g^2}{2} v^2 + \Delta_\pm. \quad (57)$$

In the leading one-loop approximation the corrections to the charged Higgs boson mass Δ_\pm in the ESSM are almost the same as in the MSSM where the parameter μ has to be replaced by $\frac{\lambda s}{\sqrt{2}}$. The explicit expressions for the leading one-loop corrections to $m_{H^\pm}^2$ in the MSSM can be found in [58].

4.4 CP-odd Higgs

The imaginary parts of the neutral components of the Higgs doublets and imaginary part of the SM singlet field S compose the CP-odd (or pseudoscalar) Higgs sector of the considered model. This sector includes two Goldstone modes G_0, G' which are swallowed by the Z and Z' bosons after EWSB, leaving only one physical CP-odd Higgs state A . In the field basis (A, G', G_0) one has

$$\begin{aligned} A &= P_S \sin \varphi + P \cos \varphi, \\ G' &= P_S \cos \varphi - P \sin \varphi, \\ G_0 &= \sqrt{2}(Im H_d^0 \cos \beta - Im H_u^0 \sin \beta), \end{aligned} \tag{58}$$

where

$$\begin{aligned} P &= \sqrt{2}(Im H_d^0 \sin \beta + Im H_u^0 \cos \beta), \\ P_S &= \sqrt{2}Im S, \quad \tan \varphi = \frac{v}{2s} \sin 2\beta. \end{aligned} \tag{59}$$

Two massless pseudoscalars G_0 and G' decouple from the rest of the spectrum whereas the physical CP-odd Higgs boson A acquires mass

$$m_A^2 = \frac{\sqrt{2}\lambda A_\lambda}{\sin 2\varphi} v + \Delta_A, \tag{60}$$

where Δ_A is the contribution of loop corrections. In the leading one-loop approximation the expressions for the mass of the pseudoscalar Higgs boson in the ESSM and PQ symmetric NMSSM coincide. The CP-odd Higgs sector of the NMSSM and one-loop corrections to it were studied in [59]. In phenomenologically acceptable models, in which the singlet VEV is much larger than v , φ goes to zero and the physical pseudoscalar is predominantly the superposition of the imaginary parts of the neutral components of the Higgs doublets, i.e. P .

4.5 CP-even Higgs

The CP-even Higgs sector involves $Re H_d^0$, $Re H_u^0$ and $Re S$. In the field space basis (h, H, N) rotated by an angle β with respect to the initial one

$$\begin{aligned} Re H_d^0 &= (h \cos \beta - H \sin \beta + v_1)/\sqrt{2}, \\ Re H_u^0 &= (h \sin \beta + H \cos \beta + v_2)/\sqrt{2}, \\ Re S &= (s + N)/\sqrt{2}, \end{aligned} \tag{61}$$

the mass matrix of the Higgs scalars takes the form [60]:

$$M^2 = \begin{pmatrix} \frac{\partial^2 V}{\partial v^2} & \frac{1}{v} \frac{\partial^2 V}{\partial v \partial \beta} & \frac{\partial^2 V}{\partial v \partial s} \\ \frac{1}{v} \frac{\partial^2 V}{\partial v \partial \beta} & \frac{1}{v^2} \frac{\partial^2 V}{\partial^2 \beta} & \frac{1}{v} \frac{\partial^2 V}{\partial s \partial \beta} \\ \frac{\partial^2 V}{\partial v \partial s} & \frac{1}{v} \frac{\partial^2 V}{\partial s \partial \beta} & \frac{\partial^2 V}{\partial^2 s} \end{pmatrix} = \begin{pmatrix} M_{11}^2 & M_{12}^2 & M_{13}^2 \\ M_{21}^2 & M_{22}^2 & M_{23}^2 \\ M_{31}^2 & M_{32}^2 & M_{33}^2 \end{pmatrix}. \quad (62)$$

Taking second derivatives of the Higgs boson effective potential and substituting m_1^2 , m_2^2 , m_S^2 from the minimisation conditions (48) one obtains:

$$\begin{aligned} M_{11}^2 &= \frac{\lambda^2}{2} v^2 \sin^2 2\beta + \frac{\bar{g}^2}{4} v^2 \cos^2 2\beta + g_1'^2 v^2 (\tilde{Q}_1 \cos^2 \beta + \tilde{Q}_2 \sin^2 \beta)^2 + \Delta_{11}, \\ M_{12}^2 &= M_{21}^2 = \left(\frac{\lambda^2}{4} - \frac{\bar{g}^2}{8} \right) v^2 \sin 4\beta + \frac{g_1'^2}{2} v^2 (\tilde{Q}_2 - \tilde{Q}_1) \times \\ &\quad \times (\tilde{Q}_1 \cos^2 \beta + \tilde{Q}_2 \sin^2 \beta) \sin 2\beta + \Delta_{12}, \\ M_{22}^2 &= \frac{\sqrt{2} \lambda A_\lambda}{\sin 2\beta} s + \left(\frac{\bar{g}^2}{4} - \frac{\lambda^2}{2} \right) v^2 \sin^2 2\beta + \frac{g_1'^2}{4} (\tilde{Q}_2 - \tilde{Q}_1)^2 v^2 \sin^2 2\beta + \Delta_{22}, \\ M_{23}^2 &= M_{32}^2 = -\frac{\lambda A_\lambda}{\sqrt{2}} v \cos 2\beta + \frac{g_1'^2}{2} (\tilde{Q}_2 - \tilde{Q}_1) \tilde{Q}_S v s \sin 2\beta + \Delta_{23}, \\ M_{13}^2 &= M_{31}^2 = -\frac{\lambda A_\lambda}{\sqrt{2}} v \sin 2\beta + \lambda^2 v s + g_1'^2 (\tilde{Q}_1 \cos^2 \beta + \tilde{Q}_2 \sin^2 \beta) \tilde{Q}_S v s + \Delta_{13}, \\ M_{33}^2 &= \frac{\lambda A_\lambda}{2\sqrt{2} s} v^2 \sin 2\beta + g_1'^2 \tilde{Q}_S^2 s^2 + \Delta_{33}. \end{aligned} \quad (63)$$

In Eq. (63) Δ_{ij} represents the contribution of loop corrections which in the leading one-loop approximation are rather similar to the ones calculated in the NMSSM. The one-loop corrections to the mass matrix of the NMSSM CP-even Higgs sector were analysed in [59], [61].

When the SUSY breaking scale M_S and VEV of the singlet field are considerably larger than the EW scale the mass matrix (62)–(63) has a hierarchical structure. Therefore the masses of the heaviest Higgs bosons are closely approximated by the diagonal entries M_{22}^2 and M_{33}^2 which are expected to be of the order of M_S^2 or even higher. All off-diagonal matrix elements are relatively small $\lesssim M_S M_Z$. As a result the mass of one CP-even Higgs boson (approximately given by H) is governed by m_A while the mass of another one (predominantly the N singlet field) is set by $M_{Z'}$. Since the minimal eigenvalue of the mass matrix (62)–(63) is always less than its smallest diagonal element at least one Higgs scalar in the CP-even sector (approximately h) remains light even when the SUSY breaking scale tends to infinity, i.e. $m_{h_1}^2 \lesssim M_{11}^2$.

The direct Higgs searches at LEP set stringent limits on the parameter space of supersymmetric extensions of the SM. In order to establish the corresponding restrictions on the parameters of the ESSM we need to specify the couplings of the neutral Higgs

particles to the Z boson. In the rotated field basis (h, H, N) the trilinear part of the Lagrangian, which determines the interaction of the neutral Higgs states with the Z boson, is simplified:

$$L_{AZH} = \frac{\bar{g}}{2} M_Z Z_{1\mu} Z_{1\mu} h + \frac{\bar{g}}{2} Z_{1\mu} \left[H(\partial_\mu A) - (\partial_\mu H)A \right]. \quad (64)$$

Here we assume that the mixing between Z and Z' is negligibly small and can be safely ignored so that $Z_1 \simeq Z$. In the considered case only one CP-even component h couples to a pair of Z bosons while another one H interacts with the pseudoscalar A and Z_1 . The coupling of h to the Z_1 pair is exactly the same as in the SM. In the Yukawa interactions with fermions the first component of the CP-even Higgs basis also manifests itself as a SM-like Higgs boson.

The couplings of the Higgs scalars to a Z_1 pair (g_{ZZi} , $i = 1, 2, 3$) and to the Higgs pseudoscalar and Z boson (g_{ZAi}) appear because of the mixing of h and H with other components of the CP-even Higgs sector. Following the traditional notations we define the normalised R -couplings as: $g_{ZZh_i} = R_{ZZi} \times \text{SM coupling}$; $g_{ZA h_i} = \frac{\bar{g}}{2} R_{ZAi}$. The absolute values of all R -couplings vary from zero to unity.

The components of the CP-even Higgs basis are related to the physical CP-even Higgs eigenstates by virtue of a unitary transformation:

$$\begin{pmatrix} h \\ H \\ N \end{pmatrix} = U^\dagger \begin{pmatrix} h_1 \\ h_2 \\ h_3 \end{pmatrix}. \quad (65)$$

Combining the Lagrangian (64) and relations (65) the normalised R -couplings may be written in terms of the mixing matrix elements according to

$$R_{ZZi} = U_{hh_i}^\dagger, \quad R_{ZAi} = U_{Hh_i}^\dagger. \quad (66)$$

If all fundamental parameters are real the CP-even Higgs mass matrix (62)–(63) is symmetric and the unitary transformation (65) reduces to an orthogonal one. The orthogonality of the mixing matrices U results in sum rules:

$$\sum_i R_{ZZi}^2 = 1, \quad \sum_i R_{ZAi}^2 = 1, \quad \sum_i R_{ZZi} R_{ZAi} = 0. \quad (67)$$

The conditions (67) allow to eliminate three R -couplings. As a result, in the limit $\alpha_{ZZ'} \rightarrow 0$ the interactions of the neutral Higgs particles with a Z boson are described by three independent R -couplings. The dependence of spectrum and couplings of the Higgs bosons on the parameters of the ESSM will be examined in the following section.

5. Higgs phenomenology

5.1 Higgs masses and couplings

5.1.1 The MSSM limit $\lambda \rightarrow 0$, $s \rightarrow \infty$

First of all we consider the spectrum and couplings of the Higgs bosons in the ESSM. Let us start from the MSSM limit of the ESSM when $\lambda \rightarrow 0$, $s \rightarrow \infty$ with $\mu_{eff} \sim \lambda s$ held fixed in order to give an acceptable chargino mass and EWSB. From the first minimisation conditions (48) it follows that such solution can be obtained for very large and negative values of m_S^2 only.

As $s \rightarrow \infty$ the CP-even Higgs state, which is predominantly a singlet field, Z' boson and all exotic quarks and non-Higgsinos become very heavy and decouple from the rest of the particle spectrum. Then by means of a small unitary transformation the CP-even Higgs mass matrix in Eq. (62) reduces to the block diagonal form [62]

$$M^2 \simeq \begin{pmatrix} M_{11}^2 - \frac{M_{13}^4}{M_{33}^2} & M_{12}^2 - \frac{M_{13}^2 M_{32}^2}{M_{33}^2} & 0 \\ M_{21}^2 - \frac{M_{23}^2 M_{31}^2}{M_{33}^2} & M_{22}^2 - \frac{M_{23}^4}{M_{33}^2} & 0 \\ 0 & 0 & M_{33}^2 + \frac{M_{13}^4}{M_{33}^2} + \frac{M_{23}^4}{M_{33}^2} \end{pmatrix}. \quad (68)$$

For small values of λ the top-left 2×2 submatrix in Eq. (68) reproduces the mass matrix of the CP-even Higgs sector in the MSSM. So at tree-level we find

$$\begin{aligned} m_{H^\pm}^2 &\simeq m_A^2 + m_W^2, & m_A^2 &= \frac{\sqrt{2}\lambda A_\lambda}{\sin 2\beta} s, \\ m_{h_1, h_2}^2 &\simeq \frac{1}{2} \left[m_A^2 + M_Z^2 \mp \sqrt{(m_A^2 + M_Z^2)^2 - 4m_A^2 M_Z^2 \cos^2 2\beta} \right], \\ m_{h_3}^2 &\simeq g_1'^2 \tilde{Q}_S^2 s^2. \end{aligned} \quad (69)$$

In Eq. (69) the terms of $O(\lambda^2 v^2)$ are omitted, and $s^2 \gg v^2$ is assumed.

Since the enlargement of s leads to the growth of the mass of the singlet dominated Higgs state m_{h_3} , which is very close to $M_{Z'}$, the mixing between N and neutral components of the Higgs doublets diminishes when λ tends to zero. Thus in the MSSM limit of the ESSM the couplings of the heaviest CP-even Higgs boson to the quarks, leptons and gauge bosons vanish and the MSSM sum rules for the masses and couplings of the two lightest Higgs scalars and pseudoscalar are recovered. As in the minimal SUSY model the masses of MSSM-like Higgs bosons are defined by m_A and $\tan \beta$. They grow if m_A increases and at large values of m_A ($m_A^2 \gg M_Z^2$) the mass of the lightest CP-even Higgs boson attains its theoretical upper bound which is determined by the Z boson mass at tree-level, i.e. $m_{h_1} \leq M_Z |\cos 2\beta|$ [63].

5.1.2 $\lambda \gtrsim g_1$

When $\lambda \gtrsim g'_1 \approx g_1 \approx 0.46$ the qualitative pattern of the spectrum of the Higgs bosons is rather similar to the one which arises in the PQ symmetric NMSSM [62], [64]. We first give an analytic discussion of the spectrum at tree-level, then discuss the spectrum numerically including one-loop radiative corrections.

Assuming that in the allowed part of the parameter space $M_{22}^2 \gg M_{33}^2 \gg M_{11}^2$ the perturbation theory method yields

$$\begin{aligned} m_{h_3}^2 &\simeq M_{22}^2 + \frac{M_{23}^4}{M_{22}^2}, \\ m_{h_2}^2 &\simeq M_{33}^2 - \frac{M_{23}^4}{M_{22}^2} + \frac{M_{13}^4}{M_{33}^2}, \\ m_{h_1}^2 &\simeq M_{11}^2 - \frac{M_{13}^4}{M_{33}^2}. \end{aligned} \tag{70}$$

Here we neglect all terms suppressed by inverse powers of m_A^2 or $M_{Z'}^2$, i.e. $O(M_Z^4/m_A^2)$ and $O(M_Z^4/M_{Z'}^2)$.

At tree-level the masses of the Higgs bosons can be written as

$$\begin{aligned} m_A^2 &= \frac{2\lambda^2 s^2 x}{\sin^2 2\beta} + O(M_Z^2), & m_{H^\pm}^2 &= m_A^2 + O(M_Z^2), \\ m_{h_3}^2 &= m_A^2 + O(M_Z^2), & m_{h_2}^2 &= g_1'^2 \tilde{Q}_S^2 s^2 + O(M_Z^2), \end{aligned} \tag{71}$$

$$\begin{aligned} m_{h_1}^2 &\simeq \frac{\lambda^2}{2} v^2 \sin^2 2\beta + \frac{\bar{g}^2}{4} v^2 \cos^2 2\beta + g_1'^2 v^2 \left(\tilde{Q}_1 \cos^2 \beta + \tilde{Q}_2 \sin^2 \beta \right)^2 - \\ &\quad - \frac{\lambda^4 v^2}{g_1'^2 Q_S^2} \left(1 - x + \frac{g_1'^2}{\lambda^2} \left(\tilde{Q}_1 \cos^2 \beta + Q_2 \sin^2 \beta \right) Q_S \right)^2 + O(M_Z^4/M_{Z'}^2), \end{aligned} \tag{72}$$

where

$$x = \frac{A_\lambda}{\sqrt{2}\lambda s} \sin 2\beta.$$

As evident from the explicit expression for $m_{h_1}^2$ given above at $\lambda^2 \gg g_1^2$ the last term in Eq. (72) dominates and the mass of the lightest Higgs boson tends to be negative if the auxiliary variable x is not close to unity. In this case the vacuum stability requirement constrains the variable x around unity. As a consequence m_A is confined in the vicinity of $\mu \tan \beta$ and is much larger than the masses of the Z' and lightest CP-even Higgs boson. At so large values of m_A the masses of the heaviest CP-even, CP-odd and charged states are almost degenerate around m_A .

In Fig. 4 we plot masses and couplings of the Higgs bosons as a function of m_A . As a representative example we fix $\tan \beta = 2$ and VEV of the singlet field $s = 1.9 \text{ TeV}$, that corresponds to $M_{Z'} \simeq 700 \text{ GeV}$ which is quite close to the current limit on the Z' boson mass. For our numerical study we also choose the maximum possible value of

$\lambda(M_t) \simeq 0.794$ which does not spoil the validity of perturbation theory up to the Grand Unification scale. In order to obtain a realistic spectrum, we include the leading one-loop corrections from the top and stop loops. The contributions of these corrections to m_A^2 , $m_{H^\pm}^2$ and mass matrix of the CP-even Higgs states (62)–(63) depend rather strongly on the soft masses of the the superpartners of the top-quark (m_Q^2 and m_U^2) and the stop mixing parameter $X_t = A_t - \frac{\lambda_s}{\sqrt{2} \tan \beta}$. Here and in the following we set $m_Q = m_U = M_S = 700 \text{ GeV}$ while the stop mixing parameter is taken to be $\sqrt{6} M_S$ in order to enhance stop-radiative effects.

From Fig. 4a it becomes clear that the mass of the lightest Higgs scalar changes considerably when m_A varies. At m_A below 2 TeV or above 3 TeV the mass squared of the lightest Higgs boson tends to be negative. A negative eigenvalue of the mass matrix (62)–(63) means that the considered vacuum configuration ceases to be a minimum and turns into a saddle point. Near this point there is a direction in field space along which the energy density decreases generating instability of the given vacuum configuration. The requirement of stability of the physical vacuum therefore limits the range of variations of m_A from below and above. Together with the experimental lower limit on the mass of the Z' boson it maintains the mass hierarchy in the spectrum of the Higgs particles seen in Figs. 4b and 4c. Relying on this mass hierarchy one can diagonalise the 3×3 mass matrix of the CP-even Higgs sector.

The numerical results in Figs. 4a–4c confirm the analytic tree-level results discussed earlier. The numerical analysis reveals that the masses of the two heaviest CP-even, CP-odd and charged Higgs states grow when the VEV of the SM singlet field (or $M_{Z'}$) increases. The masses of the heaviest scalar, pseudoscalar and charged Higgs fields also rise with increasing λ , m_A and $\tan \beta$ while the mass of the second lightest Higgs scalar is almost insensitive to variations of these parameters. The growth of the masses of heavy Higgs bosons caused by the increase of $\tan \beta$ or s does not affect much the lightest Higgs scalar mass which lies below 200 GeV (see Fig. 4a).

Turning now to a discussion of the couplings, the hierarchical structure of the mass matrix of the CP-even Higgs sector for $\lambda \gtrsim g_1$ allows one to get approximate solutions for the Higgs couplings to the Z boson. They are given by

$$\begin{aligned} |R_{ZZ1}| &\simeq 1 - \frac{1}{2} \left(\frac{M_{13}^2}{M_{33}^2} \right)^2, & |R_{ZZ2}| &\simeq \frac{|M_{13}^2|}{M_{33}^2}, & |R_{ZZ3}| &\simeq \frac{|M_{12}^2|}{M_{11}^2}, \\ |R_{ZA1}| &\simeq \left| \frac{M_{12}^2}{M_{22}^2} - \frac{M_{23}^2 M_{13}^2}{M_{22}^2 M_{33}^2} \right|, & |R_{ZA2}| &\simeq \frac{|M_{23}^2|}{M_{22}^2}, & |R_{ZA3}| &\simeq 1 - \frac{1}{2} \left(\frac{M_{13}^2}{M_{33}^2} \right)^2. \end{aligned} \quad (73)$$

The obtained approximate formulae for the Higgs couplings (73) indicate that

$$R_{ZZ1} \gg R_{ZZ2} \gg R_{ZZ3} \text{ and } R_{ZA3} \gg R_{ZA2} \gg R_{ZA1}.$$

The analytic discussion of the couplings is confirmed by the numerical results for

R_{ZZi} and R_{ZAi} shown in Figs. 4d and 4e where the results of our numerical analysis including leading one-loop corrections to the CP-even Higgs mass matrix from the top-quark and its superpartners are presented. From Eq. (73) as well as from Figs. 4d and 4e one can see that the couplings of the second lightest Higgs boson to a Z pair and to the Higgs pseudoscalar and Z are always suppressed. They are of $O(M_Z/M_{Z'})$ and $O(M_Z/m_A)$ respectively which is a manifestation of the singlet dominated structure of the wave function of the second lightest Higgs scalar. The heaviest CP-even Higgs boson is predominantly a superposition of neutral components of Higgs doublets H . This is a reason why its relative coupling to the pseudoscalar and Z is so close to unity (see Eq. (64)). The main contribution to the wave function of the lightest Higgs scalar gives the first component of the CP-even Higgs basis h . Due to this the relative coupling of the lightest CP-even Higgs boson to Z pairs tends to unity in the permitted range of the parameter space. Because mixing between H and h is extremely small the couplings R_{ZZ3} and R_{ZA1} are almost negligible, i.e. they are of $O(M_Z^2/m_A^2)$.

5.1.3 $\lambda \lesssim g_1$

With decreasing λ the qualitative pattern of the Higgs spectrum changes significantly. In Fig. 5 the masses of the Higgs particles and their couplings to Z are examined as a function of m_A for $\lambda(M_t) = 0.3$. The values of $\tan\beta$ and $M_{Z'}$ are taken to be the same as in Fig. 4. For $\lambda \lesssim g'_1 \approx g_1 \approx 0.46$ the allowed range of m_A enlarges because mixing between the first and third components of the CP-even Higgs basis reduces. In particular the mass squared of the lightest Higgs boson remains positive even when $m_A \sim M_Z$, as shown in Fig. 5a. Therefore the lower bound on the Higgs pseudoscalar mass disappears so that charged, CP-odd and second lightest CP-even Higgs states may have masses in the 200 – 300 GeV range (see Figs. 5b and 5c). But the requirement of vacuum stability still prevents having very high values of m_A (or x). Indeed from Eq. (72) it is obvious that very large values of x (or m_A) pulls the mass squared of the lightest Higgs boson below zero destabilising the vacuum. This sets upper limits on the masses of charged and pseudoscalar Higgs bosons.

At least one scalar in the Higgs spectrum is always heavy since it has almost the same mass as the Z' boson, which must be heavier than 600 GeV. The mass of this CP-even Higgs state is determined by the VEV of the singlet field and does not change much if the other parameters λ , $\tan\beta$ and m_A vary. As before the masses of the other CP-even, CP-odd and charged Higgs fields grow when m_A rises providing the degeneracy of the corresponding states at $m_A \gg M_Z$. The growth of $\tan\beta$ and s enlarges the allowed range of m_A increasing the upper limit on the pseudoscalar mass. The permitted interval for m_A is also expanded when λ diminishes.

The couplings of the neutral Higgs bosons to Z depend rather strongly on the value of the pseudoscalar mass. At small values of m_A the second lightest Higgs scalar gains a relatively low mass. Because of this the mixing between H and h is large and relative couplings of the lightest Higgs scalars to Z pairs and to the pseudoscalar and Z are of the order of unity (see Figs. 5d and 5e). The couplings of the heaviest CP-even Higgs state to other bosons and fermions are tiny in this case since it is predominantly a singlet field. If the lightest Higgs scalar and pseudoscalar had low masses and large couplings to the Z they could be produced at LEP. Non-observation of these particles at LEP rules out most parts of the ESSM parameter space for $m_A \lesssim 200$ GeV.

When m_A is much larger than M_Z but is less than $M_{Z'}$ the heaviest Higgs scalar state is still singlet dominated which makes its couplings to the observed particles negligibly small. The hierarchical structure of the CP-even Higgs mass matrix ensures that the lightest and second lightest Higgs scalars are predominantly composed of the first and second components of the CP-even Higgs basis respectively. Therefore R_{ZZ1} and R_{ZA2} are very close to unity while R_{ZZ2} and R_{ZA1} are suppressed. When m_A approaches the Z' boson mass the mixing between S and H becomes large. This leads to appreciable values of the R_{ZA2} and R_{ZA3} couplings as displayed in Fig. 5e. However both of these relative couplings may be simultaneously large only in a very narrow part of the parameter space where $m_A \simeq M_{Z'}$. At the same time the relative couplings of the heaviest Higgs scalars to Z pairs are still much less than unity in this range of parameters because the mixing between the first and the other components of the CP-even Higgs basis remains very small (see Fig. 5d). Further increasing m_A mimics the mass hierarchy of the CP-even Higgs sector appeared at $\lambda \gtrsim g_1$. As a result the pattern of the Higgs couplings is rather similar to the one shown in Figs. 4d and 4e.

5.2 Upper bound on the lightest CP-even Higgs boson mass

It is apparent from Figs. 4b and 5b, as well as our analytic considerations, that at some value of m_A (or x) the lightest CP-even Higgs boson mass attains its maximum value. This coincides with the theoretical upper bound on m_{h_1} given by the first element of the mass $\sqrt{M_{11}^2}$. In this subsection we shall obtain an absolute upper bound on the lightest CP-even Higgs boson mass in the ESSM, and compare it to similar bounds obtained in the MSSM and NMSSM.

5.2.1 Tree-level upper bound

At tree-level the lightest Higgs scalar mass is obtained from Eq. (72) where the first three terms on the right-hand side are positive definite, while the fourth term is always

negative, and the upper bound therefore corresponds to taking this term to be zero. The contribution of the extra $U(1)_N$ D -term to the upper limit on m_{h_1} may be closely approximated as

$$g_1'^2 v^2 \left(\tilde{Q}_1 \cos^2 \beta + \tilde{Q}_2 \sin^2 \beta \right)^2 \simeq \left(\frac{M_Z}{2} \right)^2 \left(1 + \frac{1}{4} \cos 2\beta \right)^2. \quad (74)$$

Using this approximation, the tree-level upper bound on the lightest CP-even Higgs boson is given by:

$$m_{h_1}^2 \lesssim \frac{\lambda^2}{2} v^2 \sin^2 2\beta + M_Z^2 \cos^2 2\beta + \frac{M_Z^2}{4} \left(1 + \frac{1}{4} \cos 2\beta \right)^2. \quad (75)$$

The first and second terms are similar to the tree-level terms in the NMSSM [14]. The extra $U(1)_N$ effect appears through the third term in Eq. (72) which is a contribution coming from the additional $U(1)_N$ D -term in the Higgs scalar potential [65].

At tree-level the theoretical restriction on the lightest Higgs mass in the ESSM depends on λ and $\tan \beta$ only. As it was noticed in section 3 the requirement of validity of perturbation theory up to the Grand Unification scale constrains the interval of variations of the Yukawa coupling λ for each value of $\tan \beta$. The allowed range of λ as a function of $\tan \beta$ was shown in Fig. 3. Using the results of the analysis of the RG flow in the ESSM one can obtain the maximum possible value of the lightest Higgs scalar for each particular choice of $\tan \beta$.

In Fig. 6a we plot maximum values of the square roots of different contributions in Eq. (75) to the tree-level upper limit on $m_{h_1}^2$ versus $\tan \beta$. It is clear that at moderate values of $\tan \beta \sim 1 - 3$ the term $\lambda^2 v^2 / 2 \sin^2 2\beta$ from the F -term involving the singlet field dominates. With increasing $\tan \beta$ it falls quite rapidly and becomes negligibly small as $\tan \beta \gtrsim 15$. In contrast the contribution of the $SU(2)$ and $U(1)_Y$ D -terms grows when $\tan \beta$ becomes larger. At $\tan \beta \gtrsim 4$ it exceeds $\lambda^2 v^2 / 2 \sin^2 2\beta$ and gives the dominant contribution to the tree-level upper bound on m_{h_1} . As one can see from Fig. 6a the D -term of the extra $U(1)_N$ gives the second largest contribution to the tree-level theoretical restriction on m_{h_1} at very large and low values of $\tan \beta$, when $\tan \beta$ is less than 1.6 or larger than 8. In the part of the ESSM parameter space where the upper limit on m_{h_1} reaches its absolute maximum value its contribution is the smallest one. According to Eq. (75) the square root of the $U(1)_N$ D -term contribution to $m_{h_1}^2$ varies from 45 to 34 GeV when $\tan \beta$ changes from 1.1 to 14.

The resulting tree-level upper bound on the mass of the lightest Higgs particle in the ESSM is presented in Fig. 6b, and compared to the corresponding bounds in the MSSM and NMSSM. In the ESSM the bound attains a maximum value of 130 GeV at $\tan \beta = 1.5 - 1.8$. Remarkably, we find that in the interval of $\tan \beta$ from 1.2 to 3.4 the absolute maximum value of the mass of the lightest Higgs scalar in the ESSM is larger than

the experimental lower limit on the SM-like Higgs boson even at tree-level. Therefore non-observation of the Higgs boson at LEP does not cause any trouble for the ESSM, even at tree-level.

The upper bound on the mass of the lightest CP-even Higgs scalar in the NMSSM exceeds the corresponding limit in the MSSM because of the extra contribution to $m_{h_1}^2$ induced by the additional F -term in the Higgs scalar potential of the NMSSM. The size of this contribution, which is described by the first term in Eq. (75), is determined by the Yukawa coupling λ whose interval of variations is constrained by the applicability of perturbation theory at high energies. The upper limit on the coupling λ caused by the validity of perturbation theory in the NMSSM is more stringent than in the ESSM due to the presence of exotic $5 + \bar{5}$ -plets of matter in the particle spectrum of the ESSM. Indeed extra $SU(5)$ multiplets of matter change the running of the gauge couplings so that their values at the intermediate scale rise when the number of new supermultiplets increases. Since $g_i(Q)$ occurs in the right-hand side of the differential equations (38) with negative sign the growth of the gauge couplings prevents the appearance of the Landau pole in the evolution of the Yukawa couplings. It means that for each value of the top-quark Yukawa coupling (or $\tan\beta$) at the EW scale the maximum allowed value of $\lambda(M_t)$ rises when the number of $5 + \bar{5}$ -plets increases. The increase of $\lambda(M_t)$ is accompanied by the growth of the theoretical restriction on the mass of the lightest CP-even Higgs particle. For instance, it was shown that the introduction of four pairs of $5 + \bar{5}$ supermultiplets in the NMSSM raised the two-loop upper limit on the lightest Higgs boson mass from 135 GeV to 155 GeV [66]. This is also a reason why the tree-level theoretical restriction on m_{h_1} in the Next-to-Minimal SUSY model is considerably less than in the ESSM at moderate values of $\tan\beta$.

At large $\tan\beta \gg 10$ the contribution of the F -term of the SM singlet field to $m_{h_1}^2$ vanishes. Therefore with increasing $\tan\beta$ the upper bound on the lightest Higgs boson mass in the NMSSM approaches the corresponding limit in the minimal SUSY model. In the ESSM the theoretical restriction on the mass of the lightest Higgs scalar also diminishes when $\tan\beta$ rises. But even at very large values of $\tan\beta$ the tree-level upper limit on m_{h_1} in the ESSM is still 6–7 GeV larger than the ones in the MSSM and NMSSM because of the $U(1)_N$ D -term contribution.

5.2.2 One-loop upper bound

So far we have discussed the bounds at tree-level. Now we shall include radiative corrections in our discussion. It is well known that the inclusion of loop corrections from the top-quark and its superpartners increases the bound on the lightest Higgs boson mass in the ESSM substantially. In the ESSM and in the NMSSM these corrections are nearly the

same as in the MSSM. The leading one-loop and two-loop corrections to the lightest Higgs boson mass in the MSSM were calculated and studied in [67] and [68]–[69] respectively. However, in contrast with the MSSM and NMSSM, the ESSM contains extra supermultiplets of exotic matter. Because it is not clear *a priori* if the corrections induced by the loops involving new particles affect the mass of the lightest Higgs scalar considerably, we include in our analysis leading one-loop corrections to $m_{h_1}^2$ from the exotic quarks since their couplings to the singlet Higgs field tend to be large at low energies enhancing radiative effects. In the leading approximation the upper bound on the lightest Higgs boson mass in the ESSM can be written as

$$m_{h_1}^2 \lesssim \frac{\lambda^2}{2} v^2 \sin^2 2\beta + M_Z^2 \cos^2 2\beta + \frac{M_Z^2}{4} \left(1 + \frac{1}{4} \cos 2\beta\right)^2 + \Delta_{11}^t + \Delta_{11}^D, \quad (76)$$

where the third term represents the $U(1)_N$ D -term contribution while Δ_{11}^t and Δ_{11}^D are one-loop corrections from the top-quark and D -quark supermultiplets respectively. When $m_{D_i}^2 = m_{\overline{D}_i}^2 = M_S^2$ the contribution of one-loop corrections to $m_{h_1}^2$ from the superpartners of D -quarks reduces to

$$\Delta_{11}^D = \sum_{i=1,2,3} \frac{3\lambda^2 \kappa_i^2 v^2}{32\pi^2} \sin^2 2\beta \ln \left[\frac{m_{D_{1,i}} m_{D_{2,i}}}{Q^2} \right]. \quad (77)$$

In Figs. 7a and 7b we explore the dependence of one-loop upper bound on the lightest Higgs boson mass on the Yukawa couplings κ_i and λ . We consider two different cases when $\kappa_1 = \kappa_2 = 0$, $\kappa_3 = \kappa$ (see Fig. 7a) and $\kappa_1 = \kappa_2 = \kappa_3 = \kappa$ (see Fig. 7b). To simplify our analysis the soft masses of the superpartners of exotic and top-quarks are set to be equal, i.e. $m_Q^2 = m_U^2 = m_{D_i}^2 = m_{\overline{D}_i}^2 = M_S^2$. In order to enhance the contribution of loop effects we assume maximal mixing in the stop sector ($X_t = \sqrt{6}M_S$) and minimal mixing between the superpartners of exotic quarks D and \overline{D} , i.e. $A_{\kappa i} = 0$. As before we keep $M_S = M_{Z'} = 700$ GeV and $\tan \beta = 2$. Then the theoretical restriction on the mass of the lightest Higgs scalar (76) is defined by the couplings λ and κ only.

In the plane $\lambda/h_t - \kappa/h_t$ the set of points that results in the same upper limit on m_{h_1} forms a line. For any choice of λ and κ lying below the line the lightest Higgs particle has a mass which is less than the theoretical restriction that corresponds to this line. Curvature of the line characterises the dependence of the upper bound on the lightest Higgs boson mass on the Yukawa coupling κ . If κ is zero the one-loop contribution of the exotic squarks to $m_{h_1}^2$ vanishes. When κ grows the exotic squark contribution to $m_{h_1}^2$ and the upper limit on the mass of the lightest Higgs scalar rise. As a consequence the same theoretical restriction on m_{h_1} is obtained for smaller values of $\lambda(M_t)$. But from Figs. 7a and 7b one can see that the increase of $\kappa(M_t)$ within the allowed range of the parameter space does not lead to the appreciable decrease of $\lambda(M_t)$ that should compensate the growth of exotic squark contribution to $m_{h_1}^2$. It means that the contribution of the exotic

squarks is always much smaller than the first term in Eq. (76). Numerically the increase of the lightest Higgs boson mass caused by the inclusion of the exotic squark contribution does not exceed a few GeV.

5.2.3 Two-loop upper bound

We also include in our analysis leading two-loop corrections to $m_{h_1}^2$ from the top-quark and its superpartner. In the two-loop leading-log approximation the upper bound on the lightest Higgs boson mass in the ESSM can be written in the following form

$$\begin{aligned}
m_h^2 \lesssim & \left[\frac{\lambda^2}{2} v^2 \sin^2 2\beta + M_Z^2 \cos^2 2\beta + \frac{M_Z^2}{4} \left(1 + \frac{1}{4} \cos 2\beta \right)^2 \right] \times \\
& \times \left(1 - \frac{3h_t^2}{8\pi^2} l \right) + \frac{3h_t^4 v^2 \sin^4 \beta}{8\pi^2} \left\{ \frac{1}{2} U_t + l + \frac{1}{16\pi^2} \left(\frac{3}{2} h_t^2 - 8g_3^2 \right) (U_t + l) l \right\} + \Delta_{11}^D, \\
U_t = & 2 \frac{X_t^2}{M_S^2} \left(1 - \frac{1}{12} \frac{X_t^2}{M_S^2} \right), \quad l = \ln \left[\frac{M_S^2}{m_t^2} \right].
\end{aligned} \tag{78}$$

Here we keep one-loop leading-log corrections from the exotic squarks. Eq. (78) is a simple generalisation of the approximate expressions for the theoretical restriction on the mass of the lightest Higgs particle obtained in the MSSM [69] and NMSSM [70]. The inclusion of leading two-loop corrections reduces the upper limit on m_{h_1} significantly and nearly compensates the growth of the theoretical restriction on m_{h_1} with increasing SUSY breaking scale M_S which is caused by one-loop corrections.

The dependence of the two-loop upper bound (78) on λ and κ for two different choices of the Yukawa couplings of exotic quarks described above is examined in Figs. 7c and 7d. After the incorporation of two-loop corrections the line that corresponds to the 160 GeV upper limit on the lightest Higgs boson mass lies beyond the permitted range of the parameter space while in the one-loop approximation even larger values of m_{h_1} are allowed. The distortion of the lines, which represent different theoretical restrictions on the mass of the lightest Higgs scalar in the ESSM, still remains negligible. It demonstrates the fact that the exotic squark contribution to $m_{h_1}^2$ is much less than the leading two-loop corrections from the top-quark and its superpartners to $m_{h_1}^2$.

From Fig. 7 it follows that for each given value of $\tan \beta$ the mass of the lightest Higgs particle attains its maximum when $\lambda(M_t) \rightarrow \lambda_{\max}$ and $\kappa \rightarrow 0$. Nevertheless the dependence of the upper limit (78) on κ is rather weak so that the theoretical restriction on the lightest Higgs boson mass for $\kappa = 0$ and for $\kappa = g_1'$ are almost identical. The upper limit on m_{h_1} is very sensitive to the choice of λ and $\tan \beta$. Therefore at the last stage of our analysis we explore the dependence of the two-loop upper bound (78) on $\tan \beta$ keeping $\kappa = 0$ (i.e. $\Delta_{11}^D = 0$) and relying on the results of our study of the RG flow summarised in Fig. 3.

The dependence of the two-loop theoretical restrictions on m_{h_1} on $\tan\beta$ shown in Figs. 8a and 8b resembles the tree-level one. But the interval of variations of the upper bound on m_{h_1} shrinks. In Figs. 8a and 8b we consider maximal ($X_t = \sqrt{6}M_S$) and minimal ($X_t = 0$) mixing in the stop sector respectively. Again at moderate values of $\tan\beta = 1.6 - 3.5$ the upper bound on the lightest Higgs boson mass in the ESSM is considerably higher than in the MSSM and NMSSM because of the enhanced contribution of the F -term of the SM singlet field to $m_{h_1}^2$. Although the two-loop theoretical restriction on m_{h_1} in the ESSM reduces with increasing $\tan\beta$ it still remains 4–5 GeV larger than the corresponding limits in the MSSM and NMSSM owing to the $U(1)_N$ D -term contribution. This contribution is especially important in the case of minimal mixing between the superpartners of the top quark. In the considered case the two-loop theoretical restriction on m_{h_1} in the MSSM and NMSSM is less than the experimental limit on the SM-like Higgs boson mass set by LEP II. As a result the scenario with $X_t = 0$ is ruled out in the MSSM. The contribution of an extra $U(1)_N$ D -term to $m_{h_1}^2$ raises the upper bound (78) at large $\tan\beta \gtrsim 10$ slightly above the existing LEP limit thus relaxing the constraints on the ESSM parameter space (see Fig. 8b).

The growth of X_t from 0 to $\sqrt{6}M_S$ increases the theoretical restriction on the lightest Higgs boson mass in the ESSM by 10 – 20 GeV. The upper limit on m_{h_1} is most sensitive to the choice of X_t at low and large values of $\tan\beta$ where the growth of the corresponding theoretical restriction reaches 20 and 15 GeV respectively. At the same time the absolute maximum value of the lightest Higgs boson mass rises by 10 GeV only. In total leading one-loop and two-loop corrections modify the maximum possible value of the mass of the lightest Higgs scalar by 20 GeV by increasing it up to about 150 GeV.

Note that the quoted upper limits for the ESSM, as well as the MSSM and NMSSM, are sensitive to the value of the top-quark mass, and the SUSY breaking scale, and depend on the precise form of the two-loop approximations used. Here we have used an analytic approximation of the two-loop effects which slightly underestimates the full two-loop corrections. We have also taken the SUSY scale to be given by 700 GeV. The upper bounds quoted here may therefore be further increased by several GeV by making slightly different assumptions. The main point we wish to make is that the upper bound on the lightest CP-even Higgs scalar in the ESSM is always significantly larger than in the NMSSM, as well as the MSSM.

6. Charginos and Neutralinos

6.1 Chargino and neutralino states in the ESSM

After EWSB all superpartners of the gauge and Higgs bosons get non-zero masses. Since the supermultiplets of the Z' boson and SM singlet Higgs field S are electromagnetically neutral they do not contribute any extra particles to the chargino spectrum. Consequently the chargino mass matrix and its eigenvalues remain the same as in the MSSM, namely

$$m_{\chi_{1,2}^\pm}^2 = \frac{1}{2} \left[M_2^2 + \mu_{eff}^2 + 2M_W^2 \pm \sqrt{(M_2^2 + \mu_{eff}^2 + 2M_W^2)^2 - 4(M_2\mu_{eff} - M_W^2 \sin 2\beta)^2} \right], \quad (79)$$

where M_2 is the $SU(2)$ gaugino mass and $\mu_{eff} = \frac{\lambda s}{\sqrt{2}}$. Unsuccessful LEP searches for SUSY particles including data collected at \sqrt{s} between 90 GeV and 209 GeV set a 95% CL lower limit on the chargino mass of about 100 GeV [71]. This lower bound constrains the parameter space of the ESSM restricting the absolute values of the effective μ -term and M_2 from below, i.e. $|M_2|, |\mu_{eff}| \geq 90 - 100$ GeV.

In the neutralino sector of the ESSM there are two extra neutralinos besides the four MSSM ones. One of them is an extra gaugino coming from the Z' vector supermultiplet. The other one is an additional Higgsino \tilde{S} (singlino) which is a fermion component of the SM singlet superfield S . The Higgsino mass terms in the Lagrangian of the ESSM are induced by the trilinear interaction $\lambda S(H_d H_u)$ in the superpotential (19) after the breakdown of gauge symmetry. Because of this their values are determined by the coupling λ and VEVs of the Higgs fields. The mixing between gauginos and Higgsinos is proportional to the corresponding gauge coupling and VEV that the scalar partner of the considered Higgsino gets. Taking this into account one can obtain a 6×6 neutralino mass matrix that in the interaction basis $(\tilde{B}, \tilde{W}_3, \tilde{H}_1^0, \tilde{H}_2^0, \tilde{S}, \tilde{B}')$ reads

$$M_{\tilde{\chi}^0} = \begin{pmatrix} M_1 & 0 & -\frac{1}{2}g'v_1 & \frac{1}{2}g'v_2 & 0 & 0 \\ 0 & M_2 & \frac{1}{2}gv_1 & -\frac{1}{2}gv_2 & 0 & 0 \\ -\frac{1}{2}g'v_1 & \frac{1}{2}gv_1 & 0 & -\mu_{eff} & -\frac{\lambda v_2}{\sqrt{2}} & \tilde{Q}_1 g'_1 v_1 \\ \frac{1}{2}g'v_2 & -\frac{1}{2}gv_2 & -\mu_{eff} & 0 & -\frac{\lambda v_1}{\sqrt{2}} & \tilde{Q}_2 g'_1 v_2 \\ 0 & 0 & -\frac{\lambda v_2}{\sqrt{2}} & -\frac{\lambda v_1}{\sqrt{2}} & 0 & \tilde{Q}_S g'_1 s \\ 0 & 0 & \tilde{Q}_1 g'_1 v_1 & \tilde{Q}_2 g'_1 v_2 & \tilde{Q}_S g'_1 s & M'_1 \end{pmatrix}, \quad (80)$$

where M_1 , M_2 and M'_1 are the soft gaugino masses for \tilde{B} , \tilde{W}_3 and \tilde{B}' respectively. In Eq. (80) we neglect the Abelian gaugino mass mixing M_{11} between \tilde{B} and \tilde{B}' that arises

at low energies as a result of the kinetic term mixing even if there is no mixing in the initial values of the soft SUSY breaking gaugino masses near the Grand Unification or Planck scale [52]. The top-left 4×4 block of the mass matrix (80) contains the neutralino mass matrix of the MSSM where the parameter μ is replaced by μ_{eff} . The lower right 2×2 submatrix represents extra components of neutralinos in the considered model. The neutralino sector in E_6 inspired SUSY models was studied recently in [20], [25], [31], [36]–[37], [40], [72]–[73].

As one can see from Eqs. (79)–(80) the masses of charginos and neutralinos depend on λ , s , $\tan \beta$, M_1 , M'_1 and M_2 . In SUGRA models with uniform gaugino masses at the Grand Unification scale the RG flow yields a relationship between M_1 , M'_1 and M_2 at the EW scale:

$$M'_1 \simeq M_1 \simeq 0.5 M_2. \quad (81)$$

This reduces the parameter space in the neutralino sector of the ESSM drastically. It allows to study the spectrum of chargino and neutralino as a function of only one gaugino mass, for example M_1 , for each set of λ , s and $\tan \beta$.

6.2 Chargino and neutralino spectrum

The qualitative pattern of chargino and neutralino masses is determined by the Yukawa coupling λ , depending on whether λ is less than g'_1 or not. Because in the MSSM limit of the ESSM, when $\lambda \rightarrow 0$, the phenomenologically acceptable solution implies that $s \gtrsim M_Z/\lambda$, the extra $U(1)_N$ gaugino \tilde{B}' and singlino \tilde{S} decouple from the rest of the spectrum forming two eigenstates $(\tilde{B}' \pm \tilde{S})/\sqrt{2}$ with mass $M_{Z'} = \tilde{Q}_S g'_1 s$. Mixing between new neutralino states and other gauginos and Higgsinos vanishes in this case rendering the neutralino sector in the ESSM indistinguishable from MSSM at the LHC and ILC. Here it is worth to emphasise that the direct observation of extra neutralino states in the ESSM is unlikely to occur in the nearest future anyway. Since off-diagonal entries of the bottom right 2×2 submatrix of the neutralino mass matrix (80) are controlled by the Z' boson mass new neutralinos are always very heavy (~ 1 TeV) preventing the distinction between the ESSM and MSSM neutralino sectors.

When $\lambda > g'_1$ the typical pattern of the spectrum of neutralinos and charginos changes. In Figs. 9a and 9b we examine the dependence of the neutralino and chargino masses on M_1 assuming the unification of the soft gaugino mass parameters at the scale M_X . As a representative example we fix $\lambda \simeq 0.794$, $\tan \beta = 2$ and $M_{Z'} = 700$ GeV ($s \simeq 1.9$ TeV). We restrict our consideration to the most attractive part of the parameter space, in which the lightest chargino is accessible at future colliders, i.e. $|M_1| \lesssim 300$ GeV. In order to get the spectrum of neutralinos we diagonalise the mass matrix (80) numerically. As a

consequence we obtain a set of positive and negative eigenvalues of this matrix which are presented in Fig. 9a. However the physical meaning is only their absolute values.

In the considered part of the parameter space the heaviest chargino and neutralinos are almost degenerate with mass $|\mu_{eff}|$. They are formed by the neutral and charged superpartners of the Higgs bosons. As one can see from Figs. 9a and 9b the masses of the heaviest chargino and neutralinos are almost insensitive to the choice of the gaugino masses if $|M_1| \lesssim 300 \text{ GeV}$. The $U(1)_N$ gaugino \tilde{B}' and singlino \tilde{S} compose two other heavy neutralino eigenstates whose masses are closely approximated as

$$|m_{\chi_{3,4}^0}| \simeq \frac{1}{2} \left[\sqrt{M_1'^2 + 4M_{Z'}^2} \mp M_1' \right]. \quad (82)$$

The four heaviest neutralinos and chargino gain masses beyond 500 GeV range so that their observation at the LHC and ILC looks rather problematic. The masses of the heaviest neutralino and chargino states rise with increasing VEV of the SM singlet field and are practically independent of $\tan \beta$.

At low energies heavy neutralinos decouple and the spectrum of the two lightest ones is described by the 2×2 mass matrix

$$M_{\tilde{\chi}^0}' \simeq \begin{pmatrix} M_1 - \frac{g'^2 v^2}{4\mu} \sin 2\beta & \frac{gg'v^2}{4\mu} \sin 2\beta \\ \frac{gg'v^2}{4\mu} \sin 2\beta & M_2 - \frac{g^2 v^2}{4\mu} \sin 2\beta \end{pmatrix}, \quad (83)$$

whose eigenvalues are

$$|m_{\chi_{1,2}^0}| \simeq \left| M_1 + M_2 - \frac{M_Z^2}{\mu} \sin 2\beta \mp \sqrt{\left(M_1 + M_2 - \frac{M_Z^2}{\mu} \sin 2\beta \right)^2 - 4 \left(M_1 M_2 - \frac{M_Z^2}{\mu} \tilde{M} \right)} \right|, \quad (84)$$

where

$$\tilde{M} = M_2 \sin^2 \theta_W + M_1 \cos^2 \theta_W.$$

The superpartners of charged $SU(2)$ gauge bosons form the lightest chargino state with mass

$$|m_{\chi_1^\pm}| = \left| M_2 - \frac{M_W^2}{\mu} \sin 2\beta \right|. \quad (85)$$

The numerical analysis and our analytic consideration show that the masses of the lightest neutralinos and chargino do not change much when λ , s or $\tan \beta$ vary unless M_1 and M_2 are quite small. The second lightest neutralino and the lightest chargino are predominantly superpartners of the $SU(2)$ gauge bosons. Their masses are governed by $|M_2|$. The lightest neutralino state is basically bino, \tilde{B} , whose mass is set by $|M_1|$.

In Figs. 10a and 10b we explore the spectrum of neutralino and chargino in the case when λ is less than g'_1 . The Yukawa coupling λ is taken to be 0.3 while the other parameters remain the same as in Fig. 9. Now the two heaviest neutralinos are mixtures of \tilde{B}' and \tilde{S} . They get masses larger than 500 GeV as before. However unlike in the large λ limit the other four neutralinos and both charginos can be light enough. Therefore they may be observed in the nearest future. The composition of the wave functions of the lightest neutralinos and charginos depends on the choice of the parameters of the model. For the set of λ , $\tan\beta$ and s chosen in Fig. 10 the lightest neutralino is still predominantly bino, \tilde{B} . Till $|M_1|$ is less than 200 GeV, i.e. $|M_2| < |\mu_{eff}|$, the second lightest neutralino and the lightest chargino are basically formed by the superpartners of $SU(2)$ gauge bosons. When $|M_1| > 200$ GeV ($|M_2| > |\mu_{eff}|$) the wave functions of the second lightest neutralino and the lightest chargino are Higgsino dominated.

Obvious disadvantage of the considered scenarios with $\lambda < g'_1$ and $\lambda > g'_1$ in the ESSM is that any pattern of the masses and couplings of the lightest neutralino and chargino, which can be observed at the LHC and ILC, may be reproduced in the framework of the minimal SUSY model. This is a consequence of the stringent lower bound on the mass of the Z' boson set by Tevatron.

7. Z' and exotic phenomenology

7.1 Masses and couplings of new states

The presence of a Z' gauge boson and exotic multiplets of matter in the particle spectrum is a very peculiar feature that permits to distinguish E_6 inspired supersymmetric models from the MSSM or NMSSM. At tree-level the masses of these new particles are determined by the VEV of the singlet field S that remains a free parameter in the considered models. Therefore the Z' boson mass and the masses of exotic quarks and non-Higgses cannot be predicted. But collider experiments [56]–[57] and precision EW tests [74] set stringent limits on the Z' mass and $Z - Z'$ mixing. The lower bounds on the Z' mass from direct searches at the Fermilab Tevatron ($p\bar{p} \rightarrow Z' \rightarrow l^+l^-$) [57] are model dependent but are typically around 500 – 600 GeV unless couplings of ordinary particles to Z' are suppressed such as in leptophobic models [53], [75]. Similarly, bounds on the mixing angle are around $(2 - 3) \times 10^{-3}$ [56]. As has been already mentioned, even more stringent constraints on the Z' mass and mixing follow from nucleosynthesis and astrophysical observations. They imply that the equivalent number of additional neutrinos with full-strength weak interactions ΔN_ν is less than 0.3 (for a recent review, see [76]). This requires $M_{Z'} \gtrsim 4.3$ TeV [42]. However these restrictions cannot be applied to the Z' gauge boson

in the ESSM because right-handed neutrinos here are expected to be superheavy and do not change the effective number of neutrino species at low energies.

The analysis performed in [77] revealed that Z' boson in the E_6 inspired models can be discovered at the LHC if its mass is less than $4 - 4.5$ TeV. At the same time the determination of the couplings of the Z' should be possible up to $M_{Z'} \sim 2 - 2.5$ TeV [78]. Possible Z' decay channels in E_6 inspired supersymmetric models were studied in [73].

The restrictions on the masses of exotic particles are not so rigorous as the experimental bounds on the mass of the Z' boson. The most stringent constraints come from the non-observation of exotic colour states at HERA and Tevatron. But most searches imply that exotic quarks, i.e. leptoquarks or diquarks, have integer-spin. So they are either scalars or vectors. Because of this new coloured objects can be coupled directly to either a pair of quarks or to quark and lepton. Moreover it is usually assumed that leptoquarks and diquarks have appreciable couplings to the quarks and leptons of the first generation. Experiments at LEP, HERA and Tevatron excluded such leptoquarks if their masses were less than 290 GeV [79] whereas CDF and D0 ruled out diquarks with masses up to 420 GeV [80]. The production of diquarks at the LHC was studied recently in [81].

In the ESSM the exotic squarks and non-Higgses are expected to be heavy since their masses are determined by the SUSY breaking scale. Moreover, their couplings to the quarks and leptons of the first and second generation should be rather small to avoid processes with non-diagonal flavour transitions. As a result the production of exotic squarks and non-Higgses will be very strongly suppressed or even impossible at future colliders. However the exotic fermions (quarks and non-Higgsinos) can be relatively light in the ESSM since their masses are set by the Yukawa couplings κ_i and λ_i that may be small. This happens, for example, when the Yukawa couplings of the exotic particles have hierarchical structure similar to the one observed in the ordinary quark and lepton sectors. Then Z' mass lie beyond 10 TeV and the only manifestation of the considered model may be the presence of light exotic quark or non-Higgses in the particle spectrum.

The new exotic particles consist of vector-like multiplets with respect to the SM gauge group. Hence their axial couplings to the SM gauge bosons go to zero in the limit of no $Z - Z'$ mixing reducing the contribution of additional particles to the electroweak observables measured at LEP. The contribution of Z' gauge boson to the electroweak observables is also negligibly small because it is supposed to be very heavy so that the mixing between Z and Z' almost vanishes.

In order to amplify the signal coming from the presence of additional particles we shall assume further that the three families of exotic quarks and two generations of exotic non-Higgsinos, whose masses are determined by extra Yukawa couplings, are considerably lighter than the Z' and in this case they can possibly be observed at the

LHC and ILC. Since the analysis of the RG flow performed in section 3 revealed that the exotic quarks as well as non-Higgsino Yukawa couplings tend to be equal we keep $\mu_{D1} = \mu_{D2} = \mu_{D3} = \frac{\kappa(M_t)}{\sqrt{2}}s$ and $\mu_{H1} = \mu_{H2} = \frac{\lambda_{1,2}(M_t)}{\sqrt{2}}s$ ($\lambda_1(M_t) = \lambda_2(M_t)$) at the EW scale. Moreover to simplify our numerical studies we fix the masses of exotic quarks and non-Higgsinos to be equal to 300 GeV.

Before proceeding to discuss the scope of future colliders in testing the features of the ESSM in the Z' and exotic sectors, we should remind the reader that we assume the mixing angle between the Z and Z' to be extremely small. In this case, any vertex involving a Z' boson and fermions can be written as

$$-\frac{ig'_1\gamma_\mu}{2}\left(g_V - g_A\gamma_5\right). \quad (86)$$

For, e.g. $M'_Z = 1.5$ TeV, the vector $g_V(M_{Z'})$ and axial $g_A(M_{Z'})$ couplings take the following values:

- charged leptons: $g_V = \tilde{Q}_{e_L} - \tilde{Q}_{e_L^c} \simeq 0.1081$, $g_A = \tilde{Q}_{e_L^c} + \tilde{Q}_{e_L} \simeq 0.4910$;
- neutrinos: $g_V = g_A = \tilde{Q}_{\nu_L} = 0.2996$;
- u -quarks: $g_V = \tilde{Q}_{u_L} - \tilde{Q}_{u_L^c} \simeq 0.0278$, $g_A = \tilde{Q}_{u_L^c} + \tilde{Q}_{u_L} \simeq 0.2996$;
- d -quarks: $g_V = \tilde{Q}_{d_L} - \tilde{Q}_{d_L^c} \simeq -0.1637$, $g_A = \tilde{Q}_{d_L^c} + \tilde{Q}_{d_L} \simeq 0.4910$;
- exotic D -quarks: $g_V = \tilde{Q}_D - \tilde{Q}_{\bar{D}} \simeq 0.1359$, $g_A = \tilde{Q}_{\bar{D}} + \tilde{Q}_D \simeq -0.7906$;
- fermion partners of extra non-Higgs fields (non-Higgsinos):

$$g_V = \tilde{Q}_{H_1} - \tilde{Q}_{H_2} \simeq -0.1915, \quad g_A = \tilde{Q}_{H_2} + \tilde{Q}_{H_1} \simeq -0.7906;$$

- fermion partners of extra singlet fields (singlinos):

$$g_V = g_A = \tilde{Q}_S \simeq 0.7906.$$

As for additional couplings, the interaction of exotic quarks and non-Higgsinos with the neutral SM gauge bosons γ and Z takes the form

$$-ieQ_{em}\gamma_\mu, \quad -\frac{i\bar{g}}{2}g_V\gamma_\mu,$$

respectively, where Q_{em} and g_V are given as follows:

- exotic D -quarks: $Q_{em}^D = -1/3$, $g_V = -2Q_{em}^D \sin^2 \theta_W$;
- charged non-Higgsinos: $Q_{em}^E = -1$, $g_V = 2T_3^f - 2Q_{em}^f \sin^2 \theta_W \simeq -\cos 2\theta_W$;

- neutral non-Higgsinos: $Q_{em}^N = 0$, $g_V = 1$.

For completeness and to fix our conventions, we also quote the couplings of the γ and Z bosons to ordinary quarks and leptons, as

- ordinary fermions (quarks and leptons): $g_V = T_3^f - 2Q_{em}^f \sin^2 \theta_W$, $g_A = T_3^f$.

7.2 Phenomenology at future colliders

Fig. 11 shows the differential distribution in invariant mass of the lepton pair l^+l^- (for one species of lepton $l = e, \mu$) in Drell-Yan production at the LHC, assuming the SM only as well as the latter augmented, in turn, by a Z' field ($M_{Z'} = 1.5$ TeV) with and without light exotic quarks or non-Higgsinos ($\mu_{Di} = \mu_{Hi} = 300$ GeV) separately⁷. This distribution is promptly measurable at the CERN collider with a high resolution and would enable one to not only confirm the existence of a Z' state but also to establish the possible presence as well as nature of additional exotic matter, by simply fitting to the data the width of the Z' resonance [78]. In fact for our choice of μ_{Di} , μ_{Hi} and $M_{Z'}$ the Z' total width varies from ≈ 19 GeV (in case of no exotic matter) to ≈ 25 GeV (in case of light exotic D -quarks) and to ≈ 21 GeV (in case of light non-Higgsinos). (Also notice the different normalisation around the Z' resonance of the three curves in Fig. 11, as this scales like $\sim \Gamma(Z' \rightarrow l^+l^-)/\Gamma(Z' \rightarrow \text{anything})$.) Clearly, in order to perform such an exercise, the Z' couplings to ordinary matter ought to have been previously established elsewhere, as a modification of the latter may well lead to effects similar to those induced by the additional matter present in our model. (Recall that in our model Z' couplings to SM particles and exotic matter are simultaneously fixed.)

However, if exotic particles of the nature described here do exist at such low scales, they could possibly be accessed through direct pair hadroproduction. In fact, the corresponding fully inclusive cross sections are in principle sufficient to such a purpose in the case of exotic D -quarks (up to masses of the TeV order) while this statement is presumably true for non-Higgsinos only up to masses of few hundred GeV. (Notice that the former are generated via gluon-induced QCD interactions while the latter via quark-induced EW ones.) This should be manifest as a close inspection of Fig. 12.

In practice, detectable final states do depend on the underlying nature of the exotic particles. The lifetime and decay modes of the latter are determined by the operators that break the Z_2^H symmetry. When Z_2^H is broken significantly exotic fermions can produce a remarkable signature⁸. Since according to our initial assumptions the Z_2^H symmetry is

⁷Recall that we assume three identical generations of the former but only two of the latter. Besides, we allow the existence of only one at a time of either.

⁸If Z_2^H is only slightly broken exotic quarks and non-Higgsinos may live for a long time. Then exotic

mostly broken by the operators involving quarks and leptons of the third generation the exotic quarks decay either via

$$\overline{D} \rightarrow t + \tilde{b}, \quad \overline{D} \rightarrow b + \tilde{t},$$

if exotic quarks \overline{D}_i are diquarks or via

$$\begin{aligned} D &\rightarrow t + \tilde{\tau}, & D &\rightarrow \tau + \tilde{t}, \\ D &\rightarrow b + \tilde{\nu}_\tau, & D &\rightarrow \nu_\tau + \tilde{b}, \end{aligned}$$

if exotic quarks of type D are leptoquarks. Because in general sfermions decay into corresponding fermion and neutralino one can expect that each diquark will decay further into t - and b -quarks while a leptoquark will produce a t -quark and τ -lepton in the final state with rather high probability. Thus the presence of light exotic quarks in the particle spectrum could result in an appreciable enhancement of the cross section of either $pp \rightarrow t\bar{t}b\bar{b} + X$ and $pp \rightarrow b\bar{b}b\bar{b} + X$ if exotic quarks are diquarks or $pp \rightarrow t\bar{t}\tau^+\tau^- + X$ and consequently $pp \rightarrow b\bar{b}\tau^+\tau^- + X$ if new quark states are leptoquarks⁹. In compliance with our initial assumptions non-Higgsinos decay predominantly into either quarks and squarks or leptons and sleptons of the third generation as well, i.e.

$$\begin{aligned} \tilde{H}^0 &\rightarrow t + \tilde{t}, & \tilde{H}^0 &\rightarrow \bar{t} + \tilde{t}, \\ \tilde{H}^0 &\rightarrow b + \tilde{b}, & \tilde{H}^0 &\rightarrow \bar{b} + \tilde{b}, \\ \tilde{H}^0 &\rightarrow \tau + \tilde{\tau}, & \tilde{H}^0 &\rightarrow \bar{\tau} + \tilde{\tau}, \\ \tilde{H}^- &\rightarrow b + \tilde{t}, & \tilde{H}^- &\rightarrow \bar{t} + \tilde{b}, \\ \tilde{H}^- &\rightarrow \tau + \tilde{\nu}_\tau, & \tilde{H}^- &\rightarrow \bar{\nu}_\tau + \tilde{\tau}. \end{aligned}$$

If we assume again that a sfermion decays predominantly into the corresponding fermion and neutralino then also the production of non-Higgsinos should lead to a significant enlargement of the cross sections of $Q\bar{Q}Q^{(\prime)}\bar{Q}^{(\prime)}$ and $Q\bar{Q}\tau^+\tau^-$ production, where Q is a heavy quark of the third generation, that allows to identify these particles if they are light enough.

As each t -quark decays into a b -quark whereas a τ -lepton gives one charged lepton l in the final state with a probability of 35%, both these scenarios would generate an excess in the b -quark production cross section. In this respect SM data samples which should be altered by the presence of exotic D -quarks or non-Higgsinos are those involving $t\bar{t}$ quarks will form compound states with ordinary quarks. It means that at future colliders it may be possible to study the spectroscopy of new composite scalar leptons or baryons. Also one can observe quasi-stable charged colourless fermions with zero lepton number.

⁹It is worth to remind here that the production cross sections of $pp \rightarrow t\bar{t}b\bar{b} + X$ and $pp \rightarrow t\bar{t}\tau^+\tau^- + X$ in the SM are suppressed *at least* by a factor $\left(\frac{\alpha_s}{\pi}\right)^2$ and $\left(\frac{\alpha_W}{\pi}\right)^2$ respectively as compared to the cross section of $t\bar{t}$ pair production (and, similarly, for t -quarks replaced by b -quarks).

production and decay as well as direct $b\bar{b}$ production. For this reason, Fig. 13 also shows the cross sections for these two genuine SM processes alongside those for the exotica. Detailed LHC analyses will be required to establish the feasibility of extracting the excess due to the light exotic particles predicted by our model. However, Fig. 13 should clearly make the point that – for the discussed parameter configuration – one is in a favourable position in this respect, as the rates for the exotica times their BRs into the aforementioned decay channels are typically larger than the expected four-body cross sections involving heavy quarks and/or leptons.

The situation will experimentally be much easier at a future ILC. Here, under the same assumptions as above concerning their decay patterns, both species of exotic particles should contribute to the inclusive hadronic cross section, see Fig. 14. Assuming, again, the mass choice $\mu_{Di} = \mu_{Hi} = 300$ GeV, the onset at 600 GeV of the exotic pair production threshold would clearly be visible above the SM continuum (with or without a much heavier Z' , again, with $M_{Z'} = 1.5$ TeV). The rise of the hadronic cross section at $\sqrt{s} = 2\mu_{Di} = 2\mu_{Hi}$ would be different, depending on the kind of exotic particles being generated, owing to the different EW charges involved and the fact that three generations of light D 's can be allowed in our model as opposed to only two in the case of light \tilde{H} 's (as already intimated). Furthermore, the line shape of the Z' resonance would be different too, depending on whether one or the other kind of exotic matter is allowed. Both the enormous luminosity and extremely clean environment of an ILC, joined with a significant degree of control on the beam energy spread, should allow one to explore in detail all such possible features of the hadronic cross section. In fact, as the actual value of the ILC beam energy has yet to be fixed and our illustrative choice for μ_{Di} and μ_{Hi} may not correspond to what nature has chosen, we present in Fig. 15 the mass dependence of the pair production cross section for our exotic states at two reference collider energies, of 700 GeV and identical to the Z' mass. While the scope for exotic D -quark production at the ILC has probably little to add to what could be obtained earlier at the LHC, a TeV scale e^+e^- linear collider is definitely crucial in increasing the discovery reach in mass for non-Higgsinos beyond the limits obtainable at the CERN hadronic machine.

8. Conclusions

In this paper we have made a comprehensive study of the theory and phenomenology of a low energy supersymmetric standard model originating from a string-inspired E_6 grand unified gauge group, which we called Exceptional Supersymmetric Standard Model, or ESSM for short. The ESSM considered here is based on the low energy SM gauge group together with an extra Z' corresponding to an extra $U(1)_N$ gauge symmetry under which

right-handed neutrinos have zero charge. This allows right-handed neutrinos to gain large Majorana masses, resulting in the conventional (high-scale) seesaw mechanism for neutrino masses. The extra $U(1)_N$ gauge symmetry survives to the TeV scale, and forbids the term $\mu H_d H_u$ in the superpotential, but permits the term $\lambda S(H_u H_d)$, where S is a low energy singlet that carries $U(1)_N$ charge and breaks the gauge symmetry when it develops its VEV, giving rise to a massive Z' and an effective μ term. Therefore the μ problem of the MSSM is solved in a similar way to that in the NMSSM, but without the accompanying problems of singlet tadpoles or domain walls since there is no S^3 term, and the would-be Goldstone boson is eaten by the Z' .

The low energy matter content of the ESSM corresponds to three 27 representations of the E_6 symmetry group, to ensure anomaly cancellation, plus an additional pair of Higgs-like doublets as required for high energy gauge coupling unification. The ESSM is therefore a low energy alternative to the MSSM or NMSSM. The ESSM involves extra matter beyond the MSSM contained in three $5 + 5^*$ representations of $SU(5)$, plus a total of three $SU(5)$ singlets which carry $U(1)_N$ charges. Thus there are three families of new exotic charge 1/3 quarks and non-Higgs multiplets predicted in the ESSM, in addition to the Z' .

As in the MSSM, the gauge symmetry of the ESSM does not forbid baryon and lepton number violating interactions that result in rapid proton decay. The straightforward generalisation of R-parity, assuming that the exotic quarks carry the same baryon number as the ordinary ones, guarantees not only proton stability but also the stability of the lightest exotic quark. The presence of heavy stable exotic quarks, that should survive annihilation, is ruled out by different experiments. Therefore the R-parity definition in the ESSM has to be modified. There are two different ways to impose an appropriate Z_2 symmetry that lead to two different versions of the ESSM where baryon and lepton number is conserved. ESSM version I implies that exotic quarks have twice larger baryon number than the ordinary quark fields. In the ESSM version II exotic quarks carry baryon and lepton numbers simultaneously.

Because the supermultiplets of exotic matter interact with the quark, lepton and Higgs superfields the Lagrangian of the ESSM includes many new Yukawa couplings. In general these couplings give rise to the processes with non-diagonal flavour transitions that have not been observed yet. In order to suppress flavour changing processes and to provide the correct breakdown of gauge symmetry we assumed a hierarchical structure of the Yukawa interactions, and imposed an approximate Z_2^H symmetry under which all superfields are odd except Higgs doublets (H_u and H_d) and singlet field S . With these assumptions only one SM singlet field S may have appreciable couplings with exotic quarks and $SU(2)$ doublets H_{1i} and H_{2i} and the couplings are flavour diagonal. It also follows that only one

pair of $SU(2)$ Higgs doublets H_d and H_u have Yukawa couplings to the ordinary quarks and leptons of order unity. The Yukawa couplings of other exotic particles to the quarks and leptons of the first two generations must be less than 10^{-4} and 10^{-3} respectively in order to suppress FCNCs. We would like to emphasise that from the perspective of REWSB these assumptions are completely natural. Without loss of generality it is always possible to work in a basis where only one family of singlets S and Higgs doublets H_d and H_u have VEVs and the remaining states do not (the non-Higgs). Then REWSB makes it natural that the so defined Higgs fields have large couplings to third family quarks and leptons, while the non-Higgs fields have small couplings.

We have analysed the RG flow of the gauge and Yukawa couplings in the framework of the ESSM taking into account kinetic term mixing between $U(1)_Y$ and $U(1)_N$. Imposing the gauge coupling unification at high energies we have found that the gauge coupling of the extra $U(1)_N$ is very close to the $U(1)_Y$ gauge coupling while the off-diagonal gauge coupling which describes the mixing between $U(1)_Y$ and $U(1)_N$ is negligibly small. Since by construction extra exotic quarks and non-Higgses fill in complete $SU(5)$ representations the Grand Unification scale remains almost the same as in the MSSM. At the same time the overall gauge coupling g_0 that characterises gauge interactions above the scale M_X is considerably larger than in the MSSM: $g_0 \simeq 1.21$. The increase of the gauge couplings at the Grand Unification and intermediate scales in the ESSM is caused by the extra supermultiplets of exotic matter.

The growth of $g_i(Q)$ relaxes the restrictions on the Yukawa couplings coming from the validity of perturbation theory up to the scale M_X as compared with the MSSM. In particular h_t and λ can take larger values at the EW scale than in the constrained MSSM and NMSSM. If the top-quark Yukawa coupling is large at the Grand Unification scale, i.e. $h_t(M_X) \gtrsim 1$, the solutions of the RG equations for the Yukawa couplings in the gaugeless limit approach the invariant line and along this line are attracted to the quasi-fixed point where $\lambda(M_t)$ is going to zero. After the inclusion of gauge couplings, the valley along which the solutions of RG equations flow to the fixed point disappear but their convergence to the fixed point becomes even stronger. The analysis of the RG flow shows that the Yukawa couplings of top- and exotic quarks tend to dominate over the Yukawa couplings of non-Higgs supermultiplets that are considerably larger than λ at the EW scale. However the solutions for the Yukawa couplings are concentrated near the fixed points only when $h_t(M_X)$ is large enough that corresponds to $\tan \beta \simeq 1 - 1.1$. At moderate and large values of $\tan \beta$ the values of the Yukawa couplings at the EW scale may be quite far from the stable fixed point. As a result for values of $\tan \beta \gtrsim 1.5$ the coupling $\lambda(M_t)$ can be comparable with the top-quark Yukawa coupling.

We have used the above theoretical restrictions on $\tan \beta$ and λ for the analysis of the

Higgs, neutralino and chargino sectors of the ESSM. Although the particle content of the ESSM involves many particles with similar quantum number only one singlet field S and two Higgs doublets H_u and H_d acquire VEVs breaking the $SU(2) \times U(1)_Y \times U(1)_N$ symmetry. Since the Higgs sector of the ESSM contains only one new field S and one additional parameter compared to the MSSM it can be regarded as the simplest extension of the Higgs sector of the MSSM. As in the MSSM, the ESSM Higgs sector does not provide extra sources for the CP-violation at tree-level. The ESSM Higgs spectrum includes three CP-even, one CP-odd and two charged states. The singlet dominated CP-even state is always almost degenerate with the Z' gauge boson. The masses of another CP-even and charged Higgs fields are set by the mass of pseudoscalar state m_A . The lightest CP-even Higgs boson is confined around the EW scale. The superpartners of the Z' boson and singlet field S also contribute to the ESSM neutralino spectrum while the number of states in the chargino sector remain the same as in the MSSM. The masses of extra states in the neutralino sector are governed by $M_{Z'}$.

The qualitative pattern of the Higgs, neutralino and chargino spectra in the ESSM is determined by the Yukawa coupling λ . When $\lambda \ll g_1$ (the MSSM limit of the ESSM) new states in the Higgs and neutralino sectors become very heavy and decouple from the rest of the spectrum making them indistinguishable from the MSSM ones. In the case when $\lambda \gtrsim g_1$ the lightest Higgs scalar can be heavier than in the MSSM and NMSSM. In this case the vacuum stability requirement constrains m_A so that the heaviest CP-even, CP-odd and charged states lie beyond the TeV range. It means that in this case only the lightest Higgs scalar can be discovered at the LHC and ILC. We have found that the mass of the lightest Higgs particle does not exceed 150 GeV.

If $\lambda \gtrsim g_1$ then the heaviest chargino and neutralino are formed by the neutral and charged superpartners of the Higgs doublets H_u and H_d . Extra neutralino states are lighter than the heaviest one but still too heavy to be observed in the near future. The lightest chargino is predominantly superpartner of W^\pm gauge bosons while the lightest neutralino state is basically bino. We have obtained the approximate solutions for the masses and couplings of the Higgs particles as well as for the masses of the lightest neutralino and chargino.

As we have already mentioned the ESSM predicts the existence of many new exotic quarks and non-Higgsinos. They compose vector-like multiplets of matter with respect to the SM gauge group, so that the axial couplings of the SM gauge bosons to exotic particles vanish. As a consequence their contributions to the EW observables measured at LEP are suppressed by inverse powers of their masses. The contribution of the Z' is also negligibly small since the latter is supposed to be very heavy and practically does not mix with the Z boson. At the same time Z' , exotic quarks and non-Higgsinos can be

produced directly at future colliders if they are light enough. The lifetime of new exotic particles is defined by the extent to which the Z_2^H symmetry is broken. If Z_2^H was exact the lightest exotic quark would be absolutely stable. Since we have assumed that Z_2^H is mainly broken by the operators involving quarks and leptons of the third generation the exotic quarks decay into either two heavy quarks $Q\bar{Q}$ or a heavy quark and a lepton $Q\tau(\nu_\tau)$, where Q is either a b - or t -quark. If exotic quarks are light enough they will be intensively produced at the LHC. In the case when Z_2^H is broken significantly this results in the growth of the cross section of either $pp \rightarrow Q\bar{Q}Q^{(\prime)}\bar{Q}^{(\prime)} + X$ or $pp \rightarrow Q\bar{Q}l^+l^- + X$, with $l = e, \mu$. If the violation of the Z_2^H invariance is extremely small then a set of new baryons or composite leptons containing quasi-stable exotic quarks could be discovered at the LHC. As compared with the exotic quarks the production of non-Higgsinos will be rather suppressed at the LHC. In contrast, at an ILC the production rates of exotic quarks and non-Higgsinos can be comparable allowing their simultaneous observation. The Z' gauge boson has to be detected at the LHC if it has a mass below $4 - 4.5$ TeV.

The ESSM can in principle be derived from a rank-6 model which naturally arises after the breakdown of the E_6 symmetry via the Hosotani mechanism near the string or Grand Unification scale M_X . The discovery at future colliders of the exotic particles and extra Z' boson predicted by the ESSM would therefore represent a possible indirect signature of an underlying E_6 gauge structure at high energies, and provide circumstantial evidence for superstring theory.

Acknowledgements

The authors are grateful to A. Djouadi, J. Kalinowski, D. J. Miller and P. M. Zerwas for valuable comments and remarks. RN would also like to thank E. Boos, D. I. Kazakov and M. I. Vysotsky for fruitful discussions. The authors acknowledge support from the PPARC grant PPA/G/S/2003/00096, the NATO grant PST.CLG.980066 and the EU network MRTN 2004-503369.

Figure captions

Fig. 1. (a) RG flow of a set of points in the $(\lambda/h_t)-(\kappa/h_t)$ plane in the gaugeless limit ($g_0 = 0$). (b) The running of $\left(\frac{\lambda(\mu)}{h_t(\mu)}\right)$ versus $\left(\frac{\kappa(\mu)}{h_t(\mu)}\right)$. The gauge couplings are included. In both cases the energy scale μ is varied from M_X to M_t , $h_t(M_X) = 10$, while the Yukawa couplings of the exotic quark and non-Higgs supermultiplets of the first and second generations are set to zero. Different trajectories correspond to different initial conditions for λ and κ at the scale M_X .

Fig. 2. (a) The allowed range of the parameter space in the $(\kappa/h_t)-(\lambda/h_t)$ plane for $\kappa_1 = \kappa_2 = \lambda_1 = \lambda_2 = 0$ and $\tan\beta = 2$ where the couplings are evaluated at the top mass $\mu = M_t$. (b) RG flow of $\left(\frac{\kappa(\mu)}{h_t(\mu)}\right)$ versus $\left(\frac{\lambda(\mu)}{h_t(\mu)}\right)$ for $\tan\beta = 2$. The Yukawa couplings of the exotic quark and non-Higgs supermultiplets of the first and second generations are taken to be zero. Different trajectories correspond to different initial conditions at the EW scale. The solutions of the RG equations flow from the left to the right when the RG scale changes from M_t to M_X . (c) Upper limit on (κ/h_t) versus (λ/h_t) for $\kappa_1 = \kappa_2 = \kappa$, $\lambda_1 = \lambda_2 = 0$ and $\tan\beta = 2$. (d) The allowed part of the parameter space in the $(\kappa/h_t)-(\lambda/h_t)$ plane for $\kappa_1 = \kappa_2 = \kappa$, $\lambda_1(M_t) = \lambda_2(M_t) = \lambda(M_t)$ and $\tan\beta = 2$.

Fig. 3. Upper limit on λ versus $\tan\beta$.

Fig. 4. Higgs masses and couplings for $\lambda(M_t) = 0.794$, $\tan\beta = 2$, $M_{Z'} = M_S = 700$ GeV and $X_t = \sqrt{6}M_S$. (a) The dependence of the lightest Higgs boson mass on m_A . (b) One-loop masses of the CP-even Higgs bosons versus m_A . Solid, dashed and dashed-dotted lines correspond to the masses of the lightest, second lightest and heaviest Higgs scalars respectively. (c) One-loop masses of the CP-odd, heaviest CP-even and charged Higgs bosons versus m_A . Dotted, dashed-dotted and solid lines correspond to the masses of the charged, heaviest scalar and pseudoscalar states. (d) Absolute values of the relative couplings R_{ZZh_i} of the Higgs scalars to Z pairs. Solid, dashed and dashed-dotted curves represent the dependence of the couplings of the lightest, second lightest and heaviest CP-even Higgs states to Z pairs on m_A . (e) Absolute values of the relative couplings $R_{ZA h_i}$ of the CP-even Higgs bosons to the Higgs pseudoscalar and Z as a function of m_A . The notations are the same as in Fig. 4c.

Fig. 5. Higgs masses and couplings for $\lambda(M_t) = 0.3$, $\tan\beta = 2$, $M_{Z'} = M_S = 700$ GeV and $X_t = \sqrt{6}M_S$. (a) The dependence of the lightest Higgs boson mass on m_A . (b) One-loop masses of the Higgs scalars versus m_A . (c) One-loop masses of the CP-odd, heaviest CP-even and charged Higgs states versus m_A . (d) Absolute values of the relative

couplings R_{ZZh_i} of the CP-even Higgs bosons to Z pairs. (e) Absolute values of the relative couplings $R_{ZA h_i}$ of the Higgs scalars to the Higgs pseudoscalar and Z as a function of m_A . The notations are the same as in Fig. 4.

Fig. 6. (a) Different contributions to the tree-level upper bound on m_{h_1} in the ESSM versus $\tan\beta$. Solid line represents the tree-level theoretical restriction on the lightest Higgs boson mass in the MSSM: $M_Z|\cos 2\beta|$. Dash-dotted line is a contribution of extra $U(1)_N$ D -term: $g'_1 v \left| \tilde{Q}_1 \cos^2 \beta + \tilde{Q}_2 \sin^2 \beta \right|$. Dotted line is the maximum possible contribution of the F -term corresponding to the SM singlet field S : $\frac{\lambda}{\sqrt{2}} v \sin 2\beta$. (b) tree-level upper bound on the lightest Higgs boson mass as a function of $\tan\beta$. The solid, lower and upper dotted lines correspond to the theoretical restrictions on m_{h_1} in the MSSM, NMSSM and ESSM respectively.

Fig. 7. (a) One-loop upper bound on the lightest Higgs boson mass as a function of the Yukawa couplings in the $(\lambda/h_t)-(\kappa/h_t)$ plane for $\kappa_1(M_t) = \kappa_2(M_t) = 0$ and $\kappa_3(M_t) = \kappa$. (b) One-loop upper limit on m_{h_1} versus Yukawa couplings in the $(\lambda/h_t)-(\kappa/h_t)$ plane for $\kappa_1(M_t) = \kappa_2(M_t) = \kappa_3(M_t) = \kappa$. (c) Two-loop upper limit on m_{h_1} as a function of the Yukawa couplings in the $(\lambda/h_t)-(\kappa/h_t)$ plane for $\kappa_1(M_t) = \kappa_2(M_t) = 0$ and $\kappa_3(M_t) = \kappa$. (d) Two-loop upper bound on the mass of the lightest Higgs scalar versus Yukawa couplings in the $(\lambda/h_t)-(\kappa/h_t)$ plane for $\kappa_1(M_t) = \kappa_2(M_t) = \kappa_3(M_t) = \kappa$. Thick, solid, dash-dotted and dashed lines in Figs. 7a–7d correspond to $m_h = 160, 150, 140, 130$ GeV respectively. The dotted line represent the allowed range of the parameter space for $\lambda_1(M_t) = \lambda_2(M_t) = 0$. Theoretical restrictions on the lightest Higgs boson mass are obtained for $\tan\beta = 2$, $m_Q^2 = m_U^2 = m_{D_i}^2 = m_{\bar{D}_i}^2 = M_S^2$, $X_t = \sqrt{6}M_S$ and $M_S = 700$ GeV.

Fig. 8. (a) The dependence of the two-loop upper bound on the lightest Higgs boson mass on $\tan\beta$ for $m_t(M_t) = 165$ GeV, $m_Q^2 = m_U^2 = M_S^2$, $X_t = \sqrt{6}M_S$ and $M_S = 700$ GeV. The solid, lower and upper dotted lines represent the theoretical restrictions on m_{h_1} in the MSSM, NMSSM and ESSM respectively. (b) Two-loop upper bound on the mass of the lightest Higgs particle in the MSSM, NMSSM and ESSM versus $\tan\beta$ for $X_t = 0$. Other parameters and notations are the same as in Fig. 8a.

Fig. 9. (a) Neutralino spectrum in the ESSM as function of M_1 for $\lambda(M_t) = 0.794$, $\tan\beta = 2$ and $M_{Z'} = 700$ GeV. (Only the absolute values of the neutralino masses have physical meaning.) (b) Chargino masses versus M_1 . The parameters are the same as in Fig. 9a.

Fig. 10. (a) The dependence of neutralino masses in the ESSM on M_1 for $\lambda(M_t) = 0.3$, $\tan\beta = 2$ and $M_{Z'} = 700$ GeV. (Only the absolute values of the neutralino masses have physical meaning.) (b) Chargino spectrum as function of M_1 . The set of parameters is the same as in Fig. 10a.

Fig. 11. Differential cross section in the final state invariant mass, denoted by M_{l+l-} , at the LHC for Drell-Yan production ($l = e$ or μ only) in presence of a Z' with and without the (separate) contribution of exotic D -quarks or non-Higgsinos \tilde{H} (both via EW interactions), with $\mu_{Di} = \mu_{Hi} = 300$ GeV. Here, $M_{Z'} = 1.5$ TeV.

Fig. 12. Cross section at the LHC for pair production of exotic D -quarks (via QCD interactions) as well as non-Higgsinos \tilde{H} (via EW interactions), as a function of their (common) mass, denoted by M_F . Here, $M_{Z'} = 1.5$ TeV.

Fig. 13. Differential cross section in the final state invariant mass, denoted by M_{FF} , at the LHC for pair production of $b-$, $t-$ and exotic D -quarks (all via QCD interactions) as well as non-Higgsinos \tilde{H} (via EW interactions), with $\mu_{Di} = \mu_{Hi} = 300$ GeV. Note the rescaling of the rates for the first and last process. Here, $M_{Z'} = 1.5$ TeV.

Fig. 14. Energy-dependent hadronic cross section at a future ILC in the SM with an additional Z' , with and without the (separate) contribution of exotic D -quarks or non-Higgsinos \tilde{H} (both via EW interactions), with $\mu_{Di} = \mu_{Hi} = 300$ GeV. Here, $M_{Z'} = 1.5$ TeV.

Fig. 15. Cross section at a future ILC for pair production of exotic D -quarks and of non-Higgsinos \tilde{H} (both via EW interactions), as a function of their (common) mass, denoted by M_F , for two collider energies. Here, $M_{Z'} = 1.5$ TeV.

$$\frac{\lambda(\mu)}{h_t(\mu)}$$

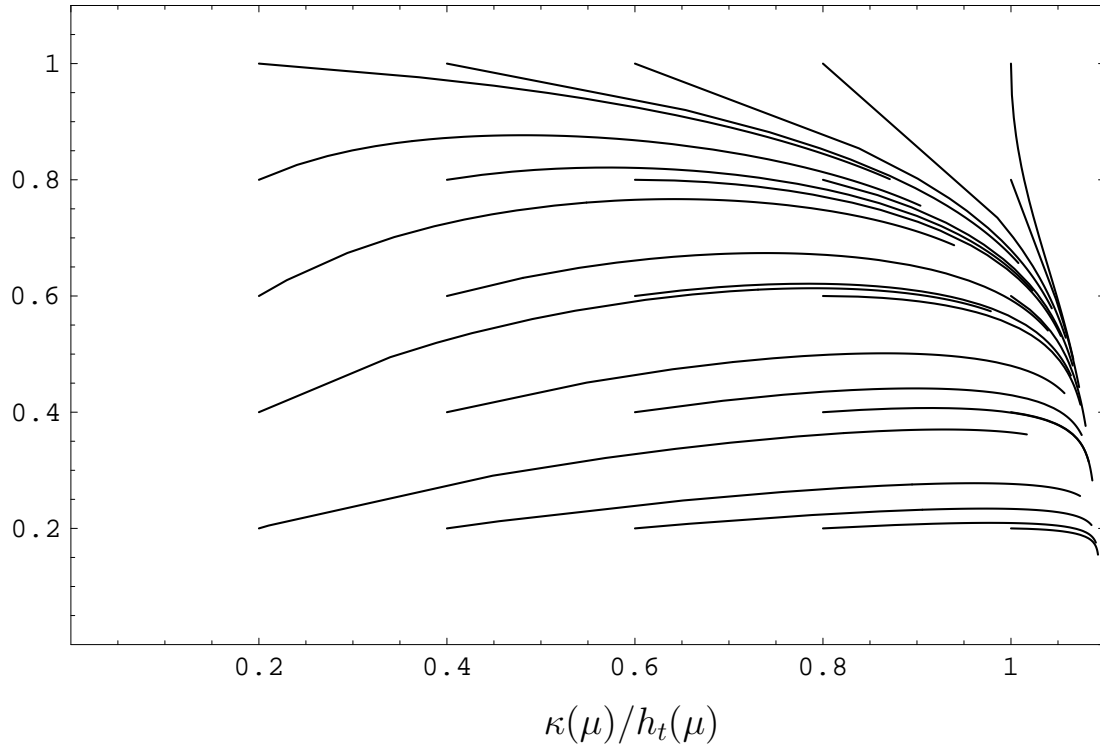


Fig. 1a

$$\frac{\lambda(\mu)}{h_t(\mu)}$$

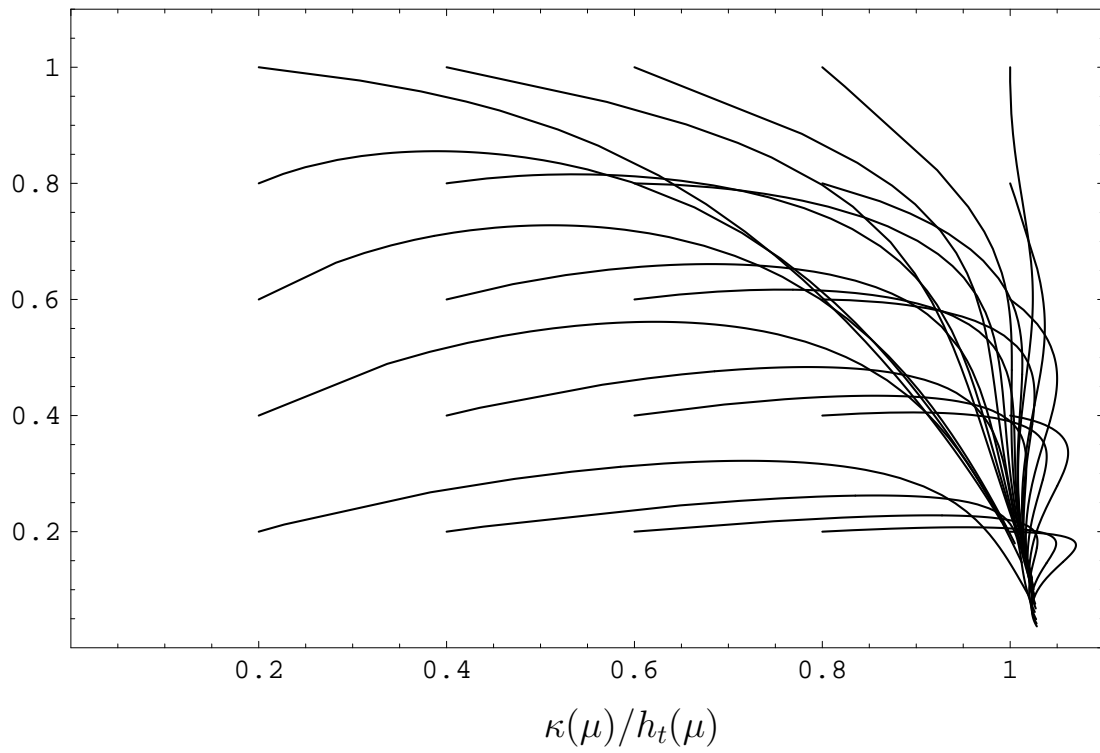


Fig. 1b

$$\frac{\kappa(M_t)}{h_t(M_t)}$$

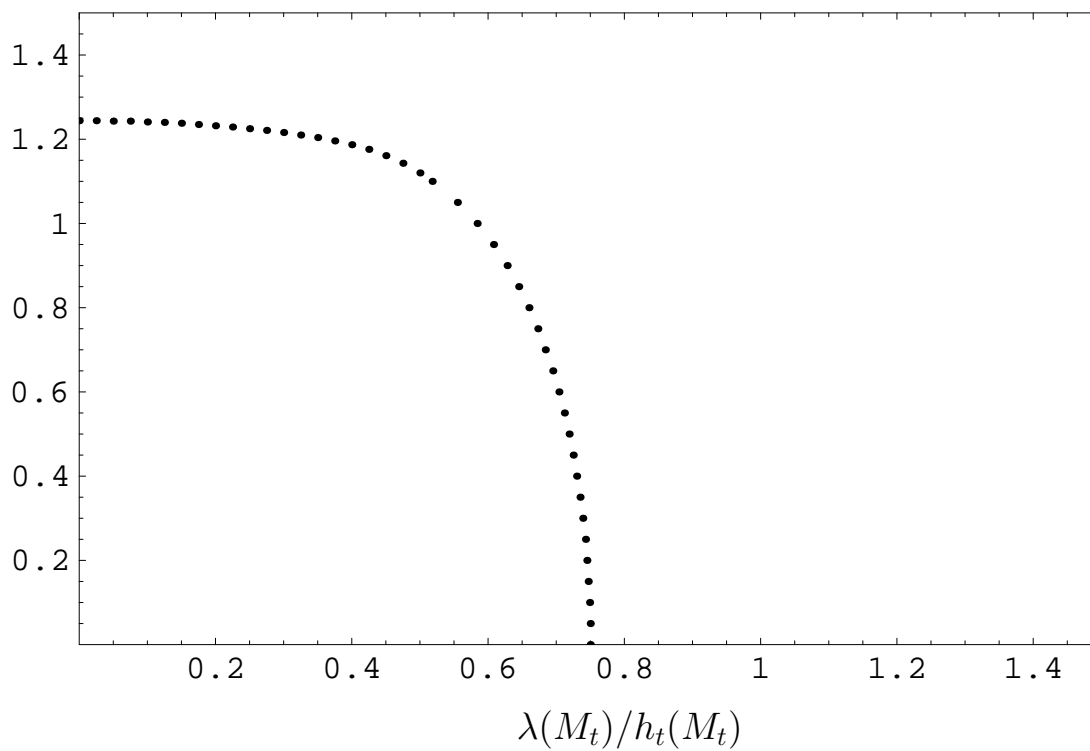


Fig. 2a

$$\frac{\kappa(\mu)}{h_t(\mu)}$$

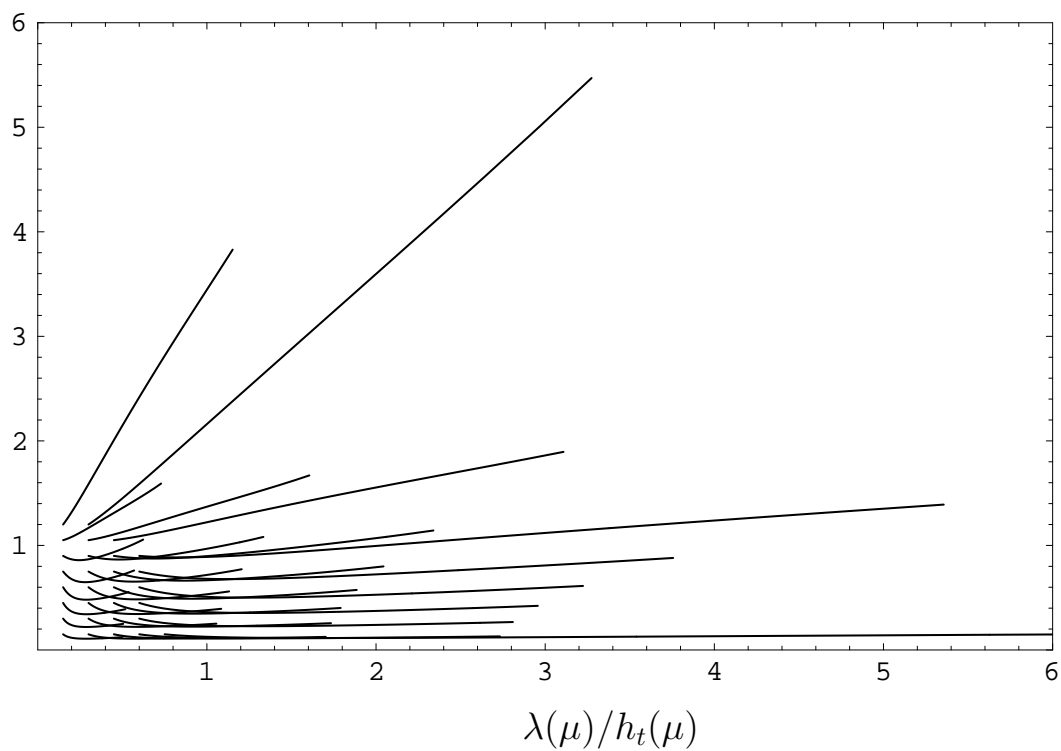


Fig. 2b

$$\frac{\kappa(M_t)}{h_t(M_t)}$$

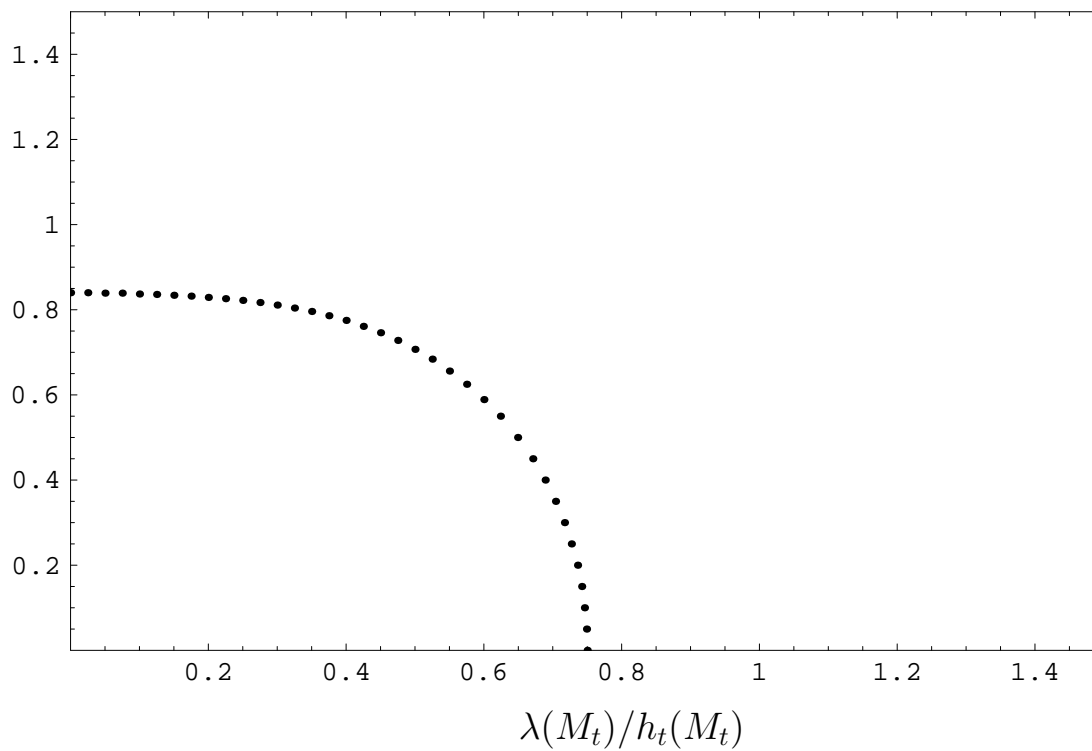


Fig. 2c

$$\frac{\kappa(M_t)}{h_t(M_t)}$$

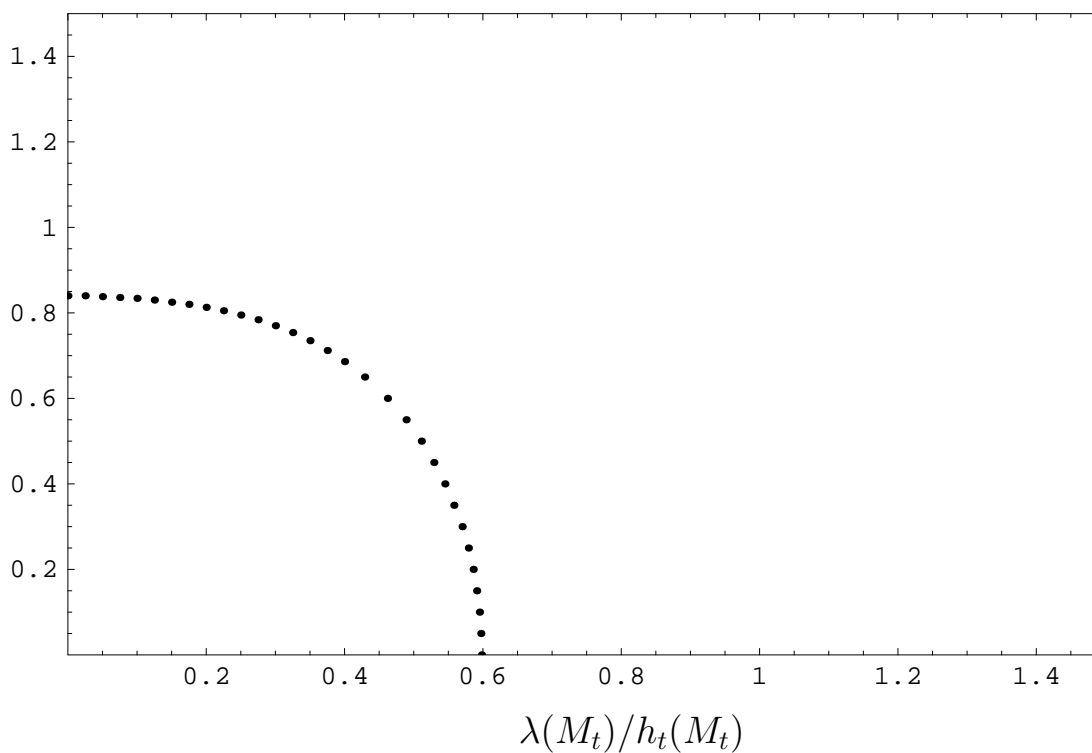


Fig. 2d

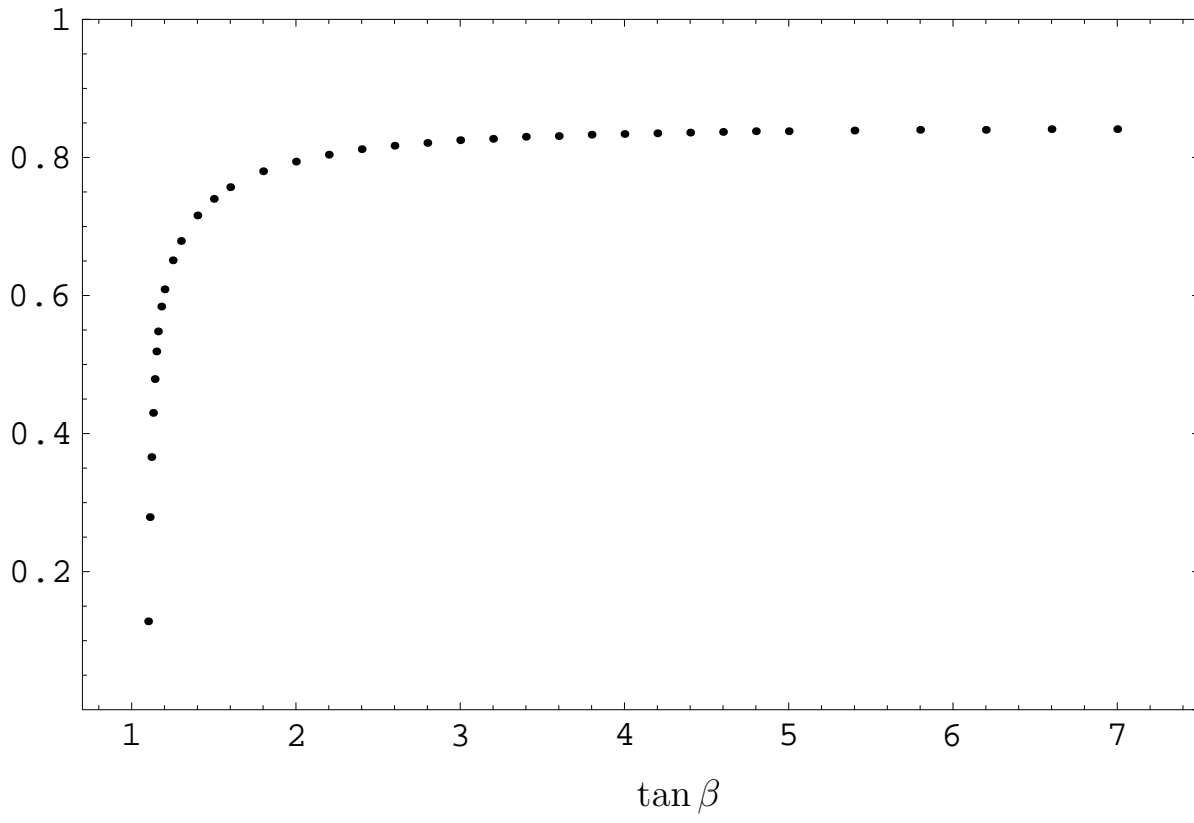
λ_{max} 

Fig. 3

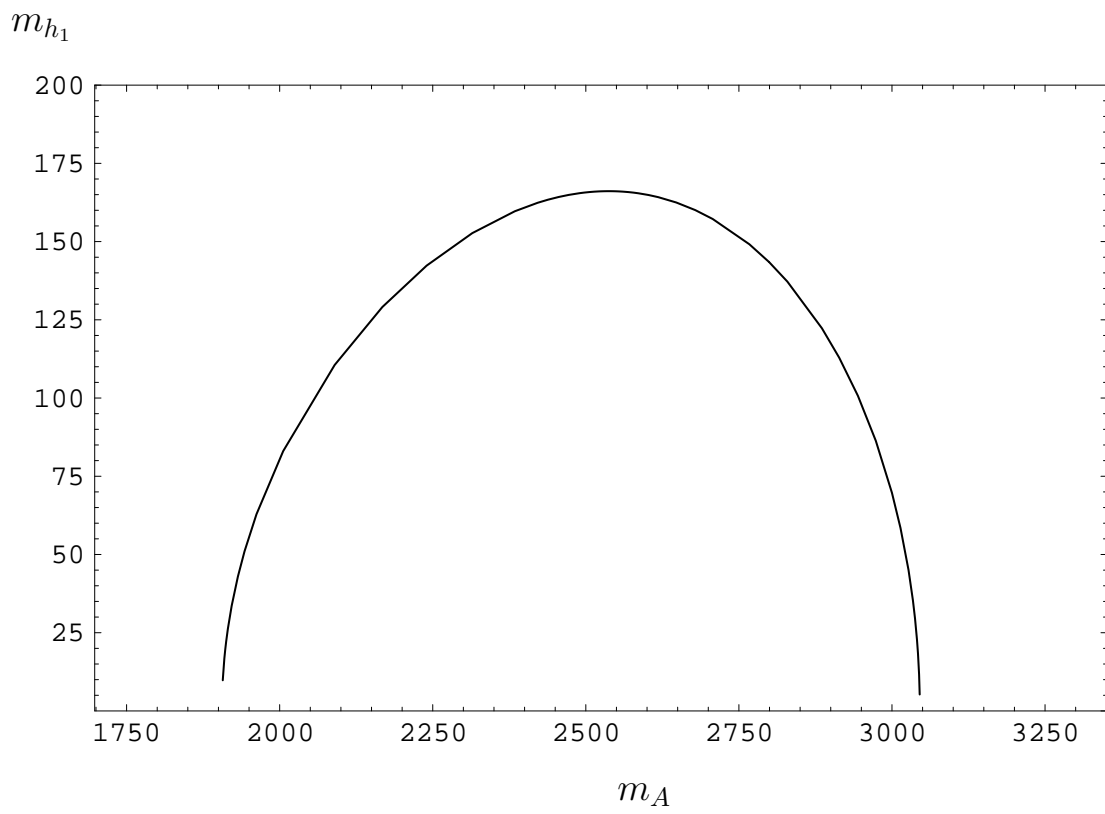


Fig. 4a

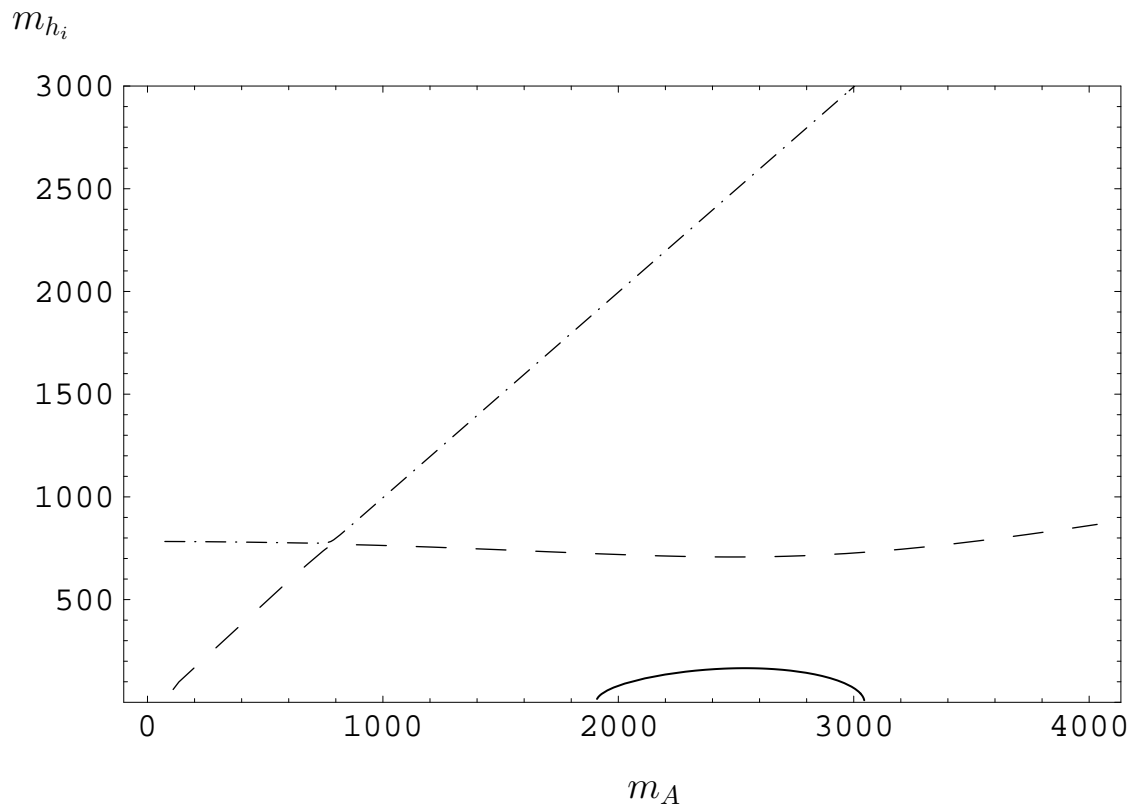


Fig. 4b

m_{A,H^\pm,h_3}

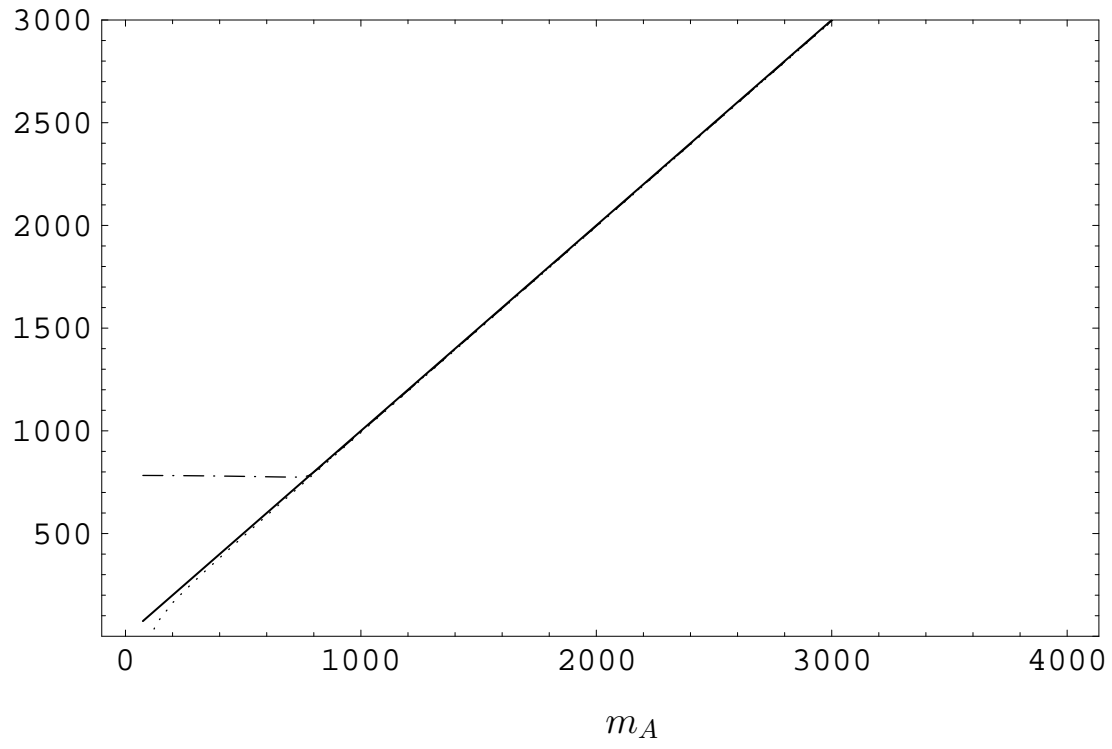


Fig. 4c

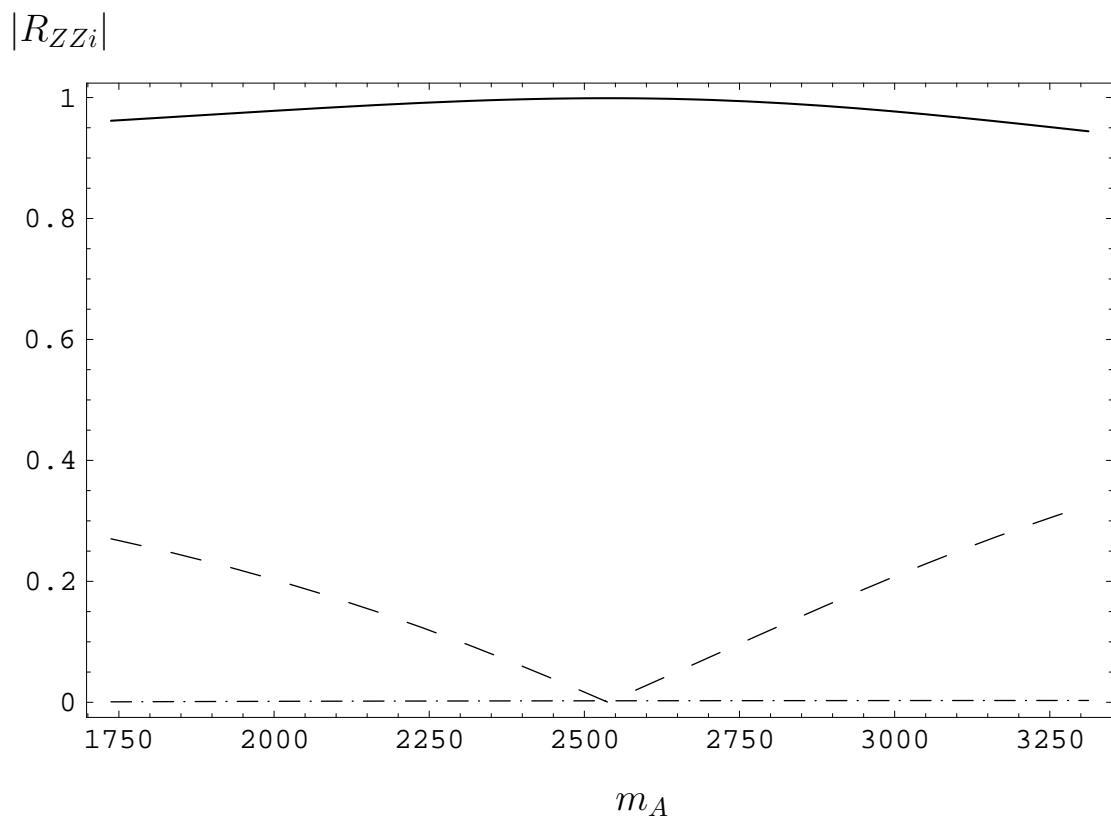


Fig. 4d

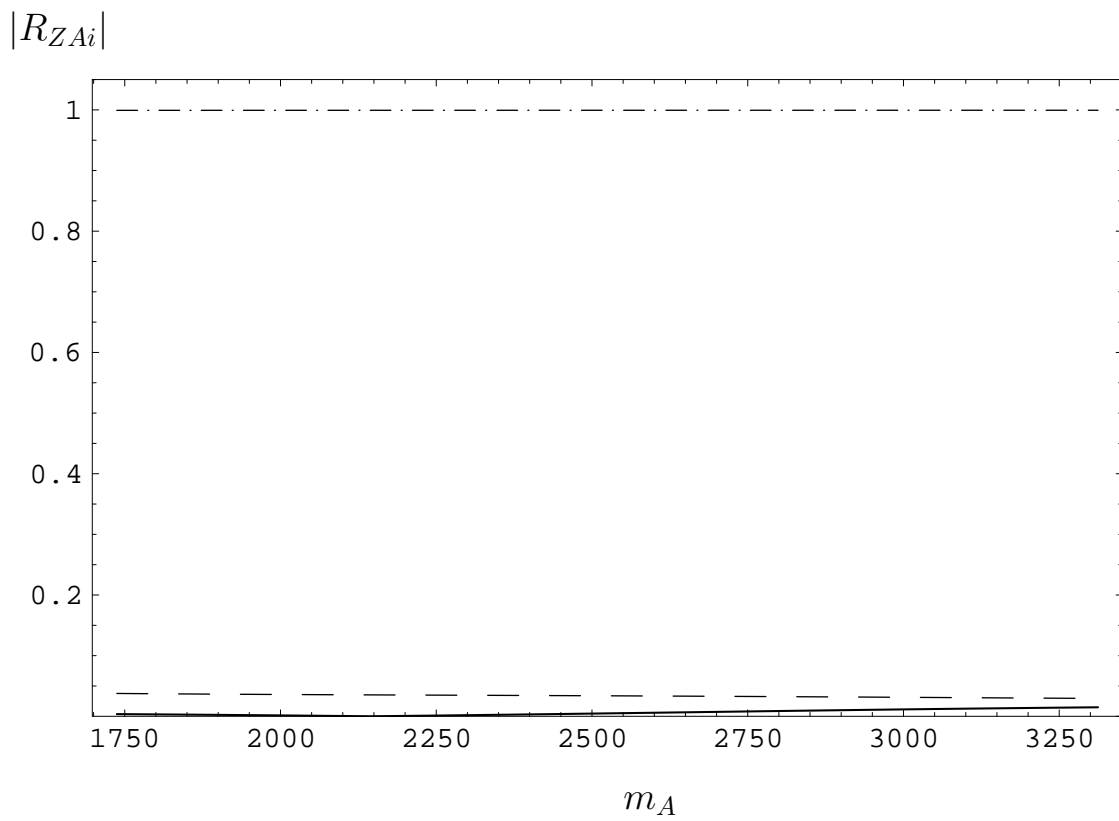


Fig. 4e

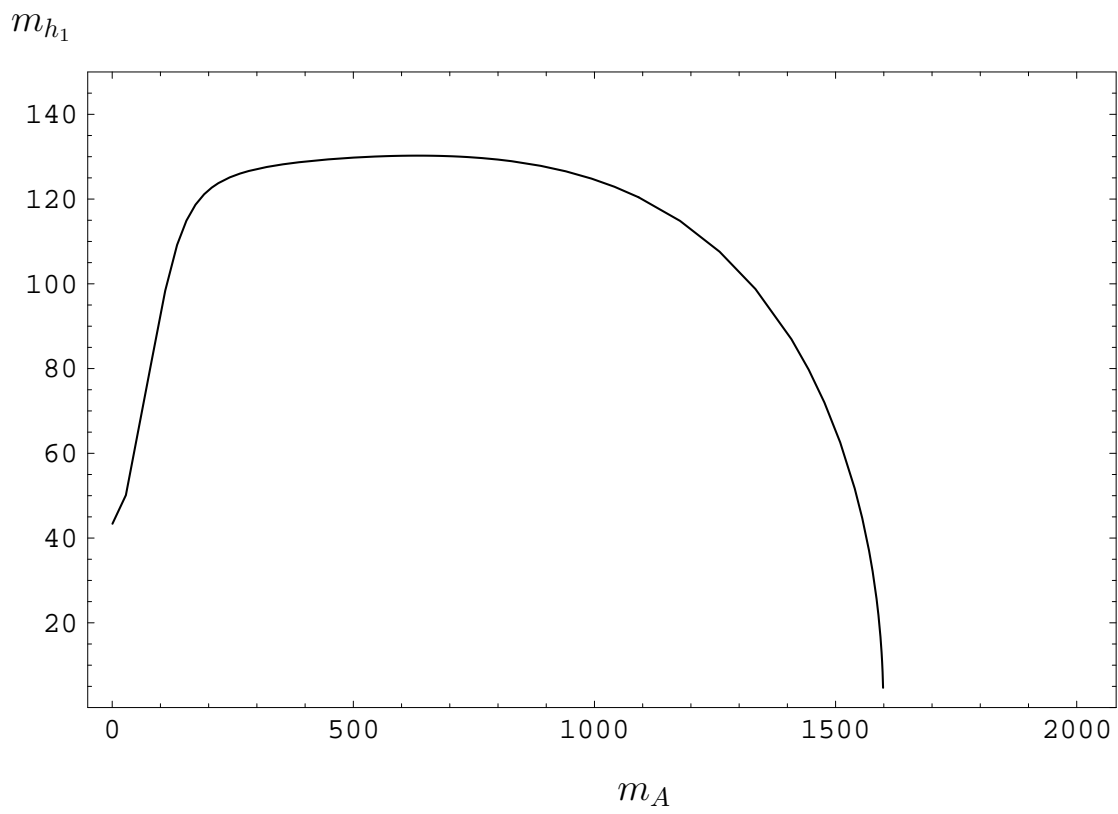


Fig. 5b

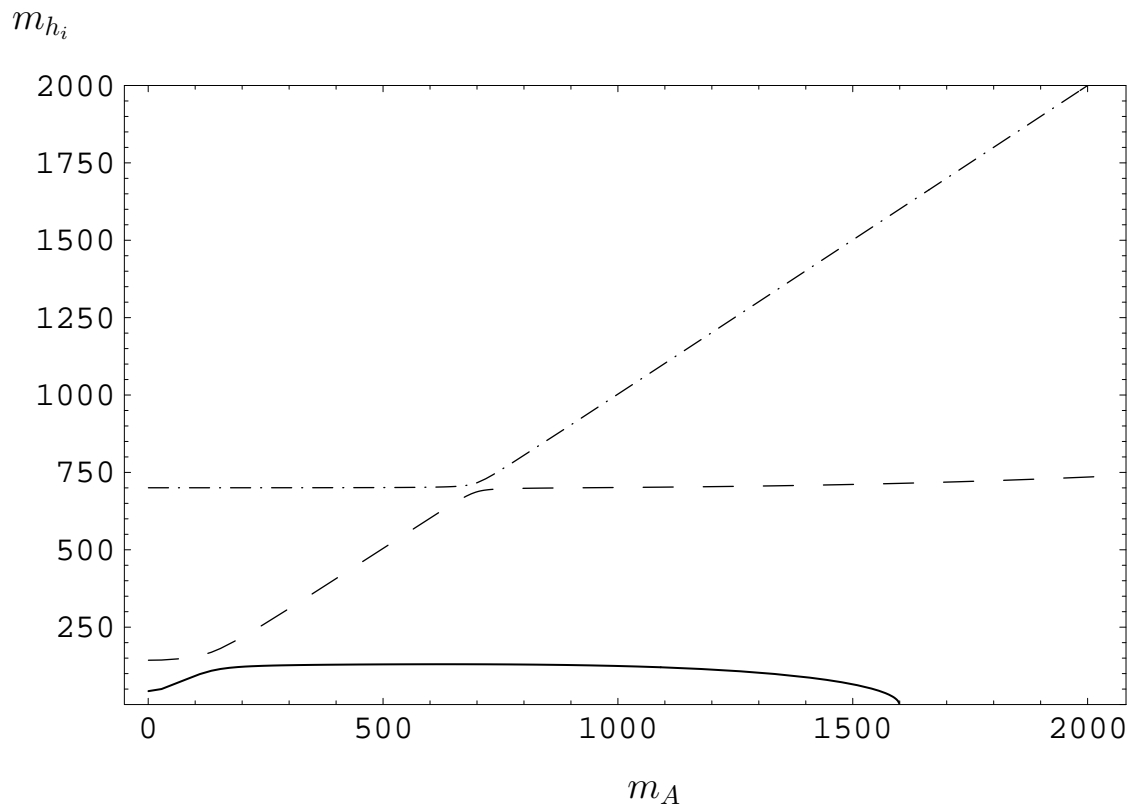


Fig. 5a

m_{A,H^\pm,h_3}

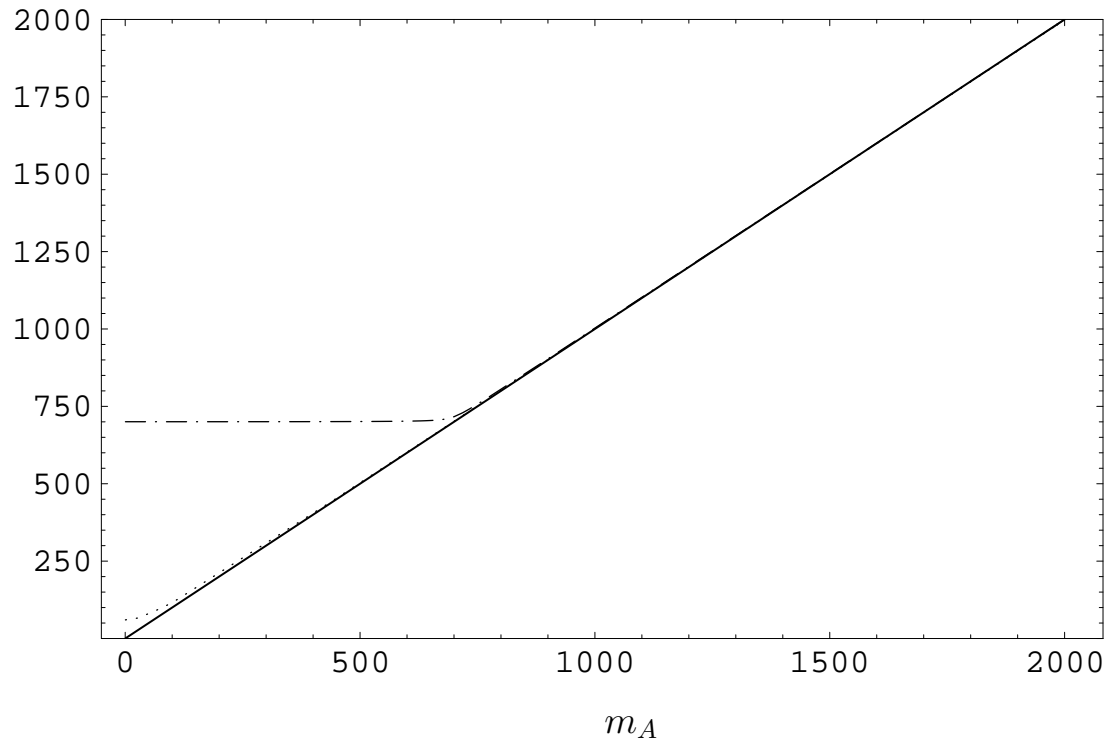


Fig. 5c

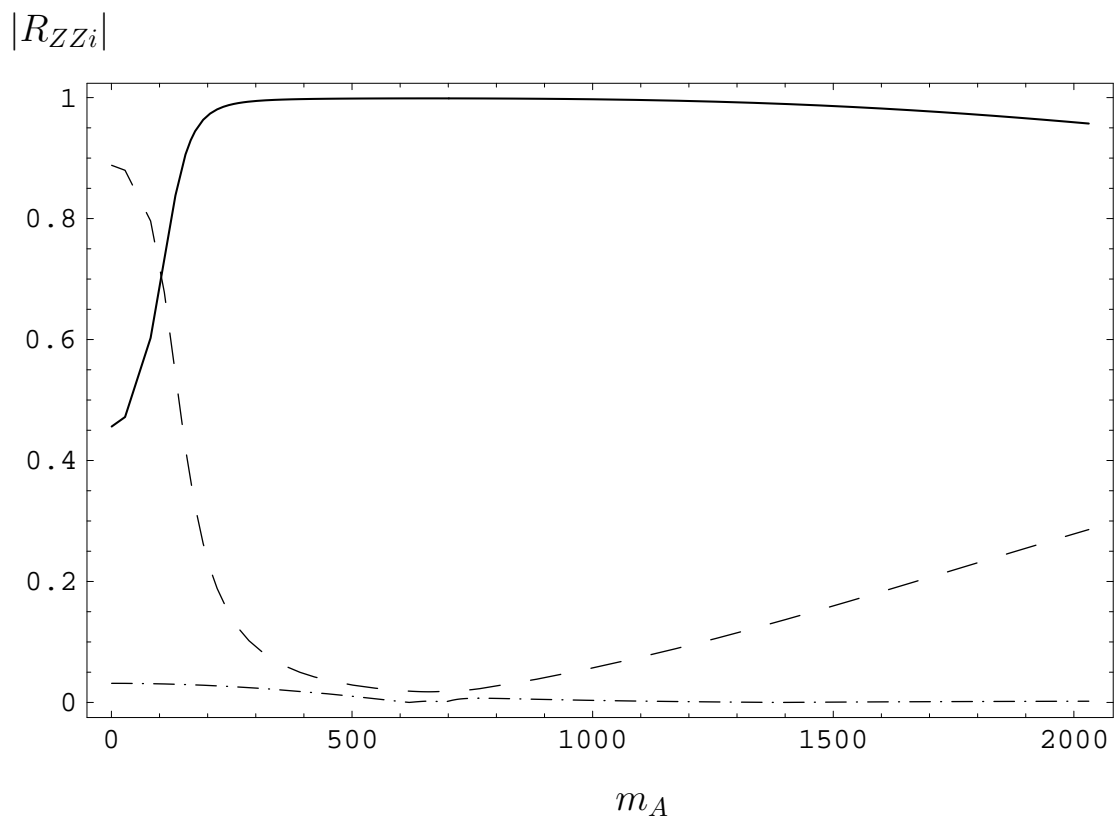


Fig. 5d

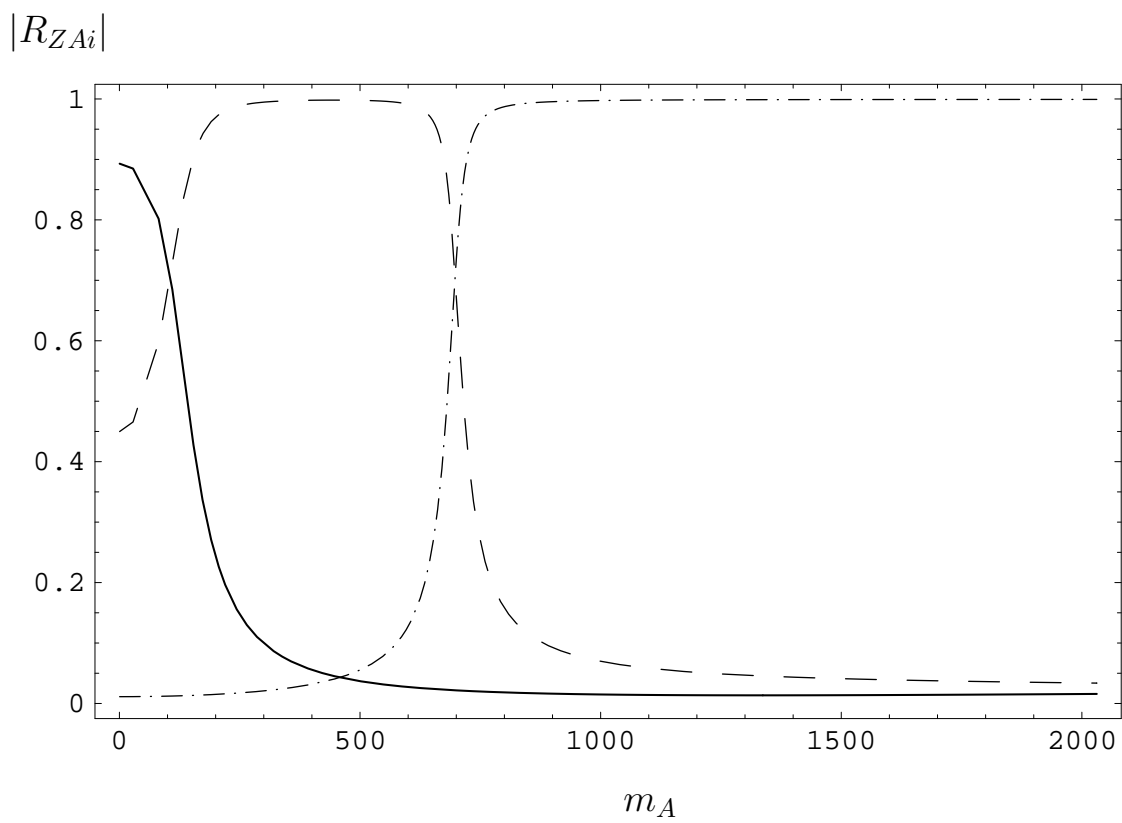


Fig. 5e

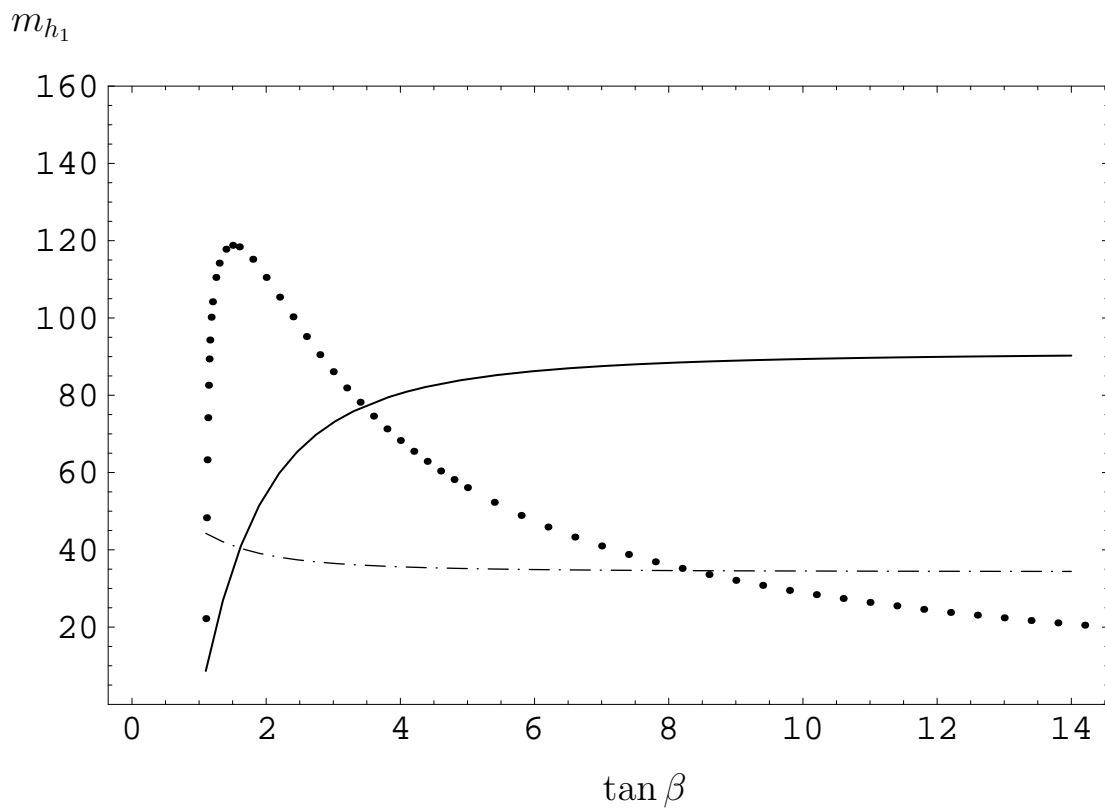


Fig. 6a

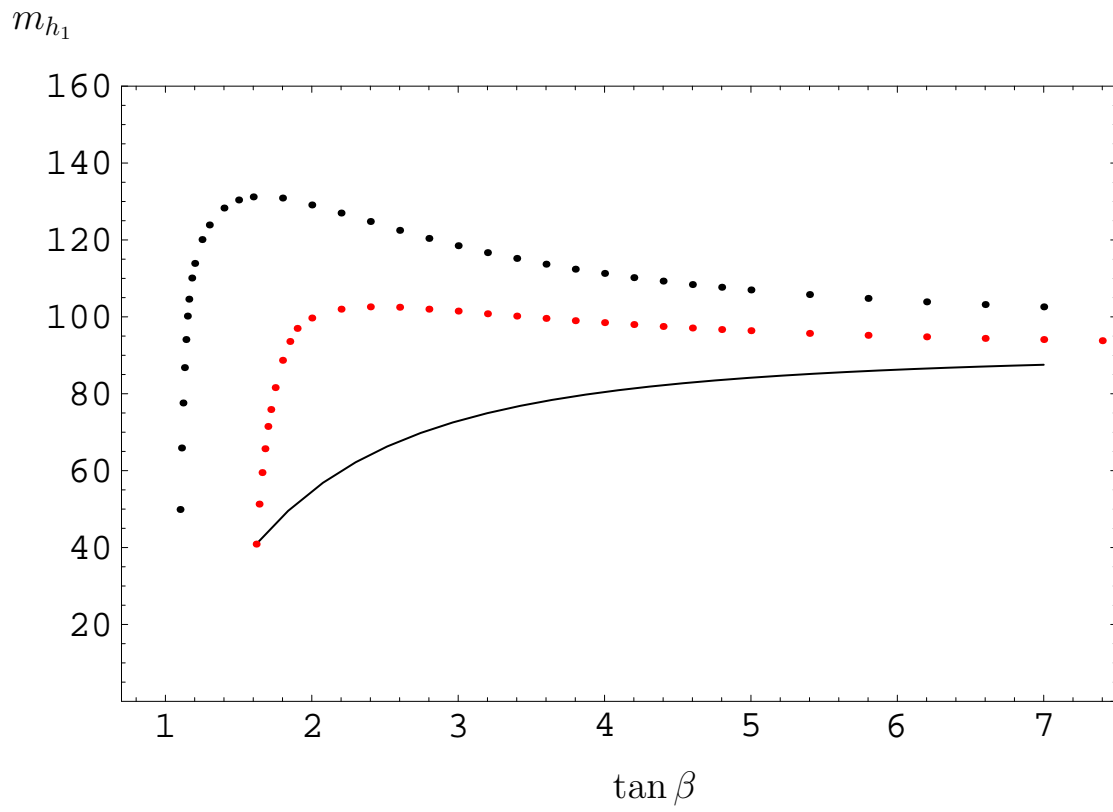


Fig. 6b

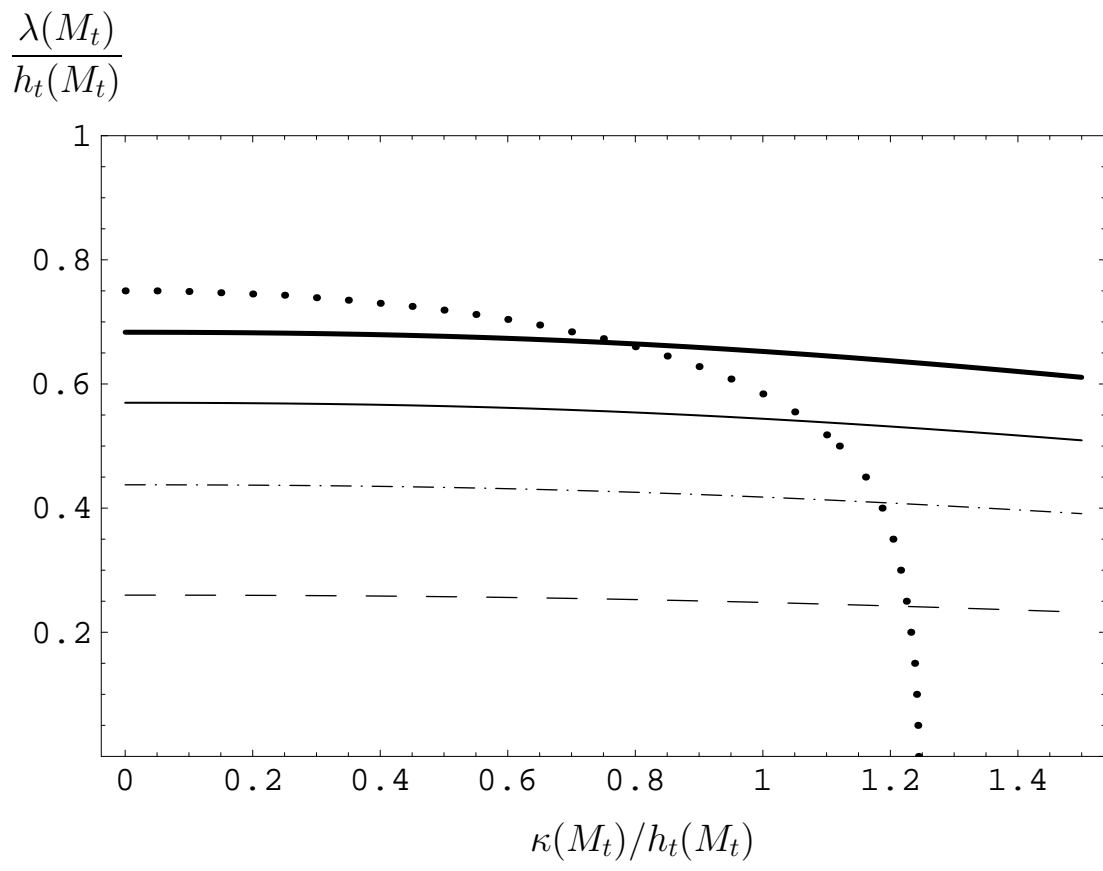


Fig. 7a

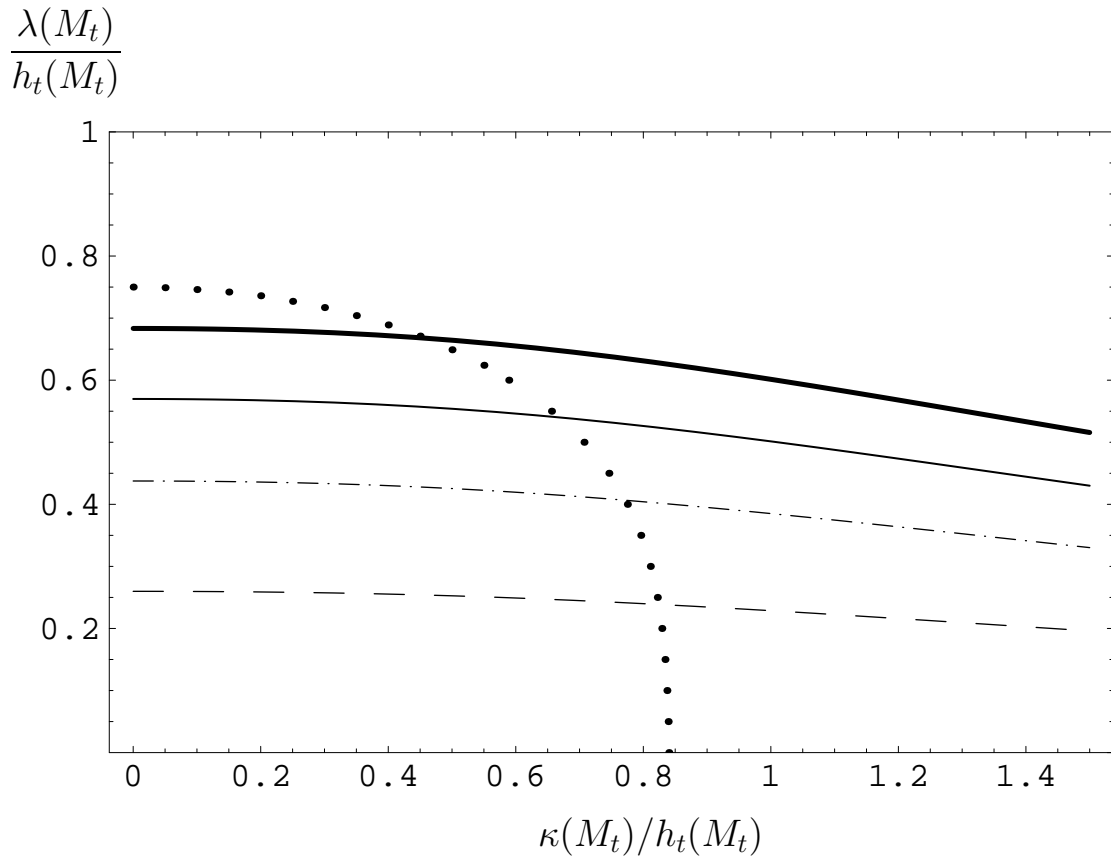


Fig. 7b

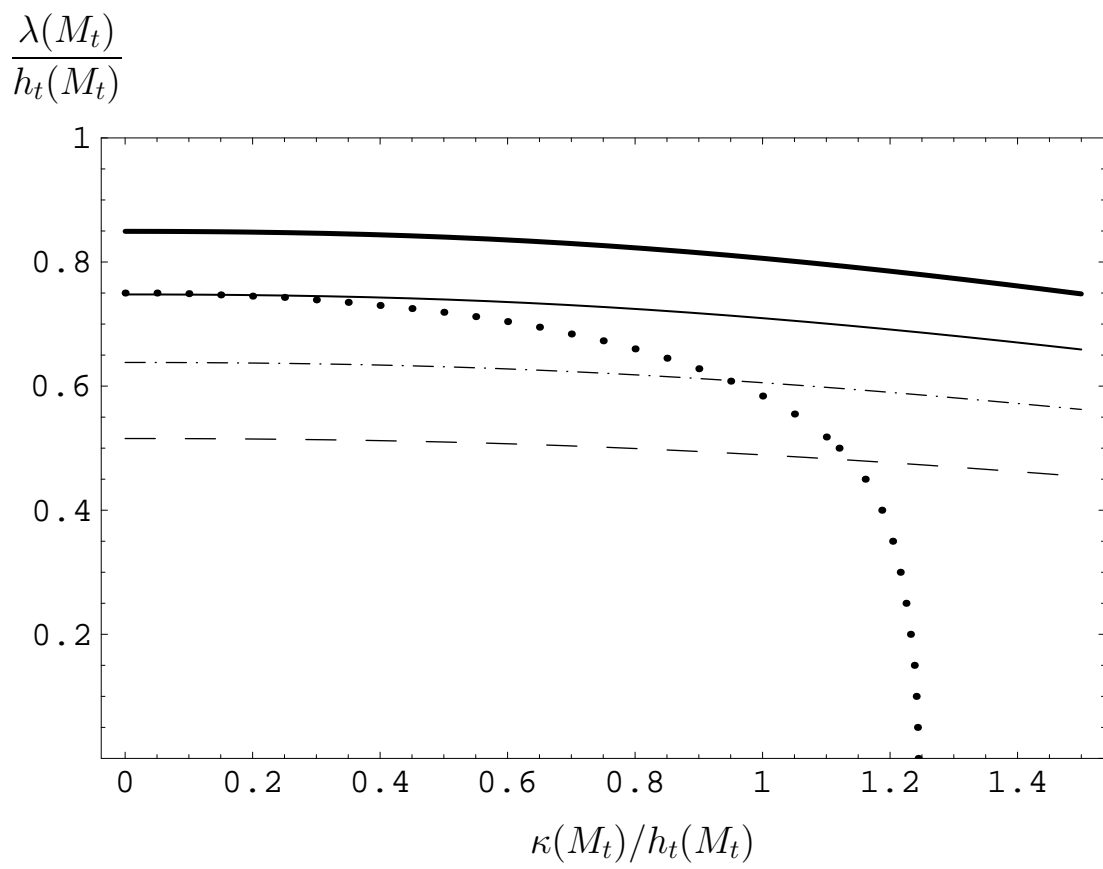


Fig. 7c

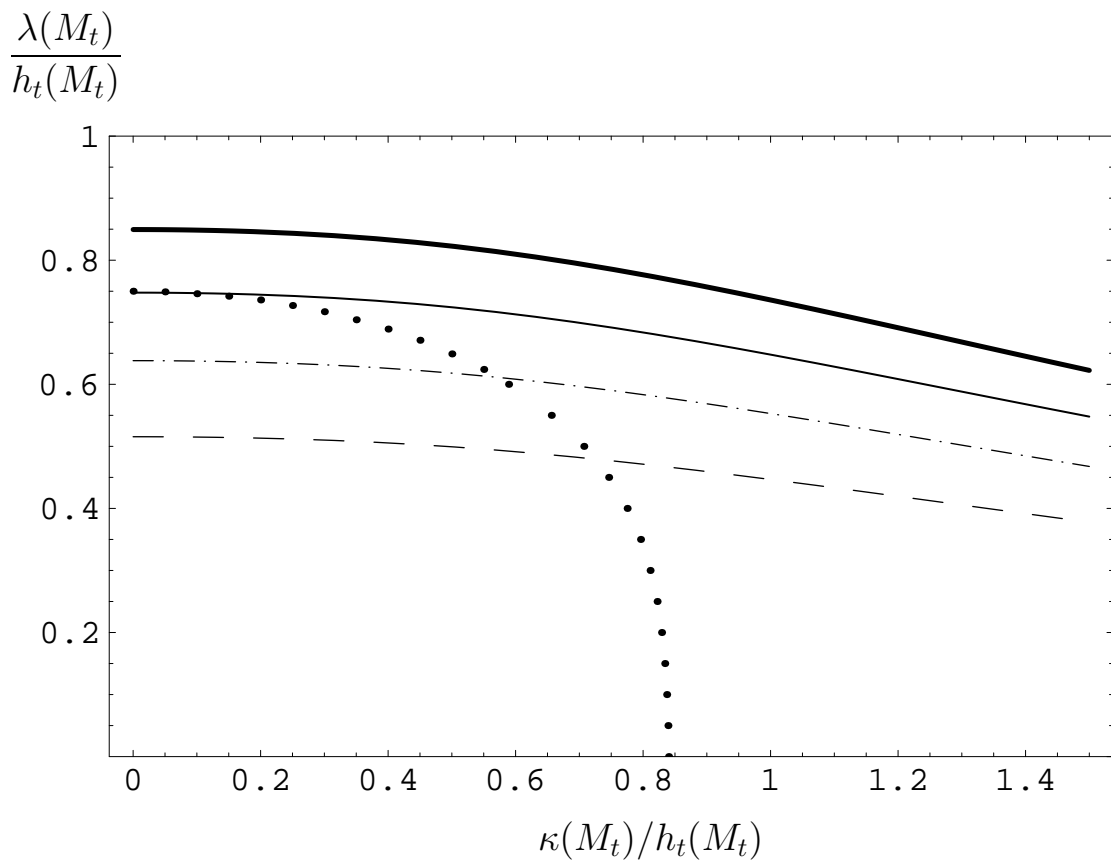


Fig. 7d

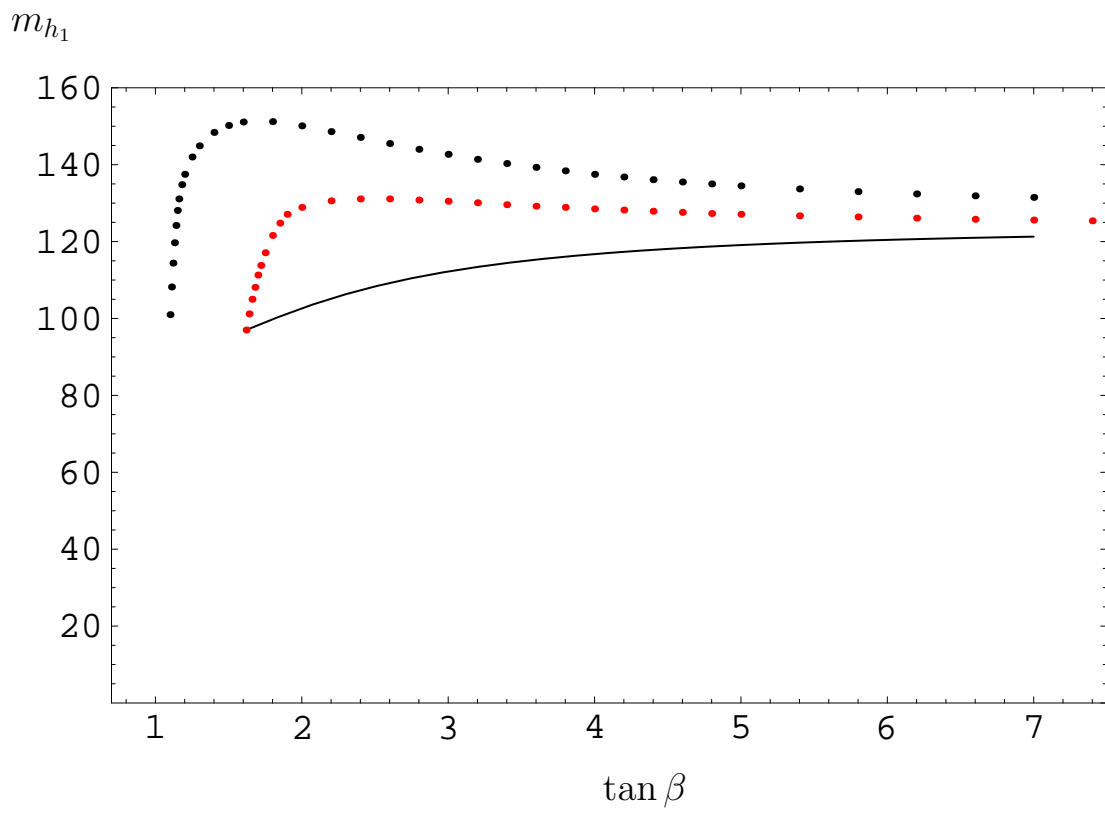


Fig. 8a

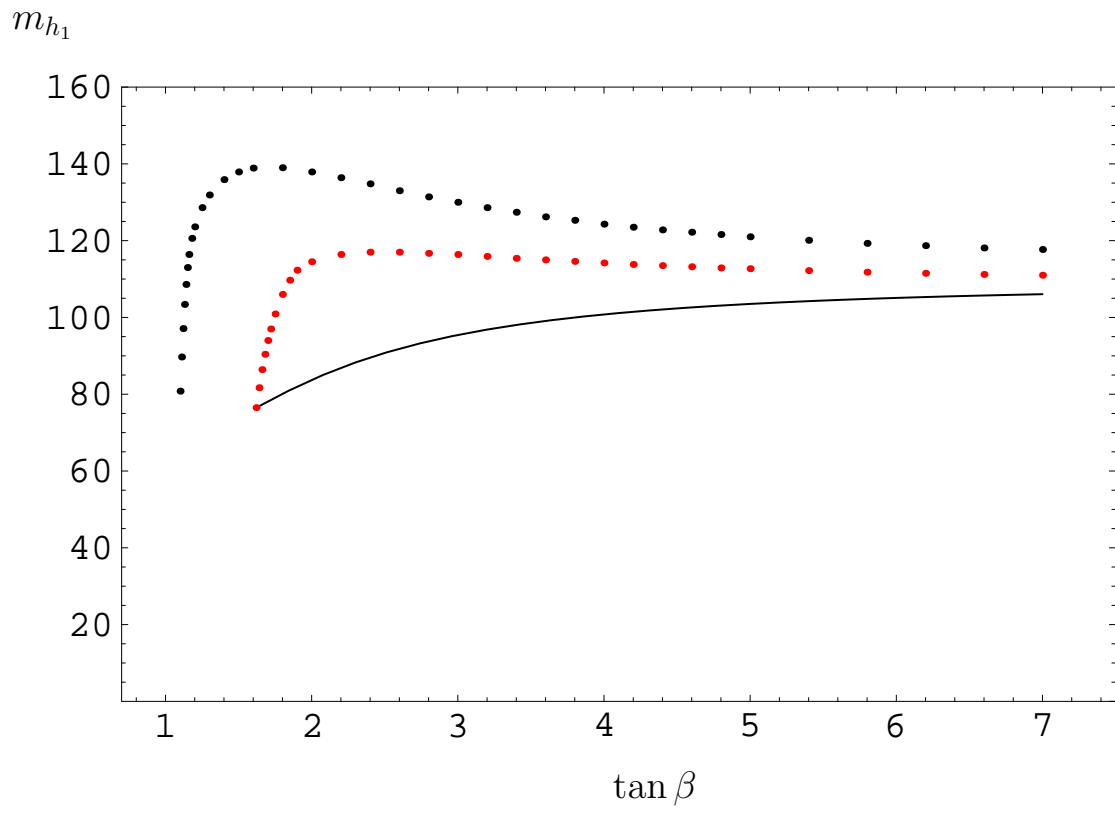
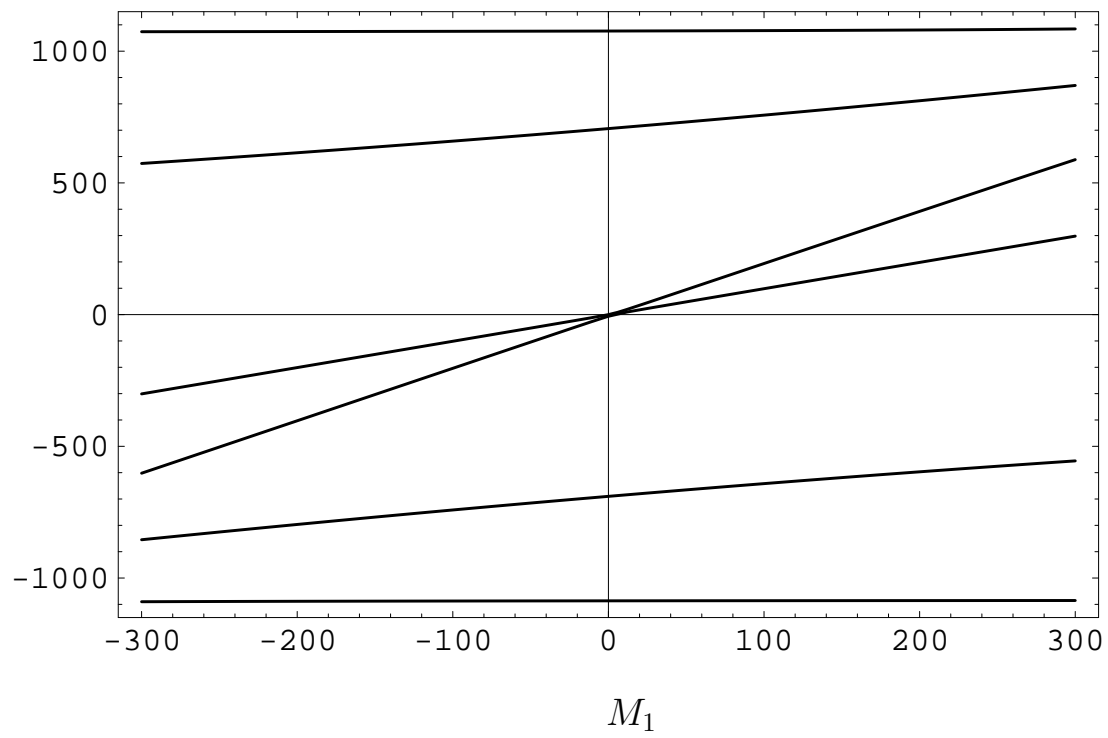
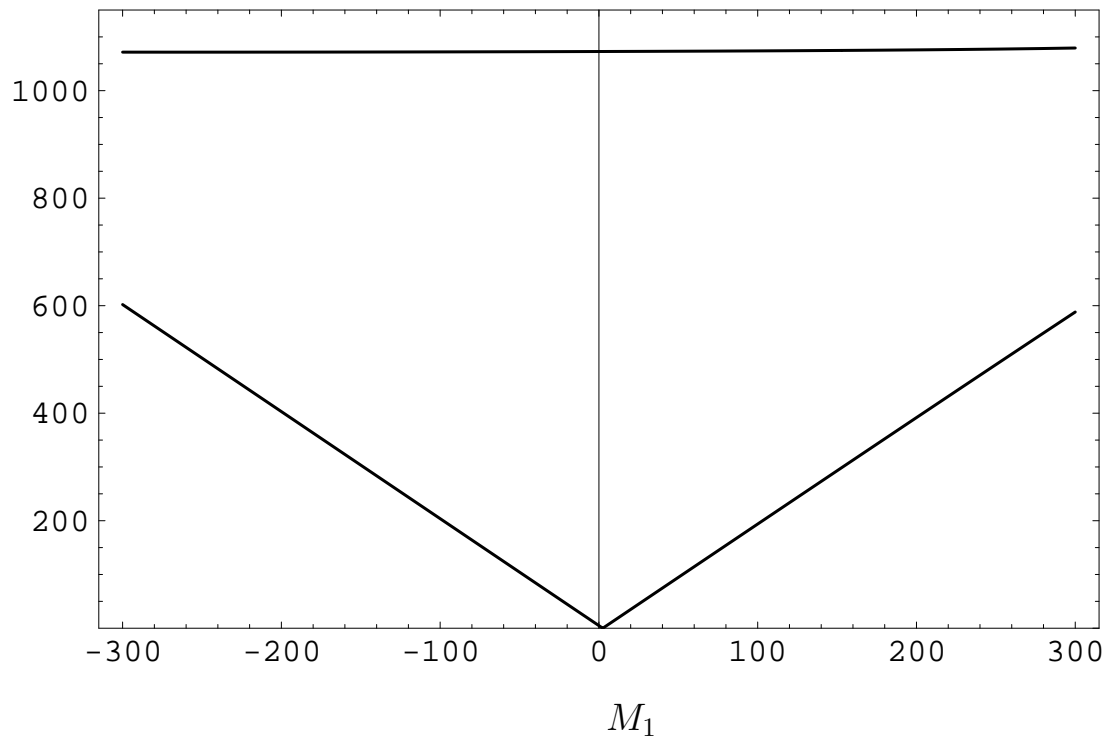


Fig. 8b

m_{χ_i} **Fig. 9a** m_{χ^\pm} **Fig. 9b**

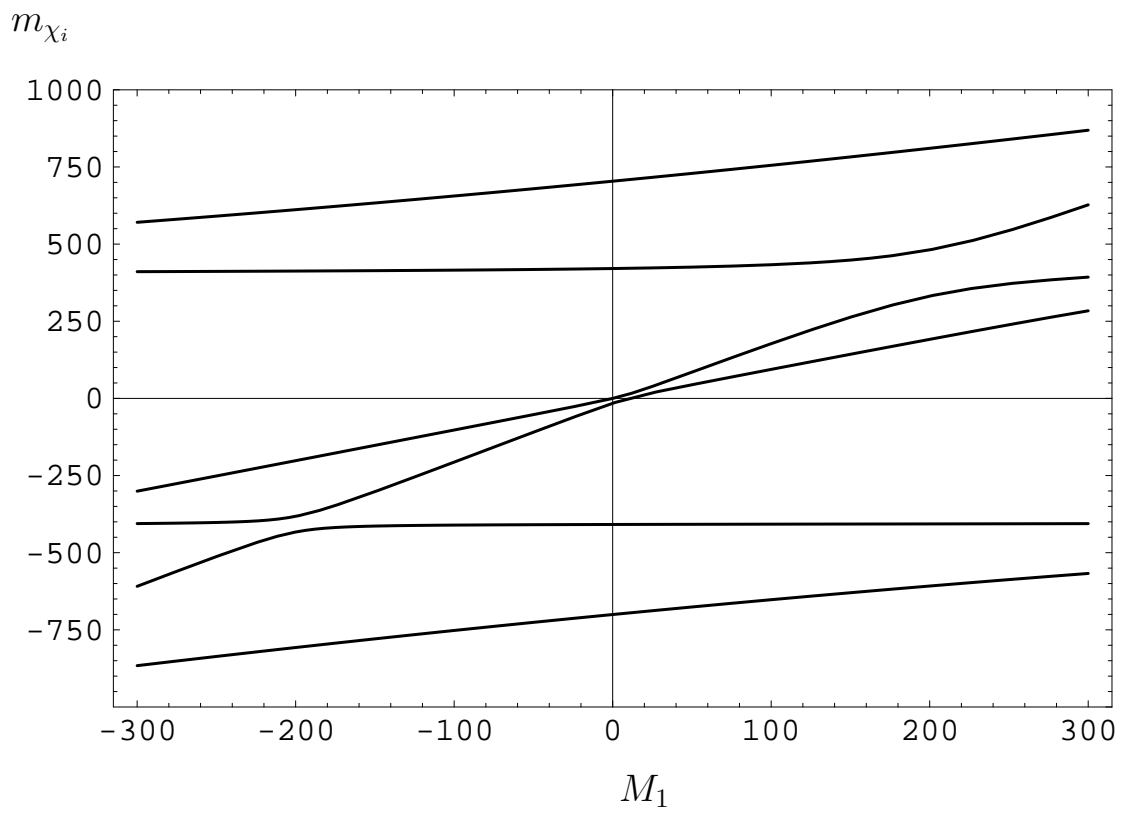


Fig. 10a

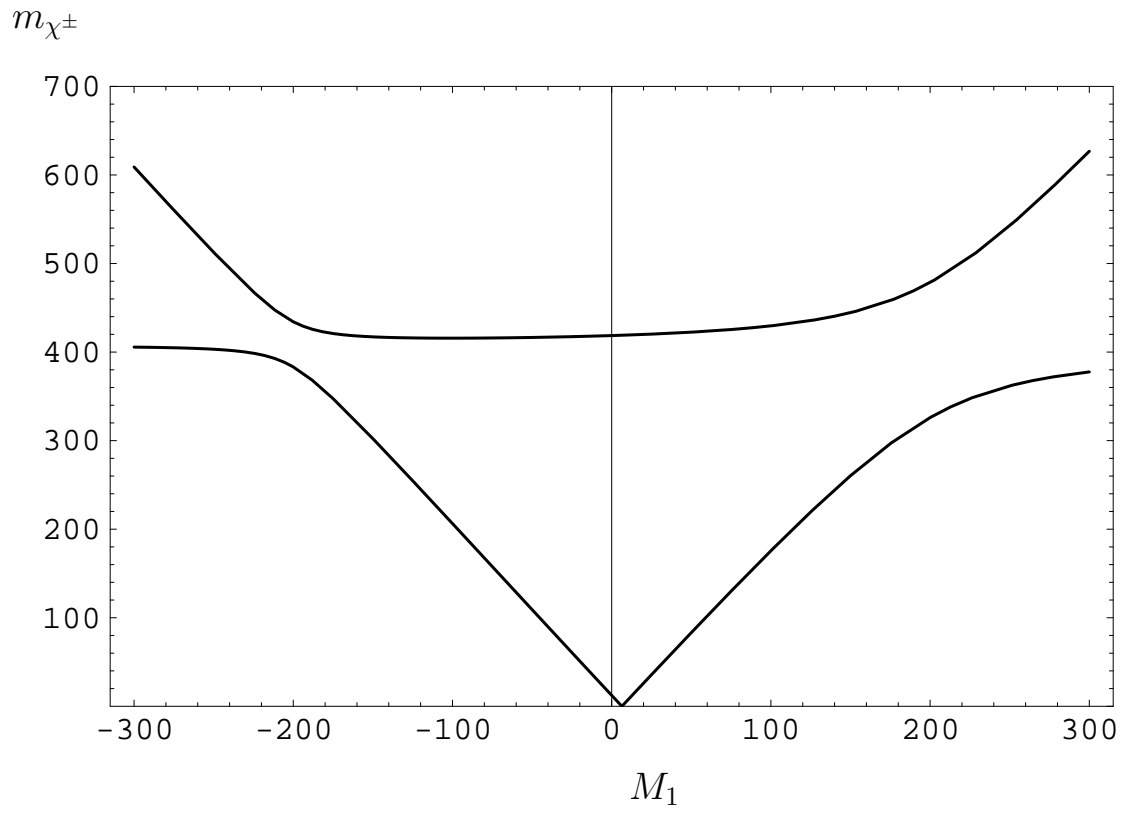


Fig. 10b

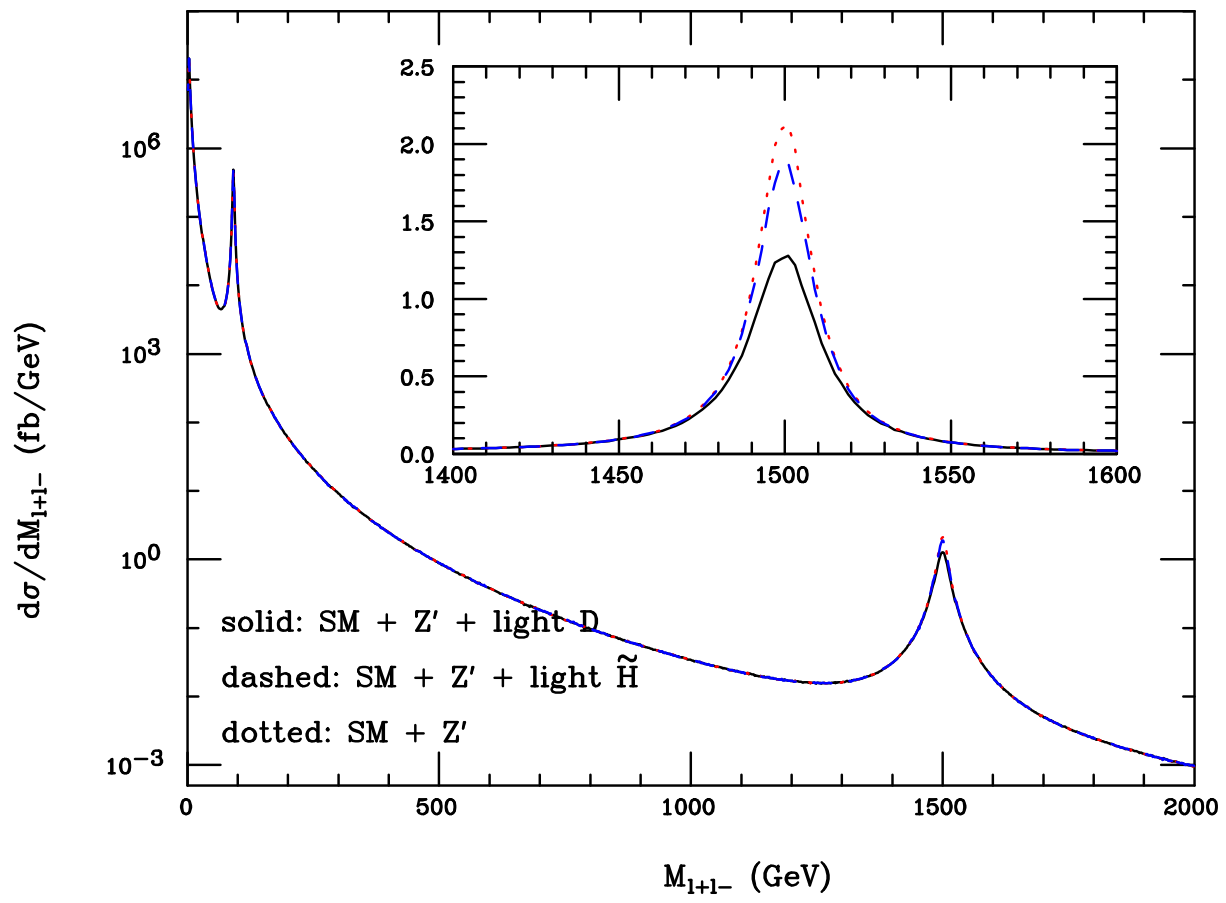


Fig. 11

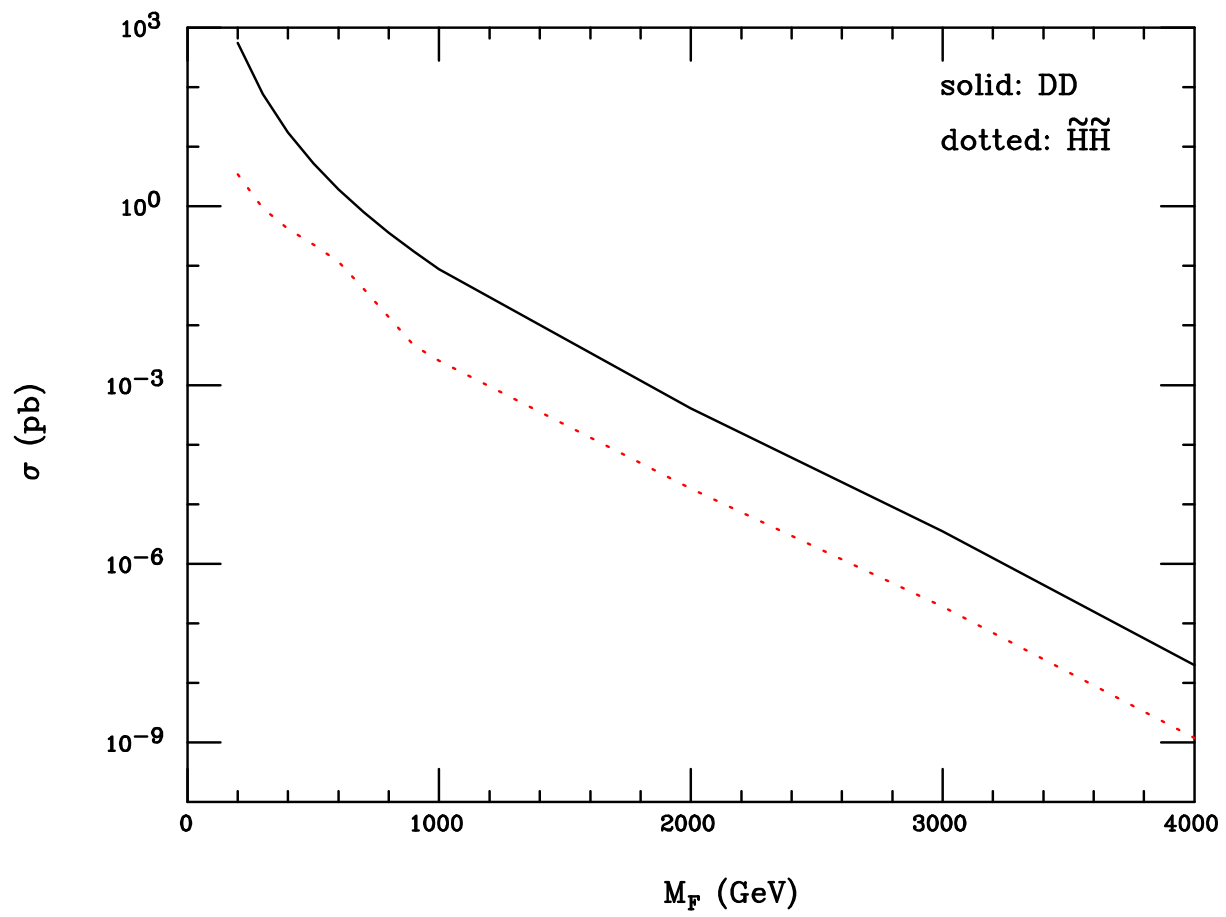


Fig. 12

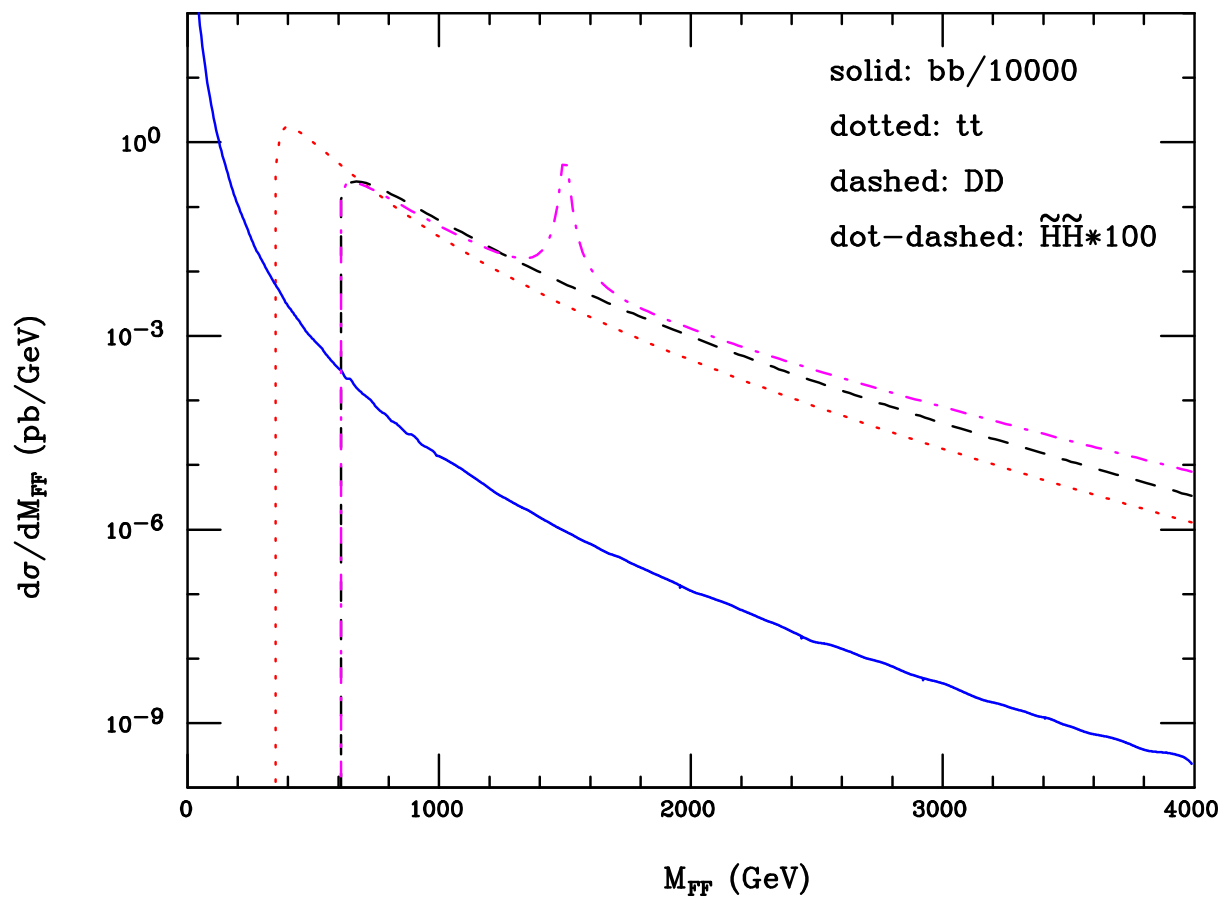


Fig. 13

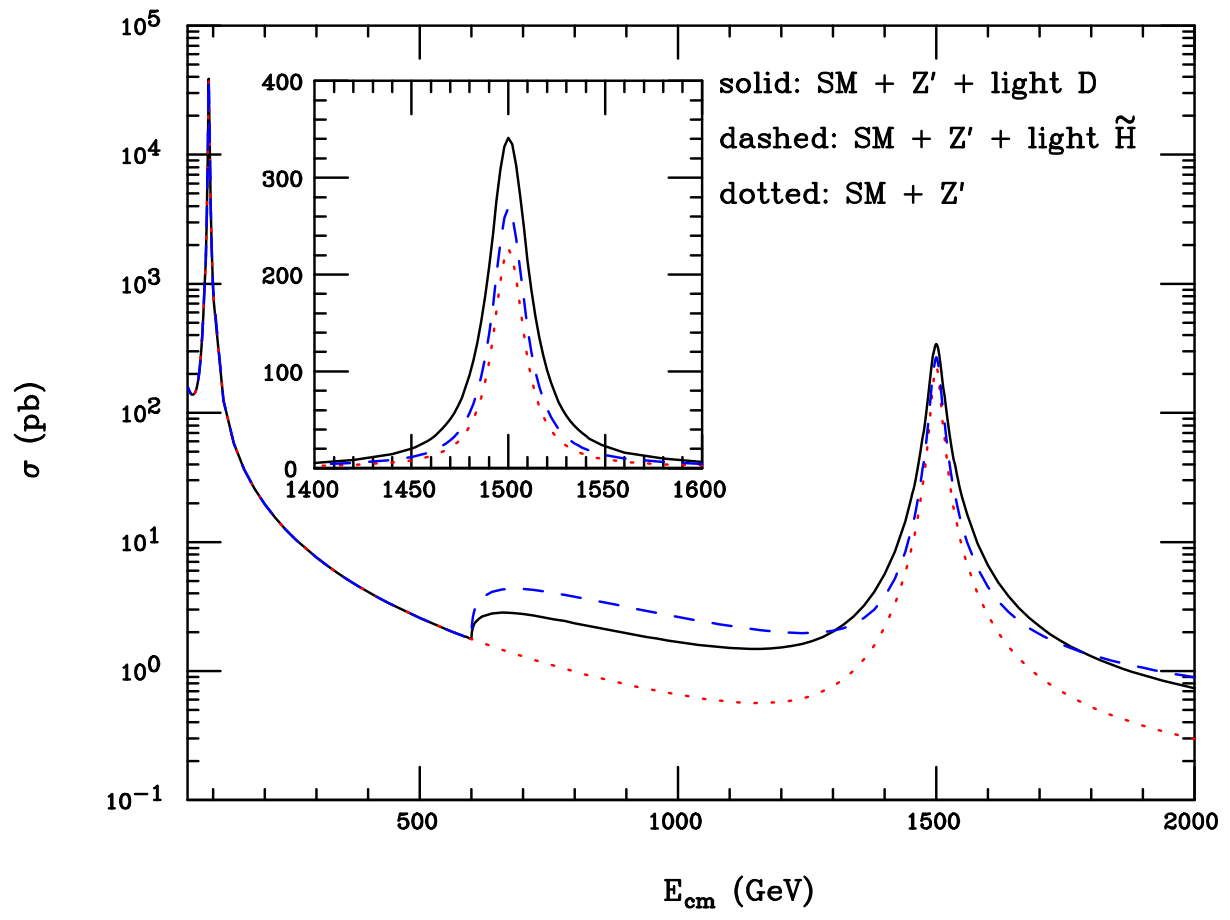


Fig. 14

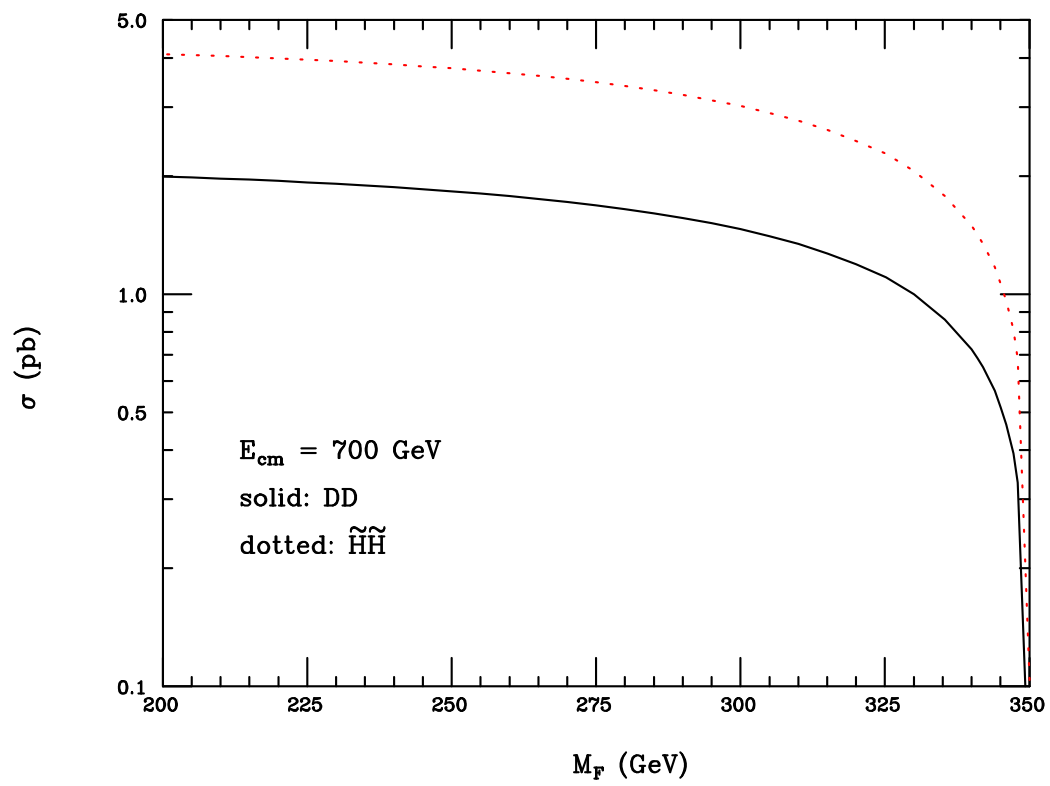


Fig. 15a

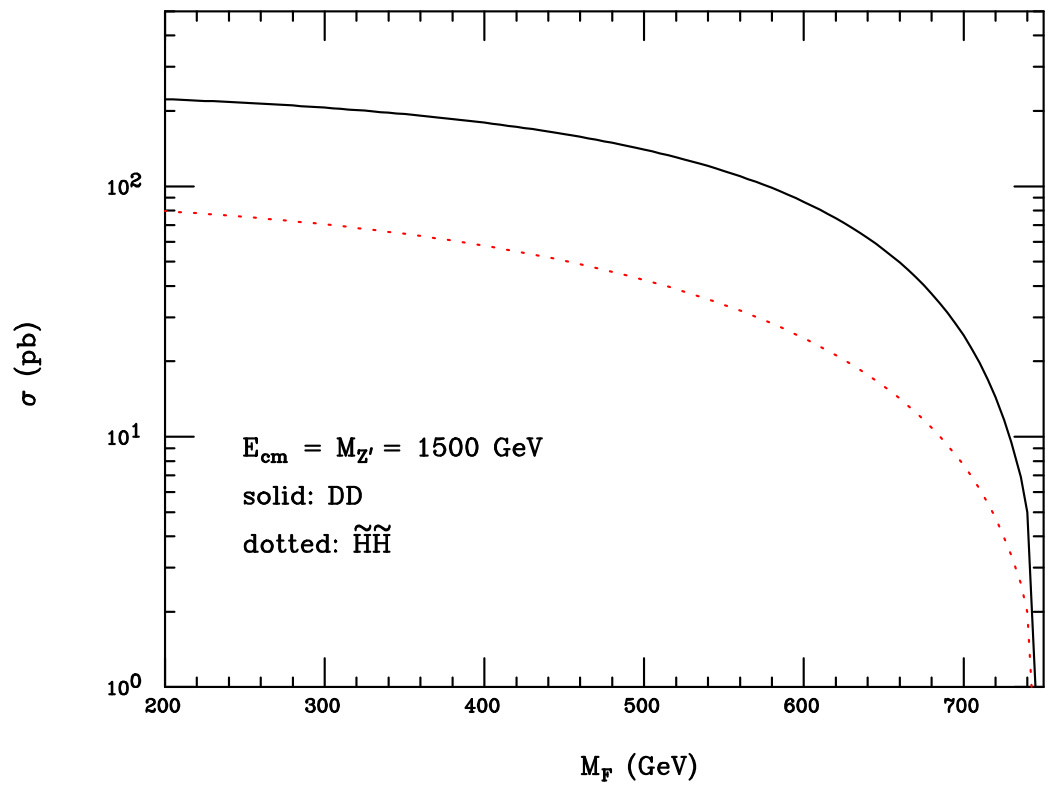


Fig. 15b

References

- [1] E. Witten, Nucl. Phys. B **188** (1981) 513; N. Sakai, Z. Phys. C **11** (1981) 153; S. Dimopoulos, H. Georgi, Nucl. Phys. B **193** (1981) 150; R. K. Kaul, P. Majumdar, Nucl. Phys. B **199** (1982) 36.
- [2] E. Gildener, S. Weinberg, Phys. Rev. D **13** (1976) 3333; E. Gildener, Phys. Rev. D **14** (1976) 1667.
- [3] D. J. H. Chung, L. L. Everett, G. L. Kane, S. F. King, J. Lykken, L. T. Wang, Phys. Rept. **407** (2005) 1.
- [4] J. Ellis, S. Kelley, D. V. Nanopoulos, Phys. Lett. B **249** (1990) 441; J. Ellis, S. Kelley, D. V. Nanopoulos, Phys. Lett. B **260** (1991) 131; U. Amaldi, W. de Boer, H. Furstenau, Phys. Lett. B **260** (1991) 447; P. Langacker, M. Luo, Phys. Rev. D **44** (1991) 817.
- [5] H. Georgi, S. L. Glashow, Phys. Rev. Lett. **32** (1974) 438.
- [6] M. B. Green, J. H. Schwarz, E. Witten, Superstring Theory (Cambridge Univ. Press, Cambridge, 1987).
- [7] P. Horava, E. Witten, Nucl. Phys. B **460** (1996) 506; Nucl. Phys. B **475** (1996) 94.
- [8] E. Witten, Nucl. Phys. B **471** (1996) 135; T. Banks, M. Dine, Nucl. Phys. B **479** (1996) 173; K. Choi, H. B. Kim, C. Muñoz, Phys. Rev. D **57** (1998) 7521.
- [9] F. del Aguila, G. A. Blair, M. Daniel, G. G. Ross, Nucl. Phys. B **272** (1986) 413.
- [10] R. Barbieri, S. Ferrara, C. Savoy, Phys. Lett. B **119** (1982) 343; H. P. Nilles, M. Srednicki, D. Wyler, Phys. Lett. B **120** (1983) 345; L. Hall, J. Lykken, S. Weinberg, Phys. Rev. D **27** (1983) 2359; S. K. Soni, H. A. Weldon, Phys. Lett. B **126** (1983) 215.
- [11] H. P. Nilles, Int. J. Mod. Phys. A **5** (1990) 4199.
- [12] A. Salam, J. Strathdee, Phys. Rev. D **11** (1975) 1521; M. T. Grisaru, W. Siegel, M. Rocek, Nucl. Phys. B **159** (1979) 429.
- [13] H. P. Nilles, M. Srednicki, D. Wyler, Phys. Lett. B **120** (1983) 346; J. M. Frere, D. R. T. Jones, S. Raby, Nucl. Phys. B **222** (1983) 11; J. P. Derendinger, C. A. Savoy, Nucl. Phys. B **237** (1984) 307; M. I. Vysotsky, K. A. Ter-Martirosian, Sov. Phys. JETP **63** (1986) 489; J. Ellis, J. F. Gunion, H. Haber, L. Roszkowski, F. Zwirner, Phys. Rev. D **39** (1989) 844.

- [14] L. Durand, J. L. Lopez, Phys. Lett. B **217** (1989) 463; L. Drees, Int. J. Mod. Phys. A **4** (1989) 3635.
- [15] Ya. B. Zel'dovich, I. Yu. Kobzarev, L. B. Okun, Sov. Phys. JETP **40** (1975) 1.
- [16] A. Vilenkin, Phys. Rept. **121** (1985) 263; A. Vilenkin, E. P. S. Shellard, Cosmic Strings and Other Topological Defects (Cambridge University Press, 1994).
- [17] S. A. Abel, S. Sarkar, P. L. White, Nucl. Phys. B **454** (1995) 663.
- [18] J. L. Hewett, T. G. Rizzo, Phys. Rept. **183** (1989) 193; J. F. Gunion, H. E. Haber, G. L. Kane, S. Dawson, “The Higgs Hunter’s Guide,” SCIPP-89/13; P. Binetruy, S. Dawson, I. Hinchliffe, M. Sher, Nucl. Phys. B **273** (1986) 501; J. R. Ellis, K. Enqvist, D. V. Nanopoulos, F. Zwirner, Nucl. Phys. B **276** (1986) 14; L. E. Ibanez, J. Mas, Nucl. Phys. B **286** (1987) 107; J. F. Gunion, L. Roszkowski, H. E. Haber, Phys. Lett. B **189** (1987) 409; H. E. Haber, M. Sher, Phys. Rev. D **35** (1987) 2206; J. R. Ellis, D. V. Nanopoulos, S. T. Petcov, F. Zwirner, Nucl. Phys. B **283** (1987) 93; M. Drees, Phys. Rev. D **35** (1987) 2910; H. Baer, D. Dicus, M. Drees, X. Tata, Phys. Rev. D **36** (1987) 1363; J. F. Gunion, L. Roszkowski, H. E. Haber, Phys. Rev. D **38** (1988) 105.
- [19] M. Cvetič, P. Langacker, Phys. Rev. D **54** (1996) 3570; Mod. Phys. Lett. A **11** (1996) 1247.
- [20] M. Cvetič, D. Demir, J. R. Espinosa, L. L. Everett, P. Langacker, Phys. Rev. D **56** (1997) 2861.
- [21] J. Erler, Nucl. Phys. B **586** (2000) 73.
- [22] D. A. Demir, G. L. Kane, T. T. Wang, hep-ph/0503290.
- [23] P. Langacker, M. Plumacher, Phys. Rev. D **62** (2000) 013006; V. Barger, C. W. Chiang, P. Langacker, H. S. Lee, Phys. Lett. B **580** (2004) 186; V. Barger, C. W. Chiang, J. Jiang, P. Langacker, Phys. Lett. B **596** (2004) 229.
- [24] D. Suematsu, Y. Yamagishi, Int. J. Mod. Phys. A **10** (1995) 4521;
- [25] E. Keith, E. Ma, Phys. Rev. D **56** (1997) 7155.
- [26] P. Langacker, J. Wang, Phys. Rev. D **58** (1998) 115010.
- [27] Y. Daikoku, D. Suematsu, Phys. Rev. D **62** (2000) 095006.
- [28] D. A. Demir, L. L. Everett, Phys. Rev. D **69** (2004) 015008.

- [29] J. -H. Kang, P. Langacker, T. -J. Li, Phys. Rev. D **71** (2005) 015012.
- [30] E. Ma, Phys. Lett. B **380** (1996) 286.
- [31] B. de Carlos, J. R. Espinosa, Phys. Lett. B **407** (1997) 12; V. Barger, C. Kao, P. Langacker, H. -S. Lee, Phys. Lett. B **600** (2004) 104.
- [32] T. Hambye, E. Ma, M. Raidal, U. Sarkar, Phys. Lett. B **512** (2001) 373.
- [33] J. Kang, P. Langacker, T. -J. Li, T. Liu, Phys. Rev. Lett. **94** (2005) 061801.
- [34] E. Ma, M. Raidal, J. Phys. G **28** (2002) 95.
- [35] V. Barger, C. Kao, P. Langacker, H. -S. Lee, Phys. Lett. B **614** (2005) 67.
- [36] D. Suematsu, Mod. Phys. Lett. A **12** (1997) 1709.
- [37] D. Suematsu, Phys. Lett. B **416** (1998) 108.
- [38] A. E. Faraggi, M. Thormeier, Nucl. Phys. B **624** (2002) 163.
- [39] J. Erler, P. Langacker, T. -J. Li, Phys. Rev. D **66** (2002) 015002; T. Han, P. Langacker, B. McElrath, Phys. Rev. D **70** (2004) 115006.
- [40] E. Keith, E. Ma, Phys. Rev. D **54** (1996) 3587. D. Suematsu, Phys. Rev. D **57** (1998) 1738.
- [41] Y. Hosotani, Phys. Lett. B **129** (1983) 193.
- [42] V. Barger, P. Langacker, H. S. Lee, Phys. Rev. D **67** (2003) 075009.
- [43] P. Di Bari, Phys. Rev. D **65** (2002) 043509.
- [44] M. Fukugita, T. Yanagida, Phys. Lett. B **174** (1986) 45.
- [45] V. A. Kuzmin, V. A. Rubakov, M. E. Shaposhnikov, Phys. Lett. B **155** (1985) 36.
- [46] J. Rich, M. Spiro, J. Lloyd–Owen, Phys. Rept. **151** (1987) 239; P. F. Smith, Contemp. Phys. **29** (1988) 159; T. K. Hemmick et al. , Phys. Rev. D **41** (1990) 2074.
- [47] S. Wolfram, Phys. Lett. B **82** (1979) 65; C. B. Dover, T. K. Gaisser, G. Steigman, Phys. Rev. Lett. **42** (1979) 1117.
- [48] E. Ma, Phys. Rev. Lett. **60** (1988) 1363.
- [49] G. F. Giudice, A. Masiero, Phys. Lett. B **206** (1988) 480; J. A. Casas, C. Muñoz, Phys. Lett. B **306** (1993) 288.

- [50] L. E. Ibáñez, G. G. Ross, Phys. Lett. B **110** (1982) 215; J. Ellis, D. V. Nanopoulos, K. Tamvakis, Phys. Lett. B **121** (1983) 123; J. Ellis, J. Hagelin, D. V. Nanopoulos, K. Tamvakis, Phys. Lett. B **125** (1983) 275; L. Alvarez-Gaumé, J. Polchinski, M. Wise, Nucl. Phys. B **221** (1983) 495.
- [51] B. Holdom, Phys. Lett. B **166** (1986) 196.
- [52] D. Suematsu, Phys. Rev. D **59** (1999) 055017.
- [53] K. S. Babu, C. Kolda, J. March–Russell, Phys. Rev. D **54** (1996) 4635; T. G. Rizzo, Phys. Rev. D **59** (1999) 015020.
- [54] K. Hagiwara et al. , Phys. Rev. D **66** (2002) 010001.
- [55] B. Schrempp, F. Schrempp, Phys. Lett. B **299** (1993) 321; B. Schrempp, Phys. Lett. B **344** (1995) 193; B. Schrempp, M. Wimmer, Prog. Part. Nucl. Phys. **37** (1996) 1.
- [56] P. Abreu et al. [DELPHI Collaboration], Phys. Lett. B **485** (2000) 45; R. Barate et al. [ALEPH Collaboration], Eur. Phys. J. C **12** (2000) 183.
- [57] F. Abe et al. [CDF Collaboration], Phys. Rev. Lett. **79** (1997) 2192.
- [58] A. Brignole, J. Ellis, G. Ridolfi, F. Zwirner, Phys. Lett. B **271** (1991) 123; P. H. Chankowski, S. Pokorski, J. Rosiek, Phys. Lett. B **274** (1992) 191; A. Brignole, Phys. Lett. B **277** (1992) 313; H. E. Haber, R. Hempfling, Phys. Rev. D **48** (1993) 4280.
- [59] T. Elliott, S. F. King, P. L. White, Phys. Lett. B **314** (1993) 56; U. Ellwanger, Phys. Lett. B **303** (1993) 271; U. Ellwanger, M. Lindner, Phys. Lett. B **301** (1993) 365; T. Elliott, S. F. King, P. L. White, Phys. Rev. D **49** (1994) 2435; S. F. King, P. L. White, Phys. Rev. D **52** (1995) 4183; S. W. Ham, S. K. Oh, B. R. Kim, Phys. Lett. B **414** (1997) 305.
- [60] P. A. Kovalenko, R. B. Nevzorov, K. A. Ter–Martirosyan, Phys. Atom. Nucl. **61** (1998) 812.
- [61] P. N. Pandita, Phys. Lett. B **318** (1993) 338; P. N. Pandita, Z. Phys. C **59** (1993) 575; S. W. Ham, S. K. Oh, B. R. Kim, J. Phys. G **22** (1996) 1575.
- [62] D. J. Miller, R. Nevzorov, P. M. Zerwas, Nucl. Phys. B **681** (2004) 3; R. Nevzorov, D. J. Miller, *Proceedings to the 7th Workshop "What comes beyond the Standard Model"*, ed. by N. S. Mankoc-Borstnik, H. B. Nielsen, C. D. Froggatt, D. Lukman, DMFA–Zaloznistvo, Ljubljana, 2004, p. 107; hep-ph/0411275.

- [63] K. Inoue, A. Kakuto, H. Komatsu, S. Takeshita, Prog. Theor. Phys. **67** (1982) 1889; R. Flores, M. Sher, Ann. Phys. **148** (1983) 95.
- [64] C. Panagiotakopoulos, A. Pilaftsis, Phys. Rev. D **63** (2001) 055003; D. J. Miller, R. Nevzorov, hep-ph/0309143; D. J. Miller, S. Moretti, R. Nevzorov, to be published in *Proceedings to the 18th International Workshop on High-Energy Physics and Quantum Field Theory (QFTHEP 2004)* (hep-ph/0501139).
- [65] H. E. Haber, M. Sher, Phys. Rev. D **35** (1987) 2206; M. Drees, Phys. Rev. D **35** (1987) 2910; D. Comelli and C. Verzegnassi, Phys. Lett. B **303** (1993) 277.
- [66] M. Masip, R. Muñoz-Tapia, A. Pomarol, Phys. Rev. D **57** (1998) 5340.
- [67] H. E. Haber, R. Hempfling, Phys. Rev. Lett. **66** (1991) 1815; Y. Okada, M. Yamaguchi, T. Yanagida, Prog. Theor. Phys. **85** (1991) 1; J. Ellis, G. Ridolfi, F. Zwirner, Phys. Lett. B **257** (1991) 83; J. Ellis, G. Ridolfi, F. Zwirner, Phys. Lett. B **262** (1991) 477; R. Barbieri, M. Frigeni, F. Caravaglios, Phys. Lett. B **258** (1991) 167; Y. Okada, M. Yamaguchi, T. Yanagida, Phys. Lett. B **262** (1991) 54; M. Drees, M. Nojiri, Phys. Rev. D **45** (1992) 2482; D. M. Pierce, A. Papadopoulos, S. Johnson, Phys. Rev. Lett. **68** (1992) 3678; P. H. Chankowski, S. Pokorski, J. Rosiek, Phys. Lett. B **274** (1992) 191; H. E. Haber, R. Hempfling, Phys. Rev. D **48** (1993) 4280; P. H. Chankowski, S. Pokorski, J. Rosiek, Nucl. Phys. B **423** (1994) 437; A. Yamada, Z. Phys. C **61** (1994) 247; A. Dabelstein, Z. Phys. C **67** (1995) 495; D. M. Pierce, J. A. Bagger, K. Matchev, R. Zhang, Nucl. Phys. B **491** (1997) 3.
- [68] J. R. Espinosa, M. Quiros, Phys. Lett. B **266** (1991) 389; R. Hempfling, A. H. Hoang, Phys. Lett. B **331** (1994) 99; M. Carena, J. R. Espinosa, M. Quiros, C. E. M. Wagner, Phys. Lett. B **355** (1995) 209; J. A. Casas, J. R. Espinosa, M. Quiros, A. Riotto, Nucl. Phys. B **436** (1995) 3; H. E. Haber, R. Hempfling, A. H. Hoang, Z. Phys. C **75** (1997) 539; S. Heinemeyer, W. Hollik, G. Weiglein, Phys. Rev. D **58** (1998) 091701; S. Heinemeyer, W. Hollik, G. Weiglein, Phys. Lett. B **440** (1998) 296; R. Zhang, Phys. Lett. B **447** (1999) 89; S. Heinemeyer, W. Hollik, G. Weiglein, Phys. Lett. B **455** (1999) 179.
- [69] M. Carena, M. Quiros, C. E. M. Wagner, Nucl. Phys. B **461** (1996) 407.
- [70] U. Ellwanger, C. Hugonie, Eur. Phys. J. C **25** (2002) 297.
- [71] A. C. Kraan, hep-ex/0505002.
- [72] S. Hesselbach, F. Franke, H. Fraas, Eur. Phys. J. C **23** (2002) 149.

- [73] T. Gherghetta, T. A. Kaeding, G. L. Kane, Phys. Rev. D **57** (1998) 3178.
- [74] J. Erler, P. Langacker, Phys. Lett. B **456** (1999) 68.
- [75] K. Agashe, M. Graesser, I. Hinchliffe, M. Suzuki, Phys. Lett. B **385** (1996) 218; J. Rosner, Phys. Lett. B **387** (1996) 113, A. Donini et al, Nucl. Phys. B **507** (1997) 51; P. Frampton, M. Wise, B. Wright, Phys. Rev. D **54** (1996) 5820.
- [76] A. D. Dolgov, Phys. Rept. **370** (2002) 333.
- [77] M. Cvetič, S. Godfrey, hep-ph/9504216; A. Leike, Phys. Rept. **317** (1999) 143; J. Kang, P. Langacker, Phys. Rev. D **71** (2005) 035014.
- [78] M. Dittmar, A. Djouadi, A-S. Nicollrat, Phys. Lett. B **583** (2004) 111.
- [79] P. Abreu *et al.* [DELPHI Collaboration], Phys. Lett. B **446** (1999) 62; J. Breitweg *et al.* [ZEUS Collaboration], Phys. Rev. D **63** (2001) 052002; C. Adloff *et al.* [H1 Collaboration], Phys. Lett. B **523** (2001) 234; G. Abbiendi *et al.* [OPAL Collaboration], Phys. Lett. B **526** (2002) 233; V. M. Abazov *et al.* [D0 Collaboration], Phys. Rev. D **71** (2005) 071104; [CDF Collaboration], hep-ex/0506074.
- [80] F. Abe *et al.* [CDF Collaboration], Phys. Rev. Lett. **77** (1996) 5336 [Erratum-ibid. **78** (1997) 4307]; B. Abbott *et al.* [D0 Collaboration], Phys. Rev. Lett. **80** (1998) 666.
- [81] E. Ma, M. Raidal, U. Sarkar, Eur. Phys. J. C **8** (1999) 301; E. Arik, O. Cakir, S. A. Cetin, S. Sultansoy, JHEP **0209** (2002) 024.